



University of Tennessee, Knoxville  
**Trace: Tennessee Research and Creative Exchange**

---

Doctoral Dissertations

Graduate School

---

8-2008

# Extraction of Proteins by Winsor III Microemulsion Systems

Javier Alejandro Gomez del Rio  
*University of Tennessee - Knoxville*

---

## Recommended Citation

Gomez del Rio, Javier Alejandro, "Extraction of Proteins by Winsor III Microemulsion Systems." PhD diss., University of Tennessee, 2008.  
[https://trace.tennessee.edu/utk\\_graddiss/439](https://trace.tennessee.edu/utk_graddiss/439)

This Dissertation is brought to you for free and open access by the Graduate School at Trace: Tennessee Research and Creative Exchange. It has been accepted for inclusion in Doctoral Dissertations by an authorized administrator of Trace: Tennessee Research and Creative Exchange. For more information, please contact [trace@utk.edu](mailto:trace@utk.edu).

To the Graduate Council:

I am submitting herewith a dissertation written by Javier Alejandro Gomez del Rio entitled "Extraction of Proteins by Winsor III Microemulsion Systems." I have examined the final electronic copy of this dissertation for form and content and recommend that it be accepted in partial fulfillment of the requirements for the degree of Doctor of Philosophy, with a major in Chemical Engineering.

Douglas Gordon Hayes, Major Professor

We have read this dissertation and recommend its acceptance:

Paul D. Frymier, Tsewei Wang, Qixin Zhong

Accepted for the Council:

Dixie L. Thompson

Vice Provost and Dean of the Graduate School

(Original signatures are on file with official student records.)

---

To the Graduate Council:

I am submitting herewith a dissertation written by Javier Alejandro Gomez del Rio entitled "Extraction of Proteins by Winsor III Microemulsion Systems." I have examined the final electronic copy of this dissertation for form and content and recommend that it be accepted in partial fulfillment of the requirements for the degree of Doctor of Philosophy, with a major in Chemical Engineering.

---

Dr. Douglas Gordon Hayes, Major Professor

We have read this dissertation  
and recommend its acceptance:

---

Dr. Paul D. Frymier

---

Dr. Tsewei Wang

---

Dr. Qixin Zhong

Accepted for the Council:

---

Carolyn R. Hodges, Vice Provost and  
Dean of the Graduate School

(Original signatures are on file with official student records.)

EXTRACTION OF PROTEINS BY WINSOR III  
MICROEMULSION SYSTEMS

A Dissertation  
Presented for the  
Doctor of Philosophy  
Degree  
The University of Tennessee, Knoxville

Javier Alejandro Gomez del Rio  
August 2008

## DEDICATION

This dissertation is dedicated to my parents, Miguel Angel Gomez del Rio and my mother Laura Esther Sitar de Gomez del Rio, and my sisters Daniela and Fernanda, and my friends. All of them supported and encourage me to reach my goals even when they sometimes seemed to be a dream at the beginning.

## ACKNOWLEDGEMENTS

I would like to thank to my advisor Dr. Douglas Hayes for his guidance, encouragement and patience in the learning process needed to complete the dissertation work. I wish to thank to my committee members, Dr. Paul Frymier, Dr. Quixin Zhong, and Dr. Tse-Wei Wang for their guidance and review of the dissertation work.

I wish to thank to the NFS grant BES-0211164, who provided the financial support for the research.

I would like to thank to the undergraduate students, Jonas Boateng (UAH), Jordan Zanetis (Univ Tenn), and Lindsey Kline (Univ Tenn) that helped me with the experimental work.

I wish to thank to my parents Miguel and Laura for the moral and economical support which made possible my travel and initial setting in United States. Also I wish thanks to the Argentineans, Dr. Ramón Cerro, Dr. Daniel Balzaretti, and Mónica Gaviola de Baker that help me with their advice and support in the process of applying to the University of Alabama in Huntsville and also in the initial setting in United State.

I would like to thank to the secretary of the Biosystems Engineering and Soil Science Department, Ms. Margaret Taylor, who help me and gave me advice for the paperwork needed by the University throughout the entire time that I studied at the University of Tennessee.

## ABSTRACT

Purification of proteins by microemulsion was improved through use of a 3-phase (“Winsor-III”) microemulsion system instead of the traditionally employed 2-phase (“Winsor-II”) water-in-oil microemulsion system. As a consequence, two of the main problems of the traditional method were improved: the low and slow rate of recovery of proteins encapsulated by the microemulsions and the low protein solubilization capacity of the microemulsions.

Microemulsion systems employed a mixture of surfactants, two pH-degradable “cyclic ketal” alkyl ethoxylates (O-[(2-tridecyl, 2-ethyl-1,3-dioxolan-4-yl) methoxy]-O'-methoxy poly(ethylene glycol)<sub>n</sub>, where n, the average degree of polymerization for the ethoxylate group, equaled 3.0 or 5.45, CK3 and CK7, respectively) and Aerosol-OT (AOT). CK7's ethoxylate size has broad molecular weight distribution. Partitioning behavior of CK7 molecules as a function of their ethoxylate size, temperature, and the addition of a second surfactant (AOT, CK3, or octyl β-D-glycoside) were investigated. A semi-empirical thermodynamic mathematical model was developed to calculate the phase inversion temperature (PIT) for a surfactant mixture of a specified composition. This information is useful to find the optimal Winsor-III for protein extraction.

Finally different Winsor-III systems formed by water, isooctane and surfactant mixtures of CK7, CK3 and AOT were tested in forward extraction of α-chymotrypsin, cytochrome-c, lysozyme, BSA and pepsin. Three approaches were used to obtain Winsor-III systems suitable for forward extraction: employment at 40°C, addition of a more hydrophobic surfactant (CK3, 25°C), and the addition of 1.5 wt. % NaCl (aq) to increase the ionic strength (25°C). Protein concentrations achieved in microemulsion phase were 10 times higher than values reported in the literature for extraction by Winsor-II microemulsion systems.

Back extraction was tested for α-chymotrypsin, cytochrome-c, and lysozyme. Aqueous stripping solutions used for back extraction contained either a high ionic strength (5 wt. % NaCl) or a high pH (12.0). Back-extraction was fast and total recovery of the

activity for  $\alpha$ -chymotrypsin was achieved. Other proteins have smaller percentage of mass recovery in the conditions tested but comparable with yields reported in the literature for microemulsion-based extraction.



# TABLE OF CONTENTS

1	Introduction.....	1
1.1	Objectives .....	1
1.2	Significance.....	3
2	Background.....	7
2.1	Introduction.....	7
2.2	Surfactants.....	8
2.2.1	Overview of Surfactant Types .....	9
2.2.2	Alkyl Ethoxylate Surfactant.....	11
2.2.3	Cleavable surfactant.....	12
2.2.4	O-[(2-tridecyl, 2-ethyl-1,3-dioxolan-4-yl)methoxy]-O'-methoxy poly(ethylene glycol) <sub>5,45</sub> (CK7) .....	15
2.2.5	Sodium Bis (2-ethylhexyl) Sulfosuccinate (AOT) .....	17
2.3	Microemulsions.....	17
2.3.1	Description and applications.....	18
2.3.2	Winsor Microemulsion systems.....	20
2.4	Microemulsion based liquid-liquid extraction-based protein purification 24	
2.4.1	Description.....	24
2.4.2	Scale up and applications.....	30
2.4.3	Role of microemulsion based liquid-liquid extraction in bioseparations 30	
3	CHEMICAL AND MOLECULAR WEIGHT-BASED CHARACTERIZATION OF CYCLIC KETAL SURFACTANTS.....	33
3.1	Introduction.....	33
3.2	Materials .....	34
3.3	Methods.....	34
3.3.1	Surfactant synthesis .....	34

3.3.1.1	Qualitative Measurement of Ketone .....	36
3.3.2	Gel permeation chromatography.....	36
3.3.3	Reverse Phase- High Performance Liquid Chromatography.....	37
3.4	Results and Discussion .....	41
3.4.1	MPEG-350 molecular weight .....	41
3.4.2	CK7 molecular weight .....	42
3.4.3	Synthesis and Chemical Characterization.....	45
3.5	Conclusions.....	48
4	Partition of CK7 in 2 and 3 phases microemulsion systems as a function of ethoxylate size and temperature in single and binary surfactant mixtures .....	50
4.1	Introduction.....	50
4.2	Theory .....	51
4.3	Materials .....	53
4.4	Methods.....	54
4.4.1	Measurement of partition coefficients .....	54
4.4.2	High performance liquid chromatography.....	54
4.4.3	Phase diagram .....	55
4.5	Results.....	56
4.5.1	The Partitioning of CK7 Between Water and Oil.....	56
4.5.2	Equilibrium Partitioning of CK7 in the presence of CK3.....	60
4.5.3	Equilibrium of CK7 in the Presence of AOT.....	65
4.5.4	Equilibrium of CK7 in the presence of C <sub>8</sub> βG <sub>1</sub> .....	70
4.5.5	CK7 Phase Diagram.....	73
4.6	Discussion .....	74
4.6.1	Use of Thermodynamic Model to Predict Phase Inversion Temperature	74
4.6.2	Thermodynamic properties .....	79
4.6.3	Model Validation .....	82
4.7	Conclusions.....	82

5	Protein Forward extraction .....	84
5.1	Introduction.....	84
5.2	Materials .....	85
5.3	Methods.....	86
5.3.1	Forward Extraction of Protein .....	86
5.3.1.1	CK7/AOT Surfactant System, Using Super-Ambient Temperature	86
5.3.1.2	CK7/AOT/CK3 Surfactant System at 25°C.....	86
5.3.1.3	CK7/AOT/ Surfactant System at 25°C, Addition of Salt.....	87
5.3.2	Quantitative Analysis of Forward Extraction Experiments .....	88
5.3.2.1	Protein Quantification.....	88
5.3.2.2	Surfactant Quantification.....	88
5.3.2.3	Volume Calibration of Vial .....	89
5.4	Results.....	90
5.4.1	W-III-Based Extraction Using AOT/CK7 at 40°C .....	91
5.4.2	Hydrophobicity Tuned by a Third Surfactant.....	96
5.4.3	Hydrophobicity Tuned by NaCl.....	99
5.4.3.1	Forward Extraction for 1 mg/ml Protein Solution .....	99
5.4.3.2	Saturation of the Middle Phase .....	100
5.5	Discussion.....	103
5.5.1	Comparison of the Three Approaches Used to Form Winsor-III Systems	103
5.5.2	Comparison of protein extraction and solubilization capacity using W-III versus W-II systems.....	104
5.6	Conclusions.....	106
6	Back extraction .....	110
6.1	Introduction.....	110
6.2	Materials .....	112
6.3	Methods.....	112

6.3.1	Backward Extraction Using 5 wt. % NaCl Solution.....	112
6.3.2	Mass Quantification.....	113
6.3.3	Activity.....	114
6.4	Results.....	115
6.4.1	Back Extraction Using a 5 wt. % NaCl(aq) Stripping Solution.....	115
6.4.2	Activity.....	117
6.5	Discussion.....	120
6.6	Conclusions.....	122
7	Conclusions and Recommendations.....	123
7.1	Conclusions.....	123
7.2	Recommendations.....	126
8	List of References.....	129
9	Vita.....	136

## LIST OF TABLES

<b>Table 3.1:</b> Mole and mass fractions of the components of MPEG-350, H-(OCH <sub>2</sub> CH <sub>2</sub> ) <sub>n</sub> -OCH <sub>3</sub> , according to the degree of polymerization, <i>n</i> , as determined from RP-HPLC using a refractive index detector .....	42
<b>Table 3.2:</b> Mole and mass fraction of CK7 molecules according to their ethoxylate group size, <i>n</i> , obtained by using ELSD detector .....	44
<b>Table 3.3:</b> Mole and mass fraction of CK7 molecules according to their ethoxylate group size, <i>n</i> obtained by using RI detector .....	45
<b>Table 4.1:</b> Coefficients of second order polynomial used to calculate molar enthalpy ( $\Delta h_n$ ) in function of number of ethoxylate monomeric units for single and binary surfactant systems, Eq. 15. Units: (J mol <sup>-1</sup> ). .....	75
<b>Table 4.2:</b> Coefficients of second order polynomial used to calculate molar entropy ( $\Delta s_n$ ) in function of number of ethoxylate monomeric units for single and binary surfactant systems, <b>Equation 4.16</b> . Units: (J mol <sup>-1</sup> K <sup>-1</sup> ). .....	76
<b>Table 4.3:</b> Phase inversion temperature calculated by using the thermodynamical model fitted to data. ....	78
<b>Table 4.4:</b> Effect of surfactant characteristics present in the interface on the PIT. ....	79
<b>Table 4.5:</b> Root mean square error (RMSE) of the ln(K <sub>n</sub> ), $\Delta h$ (J mol <sup>-1</sup> ) and $\Delta h$ (J mol <sup>-1</sup> K <sup>-1</sup> ) calculated for each surfactant mixture. ....	82
<b>Table 5.1:</b> Isoelectric point and molecular weight of the proteins used in this work. ....	95
<b>Table 5.2:</b> Summary of the characteristics of the three approaches of forward extraction by Winsor-III microemulsion systems.....	109
<b>Table 6.1:</b> Mass percent and relative activity of backward extracted $\alpha$ -chymotrypsin by three methods <sup>a</sup> .....	120

## LIST OF FIGURES

<b>Figure 2.1:</b> Picture of a surfactant in the interface oil/water. ....	10
<b>Figure 2.2:</b> Palisade structure of surfactant self assembly.....	11
<b>Figure 2.3:</b> Structure of CK <sub>2,13</sub> -O-MPEG <sub>c</sub> -O-CH <sub>3</sub> surfactant where “c” can be 7.2 or 3. .....	16
<b>Figure 2.4:</b> Sodium bis (2-ethylhexyl) sulfosuccinate (AOT) [33]. ....	17
<b>Figure 2.5:</b> Picture of the four systems classified by Winsor <i>et al.</i> In the picture orange color is oil and sky blue color is water. ....	21
<b>Figure 2.6:</b> Conceptual model of the “fish” diagram. It represents the number of phases classified by Winsor nomenclature of an ethoxylate surfactant as a function of the temperature and surfactant concentration, with the ratio of water to oil held constant (typically at a 1:1 weight or volume ratio). Blue line: phase inverse temperature (PIT).....	22
<b>Figure 2.7:</b> Increase in PIT at low concentration of a surfactant mixture which components are more soluble in oil than water observed by Ghoulam <i>et al.</i> Solid line is limit between phases. Dots line is the PIT in function of the surfactant concentration. The legend indicates the components present in the sample in the form (C <sub>12</sub> E <sub>n</sub> ) [49]. ....	23
<b>Figure 2.8:</b> A diagram illustrating the <i>forward extraction</i> process in microemulsion based protein separation. The driving force in this system shown above is the electrostatic interactions between the negatively-charged surfactant head-groups and the positively-charged protein. Iyer 2002 . ....	24
<b>Figure 2.9:</b> A diagram illustrating the <i>back extraction</i> process in microemulsion based protein separation. Iyer 2002 . ....	25
<b>Figure 2.10:</b> Diagram representing a water-in-oil microemulsion. ....	26
<b>Figure 2.11:</b> Dependence of the fraction of $\alpha$ -chymotrypsinogen A (E) the concentration of water extracted from the aqueous phase on X, the fraction of AOT based on the	

whole surfactant. $\Delta$ , E about 20 min after the contact; $\bullet$ , E about 2 days after the contact; $\circ$ , $[H_2O]_m$ [4] .....	27
<b>Figure 2.12:</b> Diagram of effects of the variables (legend in the diagram) in the phases of a system composed of oil, water and a non-ionic surfactant [1].....	29
<b>Figure 2.13:</b> Diagram of protein purification by Winsor-III microemulsion system. The sequence from the left to the right is: A) Mixing oil with surfactants and water phase with proteins and low concentration of salt. B) Proteins with charge opposite to surfactant are extracted in bicontinuous phase. C) Bottom solution is replaced by a stripping solution with a concentration of salt high enough to produce Debye shielding and the proteins are released. ....	29
<b>Figure 2.14:</b> Common steps used to purify bioproducts[60]. ....	32
<b>Figure 3.1</b> Overview of method used to synthesize CK7 and CK3. From Iyer <i>et al.</i> [5] MPEG refers to MPEG-350 and MPEG <sub>3</sub> , for CK7 and CK3, respectively. R <sub>1</sub> and R <sub>2</sub> refer to <i>n</i> -C <sub>13</sub> H <sub>27</sub> and CH <sub>3</sub> CH <sub>2</sub> , respectively.....	35
<b>Figure 3.2:</b> GPC calibration curve (natural logarithm of molecular weight vs. retention time) for poly(ethylene glycol) standards. The standard errors for the retention time values are reflected in the size of the data points.....	37
<b>Figure 3.3:</b> Chromatograms of pure CK7. C <sub>18</sub> reverse phase column, isocratic mobile phase of 98 vol% acetone and 2 vol % acetic acid at 1 ml/min. ELSD detector. n refers to the degree of polymerization of the surfactant molecule's ethoxylate group. ....	39
<b>Figure 3.4:</b> Molar distribution of of MPEG-350, H-(OCH <sub>2</sub> CH <sub>2</sub> ) <sub>n</sub> -OCH <sub>3</sub> , versus degree of polymerization, n, as determined from RP-HPLC. Blue curve represents the Poisson distribution (Section 2.2.2) centered at n=7.21. ....	43
<b>Figure 3.5:</b> Mole fraction of the species present in CK7 surfactant based on the ethylene oxide number (n) of the surfactant head. ....	44
<b>Figure 3.6:</b> FTIR spectra (top: overall spectra; bottom: -carbonyl stretching region) of CK7 surfactant. Blue: CK7 surfactant synthesized by the author of this dissertation of lower purity; Magenta: highly pure CK7 surfactant synthesized by M. Alkhatib,	

Univ. Alabama-Huntsville, and (Yellow) CK7 surfactant synthesized by the author of this dissertation.....	47
<b>Figure 3.7:</b> Thin layer chromatography of CK7 surfactant indicating the presence of ketone. The bands positions of CK7 and ketal are given in the figure. Each plate includes a band to the left for ketone standard. A) Highly pure CK7 surfactant synthesized by M. Alkhatib, Univ. Alabama-Huntsville, corresponding to magenta line in <b>Figure 3.6</b> . B) CK7 surfactant synthesized by the author of this dissertation of low purity, corresponding to blue line in <b>Figure 3.6</b> . .....	48
<b>Figure 4.1:</b> Example of chromatograms for the equilibrium partitioning of CK7 in a Winsor-III system obtained from reverse-phase HPLC analysis. A) Aqueous phase (bottom). B) Oil phase (top). The degree of polymerization n corresponding to each peak is indicated in the figure. ....	55
<b>Figure 4.2:</b> Fitting of Van't Hoff equation ( <b>Equation 4.3</b> ) to partition coefficient data for CK7. Natural logarithm of equilibrium constant $K_n$ ( $C_{wn}/C_{on}$ ) versus inverse of the temperature. A) 5 wt.% overall surfactant. B) 7.5 wt.% overall surfactant. C) 10 wt.% overall surfactant. Ethylene oxide degrees of polymerization, from 3 to 10 are represented as described in the legend. The lines represent the model fit ( <b>Equation 4.3</b> ) to the data.....	57
<b>Figure 4.3:</b> Enthalpy and Entropy values divided by the gas constant (R) versus ethoxylate size for CK7. Constants of Van't Hoff equation obtained by fitting <b>Equation 4.3</b> to the data of <b>Figure 4.2</b> . A) Slopes of fitted lines ( <b>Equation 4.3</b> ) in <b>Figure 4.2</b> B) Intercepts of fitted lines ( <b>Equation 4.3</b> ) in <b>Figure 4.2</b> . Concentrations in both figures are 5 wt.%CK7, 7.5 wt.% CK7 and 10 wt.% CK7 overall surfactant as indicated in the legend Curve represents second-order polynomial fit to the data. ....	59
<b>Figure 4.4:</b> The effect of ethoxylate group size, surfactant concentration, and temperature on the partitioning of CK7. Data and values obtained by the semi-empirical model (Section 4.2). Natural logarithm of distribution constant ( $K_n=(C_{wn}/C_{on})$ ) for CK7 surfactant versus number of ethylene oxide unit as a function of temperature. A) 5	



wt.% overall concentration of CK7. B) 7.5 wt.% and 10 wt.% overall concentration of CK7. 20°C is W-I and 30°C to 50°C are W-III system. Curves represent  $\ln(K_n)$  as predicted by the model (Section 4.2). ..... 61

**Figure 4.5:** Fitting of Van't Hoff equation (**Equation 4.3**) to the partition coefficient data obtained for the CK7 / CK3 mixed surfactant system. Natural logarithm of equilibrium constant  $K_n$  ( $C_{wn}/C_{on}$ ) versus inverse of the temperature. Concentrations are 3.75 wt.% CK7 and 3.75 wt.% CK3. Ethylene oxide degrees of polymerization, from 3 to 10 are represented as described in the legend. The lines represent the model fit (**Equation 4.3**) to the data. .... 62

**Figure 4.6:** Enthalpy and Entropy values divided by the gas constant (R) versus ethoxylate size for the CK7 / CK3 mixed surfactant system. Constants of Van't Hoff equation obtained by fitting **Equation 4.3**. A) Slopes of fitted lines (**Equation 4.3**) in **Figure 4.5**. B) y-Intercepts of fitted lines (**Equation 4.3**) in **Figure 4.5**. Concentrations in both figures are 3.75 wt.% CK7 and 3.75 wt.% CK3 overall surfactant. Curve represents second-order polynomial fit to the data. .... 64

**Figure 4.7:** The effect of ethoxylate size and temperature on the partitioning data of the CK7 / CK3 mixed surfactant system. Data and values obtained by the semi-empirical model (Section 4.2). Natural logarithm of distribution constant ( $K_n=(C_{wn}/C_{on})$ ) for CK7 surfactant versus number of ethylene oxide unit as a function of temperature for a binary system of 3.75 wt.% CK7 and 3.75 wt.% CK3. Solvents are isooctane and deionized water. Solid lines are the model fitted to the data (Section 4.2). .... 65

**Figure 4.8:** Natural logarithm of distribution constant ( $K_n=C_{wn}/C_{oiln}$ ) for CK7 surfactant versus number of ethylene oxide unit as a function of ethoxylate size for a binary system of (red) 6 wt.% AOT 1.5 wt.% CK7 and (blue) 3.75 wt.% AOT 3.75 wt.% CK7. Solvents are isooctane and deionized water. Lines are linear fitting to the data. Data points were obtained for temperatures from 20°C to 50°C. .... 66

**Figure 4.9:** Fitting of Van't Hoff equation (**Equation 4.3**) to the partitioning data of CK7 in the mixed CK7 / AOT system in the presence of salt. Natural logarithm of

equilibrium constant  $K_n$  ( $C_{wn}/C_{on}$ ) versus inverse of the temperature is plotted. Concentrations are 3.75 wt.% CK7 and 3.75 wt.% AOT. Solvents are isooctane and 1 wt.%NaCl in water solution. Ethylene oxide degrees of polymerization, from 3 to 10 are represented as described in the legend. The lines represent the model fit (**Equation 4.3**) to the data. .... 67

**Figure 4.10:** Enthalpy and Entropy values divided by the gas constant (R) versus ethoxylate size for the CK7 / AOT mixed surfactant system. Constants of Van't Hoff equation obtained by fitting **Equation 4.3** to the partitioning data of CK7 for the mixed AOT / CK7 system in the presence of salt. A) Slopes of fitted lines (**Equation 4.3**) in **Figure 4.9**. B) Intercepts of fitted lines (**Equation 4.3**) in **Figure 4.9**. Concentrations are 3.75 wt.% CK7 and 3.75 wt.% AOT. Solvents are isooctane and 1 wt.%NaCl in water solution. Curve represents second-order polynomial fit to the data. .... 68

**Figure 4.11:** Effect of ethoxylate group size and temperature on the partitioning of CK7 for the AOT / CK7 mixed surfactant system in the presence of salt. Plotted are experimental data and values obtained by the semi-empirical model (Section 4.2). Natural logarithm of distribution constant ( $K_n=C_{wn}/C_{oiln}$ ) for CK7 surfactant versus number of ethylene oxide unit as a function of temperature for a binary system of 3.75 wt.%CK7 and 3.75 wt.% AOT. Solvents are isooctane and 1 wt.%NaCl in water solution. Solid lines are the model fitted to the data. .... 69

**Figure 4.12:** Fitting of Van't Hoff equation (**Equation 4.3**) to the partitioning data of CK7 in the mixed CK7 /  $C_8\beta G_1$  system in the presence of salt. Natural logarithm of equilibrium constant  $K_n$  ( $C_{wn}/C_{on}$ ) versus inverse of the temperature is plotted. Concentrations are 3.75 wt.% CK7 and 3.75 wt.%  $C_8\beta G_1$ . Solvents are isooctane and deionized water. Ethylene oxide degrees of polymerization, from 3 to 10 are represented as described in the legend. The lines represent the model fit (**Equation 4.3**) to the data. .... 70

**Figure 4.13:** Enthalpy and Entropy values divided by the gas constant (R) versus ethoxylate size for the CK7 /  $C_8\beta G_1$  mixed surfactant system. Constants of Van't

Hoff equation obtained by fitting **Equation 4.3** to the partitioning data of CK7 for the mixed CK7 / C<sub>8</sub>βG<sub>1</sub> system. A) Slopes of fitted lines (Eq. 3) in **Figure 4.12**. B) Intercepts of fitted lines (Eq. 3) in **Figure 4.12**. Concentrations are 3.75 wt.% CK7 and 3.75 wt.% C<sub>8</sub>βG<sub>1</sub>. Solvents are isooctane and water. Curve represents second-order polynomial fit to the data..... 72

**Figure 4.14:** Effect of ethoxylate group size and temperature on the partitioning of CK7 for the AOT / C<sub>8</sub>βG<sub>1</sub> mixed surfactant system. Plotted are experimental data and values obtained by the semi-empirical model (Section 4.2). Data and values obtained by the semi-empirical model (Section 4.2). Natural logarithm of distribution constant ( $K_n=(C_{wn}/C_{on})$ ) for CK7 surfactant versus number of ethylene oxide unit as a function of temperature for a binary system of 3.75 wt.%CK7 and 3.75 wt.% C<sub>8</sub>βG<sub>1</sub>. Solvents are isooctane and water. Solid lines are the model fitted to the data. .... 73

**Figure 4.15:** Part of fish diagram of CK7 in isooctane / water system. Water: isooctane ratio held constant at 1:1 g g<sup>-1</sup>. Blue dots are phase transition and red dots are concentration and temperature of samples used in pure CK7 equilibrium. Dotted lines represent approximate positions of phase boundaries..... 74

**Figure 4.16:** A) Enthalpy and B) entropy of transferring a molecule from oil to water. Dots are calculated from measured data and solid lines are second order polynomial fitted to the data. Each color corresponds to the concentration of surfactants described in the legend..... 81

**Figure 5.1:** Vial with indication of the lengths used for volume calculation. a is a distance between the two marks in the vial as indicated in the figure and s is the level of the liquid of which volume is measured. .... 89

**Figure 5.2:** Calibration curve of volume of liquid related to the level “L” calculated in **Equation 5.1**..... 90

**Figure 5.3:** Distribution of lysozyme in the bottom (blue), middle (red), and top phase(yellow) of a Winsor III system formed by AOT, CK7, water, and isooctane. Volumes of water and isooctane are the same. Aqueous solution consists of a 0.1 M

pH 7 phosphate buffer and contains 1 mg/ml of protein.  $C_s$  is overall weight percentage of surfactant and  $X_{AOT}$  is the mass fraction of AOT among the surfactants. Temperature = 40°C. .... 92

**Figure 5.4:** Distribution of AOT present in the bottom (blue), middle (red), and top phase (yellow) of W-III systems for the experiments described in **Figure 5.3**. Conditions for extraction are given in **Figure 5.3**. .... 92

**Figure 5.5:** Partition coefficients for lysozyme based on mass amounts corresponding to the systems in **Figure 5.3**. Conditions for extraction are given in **Figure 5.3**. .... 93

**Figure 5.6:** Partition coefficients for lysozyme based on relative concentrations corresponding to the systems in **Figure 5.3**. Conditions for extraction are given in **Figure 5.3**.  $C_{middle}$  is concentration of protein in the middle phase ( $g_{prot} \cdot mL_{middle\ phase}^{-1}$ ) and  $C_{bottom}$  is concentration of protein in the bottom phase ( $g_{prot} \cdot mL_{bottom\ phase}^{-1}$ ). .... 93

**Figure 5.7:** Volume fraction of bottom (blue), middle (red), and top phase (yellow) of W-III system composed by CK7, AOT, isooctane and 0.1 M pH7 phosphate buffer at 40°C, corresponding to the experiments of **Figure 5.3-Figure 5.6**. Conditions for extraction are given in **Figure 5.3**. .... 94

**Figure 5.8:** Distribution of BSA mass in the bottom (blue), middle (red), and top phase (yellow) of Winsor III system. Volumes of water and isooctane are the same and overall surfactant is 1 wt.%. Percentage of each surfactant among the surfactants is 0.7 wt. % CK7; 0.3 wt. % AOT. Temperature 40°C ..... 95

**Figure 5.9:** Distribution of protein mass in the bottom (blue), middle (red), and top phase (yellow) of W-III system. Volumes of 0.1 M pH 7 phosphate buffer and isooctane are the same and overall surfactant is 1 wt. %. Percentage of each surfactant among the surfactants were 0.30 wt. % CK7; 0.3 wt.% CK3, and 0.4 wt.% AOT. Temperature 25°C..... 97

**Figure 5.10:** Concentration partition coefficient between middle and bottom phase of the proteins during W-III-based protein extraction, displayed in **Figure 5.9**. Conditions listed in **Figure 5.9**.  $C_{middle}$  is concentration of protein in the middle phase ( $g_{prot} \cdot$

$\text{mL}_{\text{middle phase}}^{-1}$ ) and $C_{\text{bottom}}$ is concentration of protein in the bottom phase ( $\text{g}_{\text{prot}} \cdot \text{mL}_{\text{bottom phase}}^{-1}$ ).....	97
<b>Figure 5.11:</b> Volume fraction of the bottom (blue), middle (red), and top phase (yellow) of W-III-based protein extraction, displayed in <b>Figure 5.9</b> . Conditions listed in <b>Figure 5.9</b> .....	98
<b>Figure 5.12:</b> Forward extraction of cytochrome c by 1 wt.% of overall surfactant at 25°C using the conditions listed in <b>Figure 5.9</b> .....	98
<b>Figure 5.13:</b> Mass partition coefficient between middle and bottom phase of the proteins during W-III-based protein extraction for data displayed in <b>Figure 5.9</b> . Conditions listed in <b>Figure 5.9</b> .....	99
<b>Figure 5.14:</b> Equilibrium concentration of cytochrome-c, $\alpha$ -chymotrypsin, lysozyme and BSA in the middle phase versus original concentration in the aqueous phase. Volumes of 1.5 wt.% NaCl aqueous solution and isooctane are the same and overall surfactant is 1 wt. %. Percentage of each surfactant among the surfactants were 50 wt. % CK7, and 50 wt % AOT. Protein concentrations are mass per volume of the whole phase. Temperature 25°C. Standard errors were less than 2% in all the cases. ....	100
<b>Figure 5.15:</b> Equilibrium concentration of BSA in the middle and bottom phase versus original concentration in the water phase. Conditions listed in <b>Figure 5.14</b> . Errors were less than 2% in all the cases. ....	100
<b>Figure 5.16:</b> Effect of original protein concentration on the volume fraction of the middle phase for the experiments plotted in <b>Figure 5.14</b> .....	102
<b>Figure 6.1:</b> Absorbance of light at $\lambda=410\text{nm}$ versus time of the hydrolysis of GNPNA catalyzed by $\alpha$ -chymotrypsin under standard conditions, used to calculate the “standard” activity of $\alpha$ -chymotrypsin (“St” in Eq. 1). 50 $\mu\text{L}$ of 0.5 mg/ml $\alpha$ -chymotrypsin in 5 wt.% NaCl aqueous solution was mixed with 700 $\mu\text{L}$ of GNPNA substrate solution, as described in the Experimental section. (red dots): experimental data; (black line): straight-line fit to the data.....	115

**Figure 6.2:** Mass percentage of back extracted protein based in the original protein solution using a 5 wt.% NaCl aqueous stripping solution. The distribution of surfactant consists of 30% AOT, 70% CK7. Cytochrome-c, lysozyme, and  $\alpha$ -chymotrypsin were present at 1 mg/ml in the initial aqueous solution used for forward extraction. Other conditions are listed in the Experimental section..... 116

# CHAPTER 1

## INTRODUCTION

### *1.1 Objectives*

The goal of the reported research is to improve the performance of water-in-oil microemulsion-based extraction for the purification of proteins. The effort is focused to overcome the two major problems in the traditional method of protein purification by microemulsions, which utilized Winsor-II systems, an aqueous solution in equilibrium with a water-in-oil microemulsion solution: slow recovery of proteins encapsulated in the microemulsions and a small capacity for extraction of the microemulsion. In order to achieve this objective, a three-phase microemulsion system that consist of a bicontinuous middle phase in equilibrium with excess water and oil phases, called Winsor III system, is employed. Winsor-III systems were investigated in the 1970s for the secondary oil recovery but not for protein extraction. There was only one report of extraction of proteins by a Winsor-III microemulsion system; but, it was non successful [1]. Microemulsions in this work are stabilized by two pH-degradable alkyl ethoxylates (CK3 and CK7) and Aerosol-OT (AOT) as surfactants, where the former two are nonionic and the latter is anionic, and provides an electrostatic attractive driving force for protein extraction.

The overall goal will be achieved by completion of the following sub-goals:

1. Measure the equilibrium distribution between water and oil of CK7 molecules, in single and binary surfactant mixtures (with CK3, AOT and octyl glucoside,  $C_8\beta G_1$ ) that form 2- and 3-phase microemulsion systems, based on the size of their ethoxylate head group at different temperatures, ionic

strengths, concentrations, and proportions of each surfactant in the mixture. This information will lead to a better understanding of the interrelationship of the above listed parameters to enable objective to be achieved, which in turn will lead to a capability of selecting conditions and concentrations of medium components to allow for three-phase microemulsion to be formed.

2. Find three-phase microemulsion systems that contain isooctane, aqueous solution, CK7, AOT, CK3 and/or salt as major components that are suitable for the extraction of the proteins.
3. Demonstrate that microemulsion-based extraction can be used to isolate proteins (pepsin, cytochrome c,  $\alpha$ -chymotrypsin, lysozyme and bovine serum albumin) from aqueous solutions at high yield and selectivity into the middle, bicontinuous microemulsion, phase of 3-phase systems.
4. Recover proteins encapsulated in the middle, bicontinuous microemulsion phase at high yield and without loss of biological activity

This dissertation is divided in seven chapters. Chapter 2 is a background of the basic knowledge about surfactants, microemulsions formation and extraction of proteins, and bioseparations. Chapter 3 is chemical characterization of the surfactant synthesized in for this dissertation, CK7. It reports the distribution of degree of polymerization of the ethoxylate chain, the methodology employed for synthesis and purification for CK7, and the detection of ketone as impurity. Chapter 4 reports the partition equilibrium of the components of CK7 between water and oil in the range of temperature 20-50°C. CK7 is pure or mixed with a second surfactant (AOT, CK7, or  $C_8\beta G_1$ ). A semi-empirical model was developed to calculate the phase inversion temperature (PIT) from these data which is useful to determine the conditions required to form Winsor-III systems used for protein extraction (Chapter 4). Chapter 5 reports forward extraction of  $\alpha$ -chymotrypsin, cytochrome-c, lysozyme, BSA and pepsin. Three approaches were used to obtain Winsor-III systems suitable for forward extraction: an increase of temperature (40°C), the addition of a more hydrophobic surfactant (CK3, 25°C), and the use of 1.5% NaCl (aq) to



increase the ionic strength (25°C). Protein concentrations achieved in the middle, bicontinuous microemulsion, phase were 10 times higher than values reported in the literature for extraction by Winsor-II microemulsion systems. Chapter 6 reports backward extraction, or recovery, of  $\alpha$ -chymotrypsin, cytochrome-c, and lysozyme encapsulated in the middle phase. The aqueous stripping solutions used contained either a high ionic strength (5 wt. % NaCl) or a high pH (12.0). Back-extraction was fast and total recovery of the activity for  $\alpha$ -chymotrypsin was achieved. Other proteins have smaller percentage of mass recovery in the conditions tested but comparable with yields of water in oil microemulsion. Chapter 7 provides conclusions and recommendations.

## ***1.2 Significance***

Purification is more than 50% of the cost of protein production. So any improvement in the purification process can have a big impact. One reasons for high purification cost are that proteins are very susceptible to denaturation resulting from changes in the chemical or physical environment, which limits the approaches available. In addition, contaminating molecules often have chemical properties similar to proteins such as polarity and charge density. Therefore, the separation is very difficult. It is important to preserve the biological activity because it makes the protein product valuable. In addition, purified protein products are required to possess very high purity for many applications, such as for pharmaceuticals.

Examples of industries that use proteins are pharmaceutical; for example, protease is employed to remove proteins from contact lens. The food industry uses alpha-amylase for white bread production, rennin for cheese production, and papain for softening meat for cooking. The biofuel industry uses cellulases to hydrolyze cellulose into sugars and ligninase to treat the lignin waste. Many detergent products use lipases to remove fatty and oily stains, amylase to remove starch residues, and proteases for protein stains. Molecular biology uses restriction enzymes, DNA ligase, and polymerases to manipulate DNA.

Protein extraction by microemulsion is a method discovered in the 1980's that is very selective, preserves the activity of the proteins and can be scaled up easily because it is a liquid-liquid operation. Traditionally water-in-oil microemulsions are used for protein extraction. The driving force for the extraction between protein and amphiphilic molecules at the interface can be electrostatic, hydrophobic, or bioaffinity. Interactions between extracted protein and the interface have to decrease or become repulsive in order to recover the proteins from the organic microemulsion phase. These interactions can be modified by different methods such as changing the pH, salt concentration, and composition of surfactant mixture. Due to the advantages mentioned at the beginning of this chapter, protein extraction by microemulsions is promising for the early stages of a purification scheme. If protein extraction by microemulsion delivers a higher level of purity or concentration compared to chromatographic steps, it would reduce purification costs. However, it is mainly performed on a laboratory scale to date. Moreover, microemulsion based protein extraction has two major problems that must be overcome; the difficult recovery of proteins from the microemulsions and the small capacity for protein solubilization within the microemulsions.

The two disadvantages of microemulsion based protein extraction are overcome in this research by using a three-phase microemulsion system. In contrast with traditional methods used to recover proteins from microemulsion that are based on reducing the affinity between the protein and the surfactant, back extraction for three-phase systems can occur readily by invoking a phase change. The original hypothesis was that by using a pH-cleavable surfactant (CK7 or CK3) the proteins encapsulated in the microemulsion would be released after degradation of the surfactant by acidification. The change of phases in a Winsor III system due to the acidification is more rapid than the degradation of the surfactant and probably controls the release of encapsulated protein. Back-extraction requires only a few minutes to occur, for disengagement of the phases to take place, compared to traditional back-extraction approach that can take hours and often provides poor yields, particularly for proteins that possess significant hydrophobicity. In addition, the microemulsion (middle) phase of a three-phase system possesses

bicontinuous structure, which has equivalent amounts of water and oil. As a consequence, there is around 45 volume % of water to solubilize the protein instead of 5% of water for the droplet-based water-in-oil microemulsions, employed in the traditional approach, which should reduce the loss of activity during an enzyme's residence in the microemulsion phase.

The hydrophilicity of alkyl ethoxylate surfactant depends on the temperature and the distribution of surfactant molecules according to the size of their ethoxylate group, which controls the molecules' distribution between oil and water. Moreover, most ethoxylate surfactants have broad distribution of sizes for their ethoxylate polar or "head" group. So the first objective of the proposed research is to understand how the CK7 surfactant distributes between water and oil phases within 2- and 3-phase microemulsion systems as a function of ethoxylate head group size and environmental conditions, such as temperature and ionic strength. This information is useful for selecting the proper media composition and conditions in order to form a three phase system.

Stable three-phase microemulsion systems are formed for a small range of conditions in which the affinity of the surfactant's hydrophilic moiety is equivalent in strength to the hydrophobic moiety. The hydrophilicity is more easily tuned than hydrophobicity because the polarity of ethoxylate head groups is controlled by temperature. The hydrophilicity of an alkyl ethoxylate surfactant can also be tuned by changing the distribution of its ethoxylate chain length, for example, by mixing ethoxylate surfactants of different sizes and distributions of ethylene oxide units. The hydrophilicity of AOT can be tuned by changing the salt concentration, which controls the affinity of AOT's sulfonate head group and its  $\text{Na}^+$  counterion through Debye shielding. The hydrophilicity of the whole mixture can be tuned by changing the relative proportion of each surfactant.

For any 3-phase system candidate, it must be proved that proteins can be selectively extracted without significant loss of their biological activity. After completion of the forward extraction, the microemulsion system should be easily manipulated to release the encapsulated protein in a reasonable length of time and amount. The proteins

selected for this work interact with the surfactant monolayer so they are particularly difficult to recover by traditional approaches used for back extraction.

## CHAPTER 2 BACKGROUND

### *2.1 Introduction*

This chapter provides the basic concepts necessary to understand the subsequent chapters of this dissertation. First, surfactants, molecules that simultaneously have affinity for polar and non-polar solvents, or equivalently, are amphiphilic, are described. Next, categories of surfactant types are defined and described. Surfactants used in this dissertation can be classified as ionic or non-ionic. The ionic surfactant employed in this work, Aerosol-OT, imposes an electrostatic driving force for protein extraction but also can partially deactivate the proteins if not employed carefully. On the other hand, non-ionic surfactants reduce the strong electrostatic interaction between the ionic surfactant and the protein, reducing in this way the deactivation of the protein. Since the nonionic surfactants employed in this thesis are pH-degradable due to the presence of a 1,3-dioxolane linkage between their lipophilic and hydrophilic moieties, cleavable surfactants are also described, with emphasis placed on the 1,3-dioxolane surfactants. The synthesis and physical properties of the non-ionic surfactant employed in for this dissertation is studied in Chapter 3 and the properties of anionic / nonionic surfactant mixtures are studied in Chapter 4.

The surfactant mixtures referred to above form microemulsions when they are mixed with water and isooctane. Section 2.3.2 explains the Winsor classification of microemulsion systems and their dependence with variables such as temperature and salt concentration, particularly with regard to nonionic surfactants. In this dissertation three phase (Winsor-III) microemulsion systems, in which the surfactant molecules have nearly equivalent affinity to the oil and water phase, are used for protein extraction (Chapter 5). The selection of Winsor-III systems as media for extraction is because of their high

content of water and fast disengagement of the three phases. The exact point at which the affinity of the surfactant is equivalent to water and oil is called phase inversion temperature (PIT) and explained in **Figure 2.6**. In Chapter 4 a semi-empirical thermodynamic mathematical model is developed to calculate the PIT.

Finally, Section 2.4.3 is an overview of the state of the art for protein purification by microemulsions in order to understand the mechanisms, utility and limitations of this method, and to provide a basis of comparison for the data described in Chapter 5 and 6. In particular, Winsor-III systems can concentrate the proteins because their bicontinuous microemulsion phase can solubilize 10 times the concentration of proteins solubilized by reverse micelles in the traditional approach (Chapter 5). Also the recovery, or back extraction, of microemulsion-encapsulated proteins is faster than traditional methods (Chapter 6).

## **2.2 Surfactants**

“Surfactants are amphiphilic compounds which can reduce surface and interfacial tension by accumulating at the interface of immiscible fluids” [2]. Surfactants have two functions related to extraction of proteins by microemulsions. One is to stabilize the microemulsion by reducing the interfacial tension to a value lower than  $5 \times 10^{-2} \text{mN/m}$  [3]. The second function is having affinity for some of the proteins through their head group in order to provide a selective driving force for extraction [4].

In this work a pH cleavable ethoxylate non-ionic surfactant O-[(2-tridecyl, 2-ethyl-1,3-dioxolan-4-yl)methoxy]-O'-methoxy poly(ethylene glycol)<sub>5,45</sub> surfactant (CK7, the name chosen for degree of polymerization of the poly (ethylene glycol) source used for its synthesis, 7.2), is used [5]. The pH-degradable property was selected to impart a means of recovery of the microemulsions-encapsulated protein. The non-ionic characteristic of the surfactant will reduce activity loss for microemulsion-encapsulated

proteins. An ionic surfactant will be added to the nonionic surfactant, Aerosol-OT (AOT), which has a negative charge to extract positive-charged proteins [6-8].

### 2.2.1 Overview of Surfactant Types

Surfactants have two groups of atoms with completely different chemical properties. One group is polar and the other is non-polar. The polar hydrophilic group, also called “head group” of the surfactant, has affinity for polar molecules such as water. There are two main classes of surfactants, ionics and non-ionics. These classes are based on the chemistry of the head group. Ionic surfactants’ head groups dissociate in to two ions: one covalently attached to the surfactant molecule and the other as a free counterion. Non-ionic surfactants have a polarization of electrostatic charges and dissolve in water by forming hydrogen bonds. The non-polar hydrophobic group, also called the tail of the surfactant, is normally a hydrocarbon chain and has an affinity to non-polar molecules. The tail interacts with other non polar molecules (such as hydrocarbons) by Van der Waal forces. The interaction between non-polar tail and a polar solvent such as water is energetically unfavorable because hydrogen bonds have to be broken and replaced by Van der Waal forces that are weaker. A molecule with affinity for both polar and non-polar solvents is amphiphilic. **Figure 2.1** depicts a surfactant molecule in the interface of oil/water, where surfactants solubilize preferentially. The head dissolves in water and the tail in oil.

Non-ionic surfactants have a head group that does not dissociate when they dissolve in water. So the surfactants have zero overall electrostatic charge when dissolved in water. Actually, there is a polarization in their head group that makes them soluble in the water, but the surfactant does not change the overall electrostatic charge. The electrostatic effect is not as strong as it is for ionic surfactants. As a result, non-ionic surfactants bind electrostatically less strongly to proteins, often leading to less

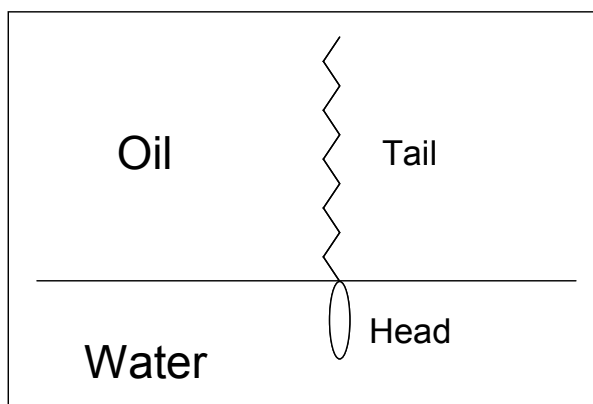


**Figure 2.1:** Picture of a surfactant in the interface oil/water.

denaturation. Also the effect of an electrolyte on the surface activity is smaller on non-ionic surfactants than it is on ionic surfactants.

Ionic surfactants have a cationic, anionic, or zwitterionic head group with a strongly bound counterion; upon solubilization in water, the ionic pair partially dissociate. Charged head groups produce electrostatic repulsion between neighboring molecules when the surfactants self-assemble with other surfactant molecules at the interface. Another effect is that the head charge attracts oppositely charged ions. These electrostatic effects are reduced by the presence of salt in the solution because the counterions reduce the distance of electrostatic interaction of the ionic surfactant, a phenomenon referred to as Debye shielding. Examples of cationic, anionic and zwitterionic surfactants are hexadecyltrimethylammonium bromide, sodium bis (2-ethylhexyl) sulfosuccinate (AOT) and phosphatidylcholine, respectively.

In a system composed of oil, water and surfactant, the surfactant is localized mostly in the liquid-liquid interface. If the concentration of the surfactant is higher than the critical micelle concentration (CMC), the surfactant at the interface will align one next to the other in a monolayer structure called a palisade (**Figure 2.2**) [9].



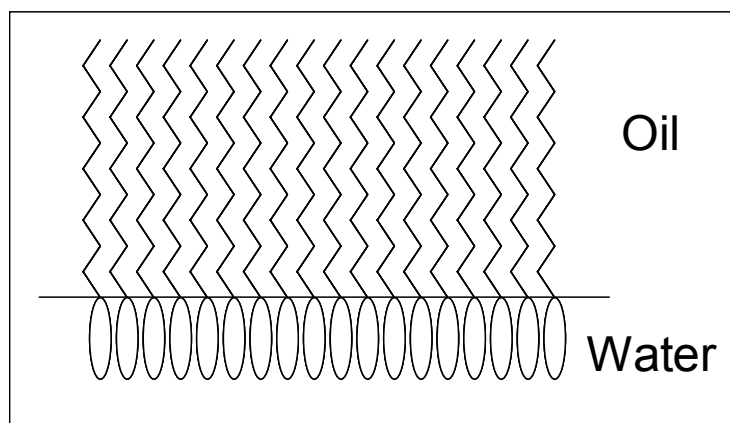


**Figure 2.2:** Palisade structure of surfactant self assembly.

## 2.2.2 Alkyl Ethoxylate Surfactant

Ethoxylated surfactants are a class of non-ionic surfactants that have a chain of polyethylene glycol (PEG) as their hydrophilic moiety. Commercial PEG surfactant preparations do not have the same PEG chain length on every molecule. The distribution of ethylene glycol monomeric units often follows a Poisson function, which predicts the probability of a certain number of random events occurring within an interval when the number of events is countable, or discrete (**Equation 2.1**).

$$f(n, \lambda) = \frac{\lambda^n \cdot e^{-\lambda}}{n!} \quad \mathbf{2.1}$$

Equation 2.1 predicts the mole fraction of a population of ethoxylate groups with chain length  $n$ , being formed, and the population's average ethoxylate size, or EON value, equals  $\lambda$ .

The cost of producing ethoxylated surfactants with a monodisperse size distribution would be prohibitively high. The disadvantage of using polydisperse

surfactant mixtures is the complexity in predicting their behavior. The reason for this difficulty is that the partitioning of each molecule between water and oil is a function of the number of ethylene glycol units in the hydrophilic chain [10]. The hydrophilicity is proportional to the mass fraction of the ethoxylate chain within the surfactant. Therefore, the longer the ethoxylate chain, the higher the concentration of surfactant is in water. The hydrophobicity of ethoxylate surfactants also increases with temperature. The ethoxylate chain undergoes more thermal motion as temperature increases, resulting in a lower number of water molecules of hydration and thus to an increased hydrophobicity.

Examples of commercial surfactants that contain ethoxylated chains are Neodol ( $C_nH_{2n+1}(OC_2H_4)_mOH$ ) from Shell Chemical Company, Igepal ( $C_nH_{2n+1}C_6H_4(OC_2H_4)_mOH$ ) from Rhone-Poulenc Inc., and Brij ( $C_nH_{2n+1}(OC_2H_4)_mOH$ ), and Tween ( $(C_nH_{2n}O_2)_iC_5H_9(OC_2H_4)_mOH$ ) from ICI Specialty Chemicals [11].

### 2.2.3 Cleavable surfactant

Cleavable surfactants typically have a weak covalent bond linking the hydrophilic head and hydrophobic tail of the molecule [12]. The surface activity of cleavable surfactants can be reduced by breaking the weak bond, and in that way is severing the tail from the head. If the surface activity of the surfactant is reduced, the surface tension increases. Increasing the surface or interfacial tension of the liquids after using a surfactant can be necessary in the next operation of the process [12, 13]. For example, this change is needed to avoid foaming formation or stable emulsification [12]. Demulsification is one means of recovering a biomolecule encapsulated in a microemulsion, relevant to this dissertation [5]. Also it may be important to reduce surface activity of surfactant monolayers present in microemulsion-based drug delivery vehicles to allow for release of microemulsion-encapsulated drugs. The other important consequence of using a cleavable surfactant is that it degrades faster than a similar

surfactant with a strong link between the head and the tail [14]. This last property makes the surfactant environmental friendly. A pH degradable surfactant, a special type of cleavable surfactants, is used in this work. Other types of cleavable surfactants include ultraviolet- (UV-) [15, 16], electrochemically- [17], and thermally-degradable [18].

The most broadly used acid labile surfactants are alkyl glucosides, introduced in 1992, as Henkel Corporation began to produce large quantities, 23000 tons/year, in US [19]. “The alkyl glucoside surfactants break down into glucose and long-chain alcohol under acidic conditions. On the alkaline side, even at very high pH, they are stable to hydrolysis.” [12] Alkyl glucosides are advantageous in that the raw materials are natural and inexpensive. The hydrophilic part is a sugar and is therefore easily biodegradable; the hydrophobic part is often a fatty acid derivative that is also found in nature [19]. A second type of surfactant, to which more academic studies has been devoted, are surfactants that contain a cleavable linkage (**Section 2.2.4**). The cyclic ketal ring can have five atoms such as 1,3 dioxolane [20, 21] or six atoms such as 1,3 dioxane [22, 23]. The cleavage of these surfactant occurs a reasonable reaction rate normally at pH lower than 5, but it changes depending on the structure of the surfactant or the presence of a catalyser or inhibitors [21]. Another type of surfactant that is interesting due to its high degradation rate is the non-cyclic acetal. This degrades several times faster than cyclic acetals [24]. Lastly, ortho esters [25, 26] can be used as an acid labile surfactant; they degrade by the same mechanisms as acetals and ketals [27].

Epstein *et al.* synthesized sodium 4-(3,3-dimethyl-1-oxotridecyl) benzenesulfonate, which is a UV (300 nm) degradable surfactant similar to sodium dodecyl sulfate. The group that is cleaved is an alkyl phenyl ketone [15]. Eastoe *et al.* used a surfactant with an azo group that was cleaved by UV, the first time that a UV cleavable surfactant was used to deconstruct a microemulsion [16]. There are also reversible photoresponsive surfactants. The most common photoresponsive group is azobenzene, which is in the tail of the surfactant. It has *trans* configuration under visible light and *cis* configuration under UV light. The *trans* configuration is more hydrophobic than *cis* configuration. So the interfacial tension change reversible with the light. These

surfactants, photocleavable surfactant and photoresponsive surfactant, are interesting in laboratory scale because the surfactant is stable at wavelength of the room light but it can be degraded by using UV in samples that do not have cell debris. In industrial scale, that is possible if the microemulsion is clear; but if it contains solids such as cell debris or other residues, the UV rays would not penetrate in the bulk of the microemulsion and would take a significant amount of time to degrade the whole mass of surfactant.

Gallardo *et al.* tested a surfactant that undergoes a surface activity change by changing the electrostatic potential [28]. Actually the phenomenon is a chemical restructuring of the molecule, not a cleavage of the surfactant. The surfactant has a ferrocenyl group at the terminus of the hydrocarbon chain and an amino in the other extreme. The ferrocenyl group can be oxidized from neutral to a positive charge. The positive charged ferrocenyl is soluble in water but the neutral state is not. The change in surface tension upon oxidation is 23 mN/m [28]. The advantage is that the change in surface tension is reversible by changing the electrostatic potential. The surfactant used by Gallardo *et al.* reduces the surface tension of water to a value insufficient to produce a microemulsion. The lowest surface tension achieved in water-air interface was 49 mN/m [28]; to produce a microemulsion, the surface tension has to be lower than  $5 \cdot 10^{-2}$  mN/m [3].

Thermolabile surfactants can be cleaved by an increase of temperature. They are interesting because they may not require an additive to the system. The problem is that the surfactants recently developed need a high temperature to degrade, the range of which is too high to maintain stable proteins. For example Hayashi *et al.* use a tertiary amine surfactant with an ether bond in between the second and third carbon from the nitrogen. This surfactant degrades at 150°C [18]. McElhanon *et al.* use Diels-Alder adducts to link the hydrophilic (phenol or carboxylic acid) and hydrophobic groups (dodecyl). This surfactant degrades at 50°C [29]. A surfactant with the cleavable group used by McElhanon *et al.* that can form a microemulsion could be used to extract proteins from thermopiles bacteria.

#### 2.2.4 O-[(2-tridecyl, 2-ethyl-1,3-dioxolan-4-yl)methoxy]-O'-methoxy poly(ethylene glycol)<sub>5.45</sub> (CK7)

CK7 and CK3 are used in this work because they are non-ionic. This property is important in order to preserve the activity of the proteins when they are solubilized into microemulsions. Also CK7 and CK3 are degradable at low pH. The rate of degradation under low pH was lower than that of protein release during back-extraction from Winsor-III microemulsion system when utilizing high ionic strength stripping solutions (Chapter 6); thus, the hydrolysis of CK7 and CK3 was not thoroughly investigated in this dissertation, but was nonetheless important for discovering the change of phases that release the protein from the microemulsion. Although the 1,3 dioxolane ring is not used as a target for hydrolysis it is important because it makes the surfactant biodegradable [14].

**Figure 2.3** depicts the chemical structure of the ethoxylate surfactant used in this work, which contains poly(ethylene glycol) monomethyl ether (MPEG) as the hydrophile and a long chain ketone as the hydrophobe. These parts were linked together by a cyclic ketal, or 1,3 dioxolane ring [5]. There were two cyclic ketal surfactant products employed in this research project. One had an average ethoxylated group size of 5.5 units of ethylene glycol (CK7; the name was chosen because the MPEG employed for the surfactant synthesis had 7.2 units of ethylene glycol on average) and the other has 3 units of ethylene glycol (CK3). CK3 differs from CK7 in the fact that CK3 had a more monodisperse distribution of ethoxylate molecular weight and, of relevance to this work, is more hydrophobic than CK7. The 1,3 dioxolane group makes the surfactant more hydrophobic. The ring is equivalent to 2 -CH<sub>2</sub>- groups when the surfactant is in a micelle state [30, 31].

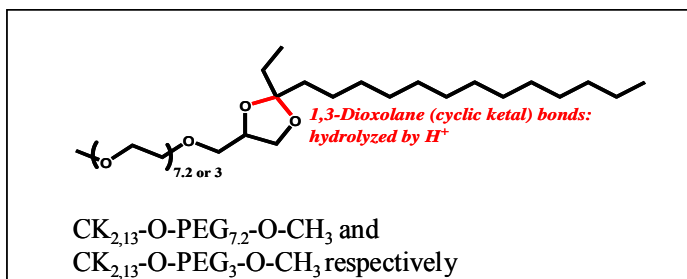


**Figure 2.3:** Structure of CK<sub>2,13</sub>-O-MPEG<sub>c</sub>-O-CH<sub>3</sub> surfactant where “c” can be 7.2 or 3.

Iyer-Raikar *et al.* used CK7 (0.15M) to solubilize lysozyme and chymotrypsin in water-in-oil microemulsions. Back extraction was done by employing a pH 5 phosphate buffer, which partially hydrolyzed the surfactant. After one hour 90 % of the protein was recovered with a loss of only  $9.6 \pm 4.0\%$  of the specific activity. The surfactant was 100% degraded in 3 hours [5]. A microemulsion solution of CK7 (1.2M) in isooctane with encapsulated lysozyme were also put in contact with pH 5 buffer to facilitate back extraction. Back extraction was achieved at 70% level after one hour. The activities of the proteins were around 90% of the original. The same result was also obtained by using a buffer pH 7 which degrades the surfactant at a significant lower rate than pH 5. This observation suggests that there are not strong attractive forces between CK7 palisade and proteins [32]. Alkhatib *et al.* studied mixtures of CK7 with sodium bis (2-ethylhexyl) sulfosuccinate (AOT) and *n*-octyl- $\beta$ -D-glucopyranoside (C<sub>8</sub> $\beta$ G<sub>1</sub>). A low concentration of surfactant mixtures, 1:1 w/w of AOT and CK7, in a system with 0-1 wt. % NaCl, and isooctane produce temperature-insensitive phase regions in the phase diagram, which makes them potential candidates for drug delivery vehicles. The mixture C<sub>8</sub> $\beta$ G<sub>1</sub> and CK7 shows similar insensitivity in a system with 1 wt. % NaCl but not in pure water [33].

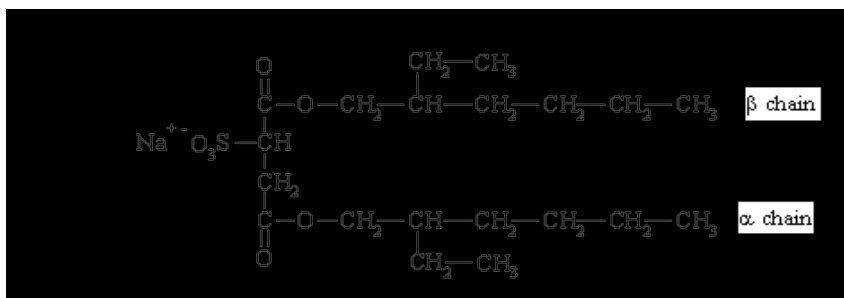


**Figure 2.4:** Sodium bis (2-ethylhexyl) sulfosuccinate (AOT) [33].

### 2.2.5 Sodium Bis (2-ethylhexyl) Sulfosuccinate (AOT)

AOT (**Figure 2.4**) is a surfactant commonly used in microemulsions because it can form the microemulsion without the need of a cosurfactant [34]. AOT does not need a cosurfactant to form water in oil microemulsion due to two reasons: the first being that its two chains give it a cone-like shape which in turn provides a very big curvature to the water, and the second reason being that the hydrophobic chains are branched, which does not allow them to form bilayer sheet-like structures [35]. The parallel arrangement makes the surfactant monolayer too rigid to form a microemulsion [35]. AOT has negative charge when it is dissolved in water, which is the reason that it is used in this work. The negative charge provides an electrostatic attraction driving force to extract positively charged proteins [8, 36].

## 2.3 Microemulsions

A microemulsion is a thermodynamically stable dispersion of a polar liquid in a non-polar liquid (water-in-oil), or vice versa (oil-in-water), stabilized by amphiphilic compounds. Amphiphilic refers to a compound that has affinity for polar and for non-

polar solvents. Microemulsions have many applications but the most important application for this work is that they can extract selectively proteins from a water solution and conserve their activity.

### **2.3.1 Description and applications**

Microemulsions are macroscopically homogeneous and optically clear because the dimensions of the structures formed by the three main components in their bulk are smaller than the wavelength of visible light. Microemulsions self assembly structures possess sizes in the range of 5-100 nm . Even though the name “microemulsion”, coined by Schulman *et al.* in 1956 [37, 38], comes from the size of the dispersion, it does not mean that all small emulsions can be called microemulsion. Nano-emulsions are in the range of 20-200 nm and they are also transparent [39]. The difference between nanoemulsions and microemulsions is that the former are thermodynamically unstable so they need external energy to disperse. Macroemulsions are larger than 200 nm, opaque, and thermodynamically unstable [38]. Nanoemulsion and macroemulsion need energy to disperse and the two components separate after some time. In contrast, microemulsions are thermodynamically stable so they disperse spontaneously and are stable through time. The polar phase is normally water; but, glycerol, ethylene glycol and ionic liquids have been employed. The non-polar liquid normally is a hydrocarbon but there are other non-polar liquids that have been employed such as supercritical CO<sub>2</sub>.

The word amphiphilic of the definition of microemulsion is used to not limit the definition to surfactants. Amphiphilic refers also to other components that may have surface activity such as block copolymers, cosurfactant, or nanoparticles [40]. Many surfactants cannot induce a microemulsion by themselves, but need a cosurfactant. Cosurfactants are molecules with short hydrophobic chain and weak hydrophilic group. Cosurfactants are too weak to function as surfactants because they partition between the bulk phases and the interface. However, in the presence of an interface, a sizable



proportion of cosurfactant molecules localize in the interface within the surfactant palisade. As a result, the short alkyl chain of the cosurfactant alters the structure of the palisade making it more flexible; therefore, the surface tension decreases. The low surface tension and flexibility of the interface increases the curvature and allow the system to become thermodynamically stable, forming a microemulsion. The same effect is achieved by surfactants that have two alkyl chains as hydrophobic group [41]. Cosurfactants historically were used to make possible the existence of a microemulsion phase. But they can be used to improve selectivity too. For example, relating to microemulsion-based protein extraction, by choosing a cosurfactant with affinity to a certain protein the extraction becomes selectively extracted with more efficiency.

Paul *et al.* reviewed the most common uses of microemulsions [42]. Applications related to protein extraction will be described in a later section of the dissertation. The most common application of microemulsion is enhanced oil recovery, which is achieved by forming a bicontinuous microemulsion between petroleum trapped within porous rock and brine present in the reservoir. The crude oil is trapped in the pores because the high interfacial tension between crude oil and brine so it is impossible to recover only by pumping. The surfactant reduces the interfacial tension from 20–25 mN/m to  $10^{-3}$  mN/m allowing for the recovery of approximately 20% of the trapped crude oil [42]. An application in the fuel formulation is improving gasoline or diesel performance by adding water or water soluble additives in microemulsions. The water reduces the temperature of the gases so the engine works more efficiently. The additives are for increasing the octane number in gasoline or cetane number in diesel [42]. Lubricants with water-in-oil microemulsions can prevent corrosion by keeping the corrosive agent encapsulated in the microemulsion droplet and covering the metal surface with a surfactant layer [42]. Microemulsions are also used for smoothing textile fibers to protect them from abrasion [42]. Microemulsions are good for cleaning because they can dissolve water and oil. They are used to clean contaminated soils [42]. Microemulsions are useful in cosmetics because the active principle can better penetrate the skin than using macroemulsions [42]. Pesticides and herbicides are easier to handle and sometimes more effective if they are in

oil-water microemulsion than dissolved directly in an organic solvent [42]. In food technology there is potential value for the microemulsions in encapsulating flavors, preservatives and vitamins, but the technology still is not very well developed [42]. There are limitations in the choice of the surfactant because they must be of food grade and often must solubilize in triglyceride [38]. In medicine microemulsions can be used for drug delivery of hydrophobic molecules, or of medicines that degrade fast but they are absorbed slowly. Rate of releasing of the medicine can be controlled by microemulsions [43, 44]. Chemical and enzyme-catalyzed reactions involving combinations of hydrophilic and hydrophobic reactants can be accelerated in microemulsions [45]. Nanoparticles with a narrow size distribution can be synthesized in microemulsions [42, 45].

### 2.3.2 Winsor Microemulsion systems

Winsor *et al.* classified systems composed of a lipophilic species (alkane oil), a hydrophilic species (water plus salt), and an amphiphilic species (surfactant) to four categories depending on the number and chemical nature of the excess phase(s) in equilibrium with the microemulsion phase [46]. **Figure 2.5** is a cartoon showing the Winsor system classification. Winsor I (W-I) is a two phase system with oil dispersed in continuous water phase in equilibrium with a phase enriched in oil. Winsor II (W-II) is also a two phase system with water dispersed in a continuous oil phase in equilibrium with an excess water phase. Winsor III (W-III) is a three phase system with a microemulsion phase residing between oil and water in equilibrium with excess water and excess oil, with the microemulsion phase possessing nearly equivalent amounts of water and oil. Winsor III microemulsion systems exist when the affinity of the surfactant for the water is equivalent to the affinity to the oil, producing an interface that has the minimum interfacial tension. Winsor IV (W-IV) systems have only one phase. The microemulsion phase can be either water droplets in oil (w/o  $\mu$ E) or oil droplets in water

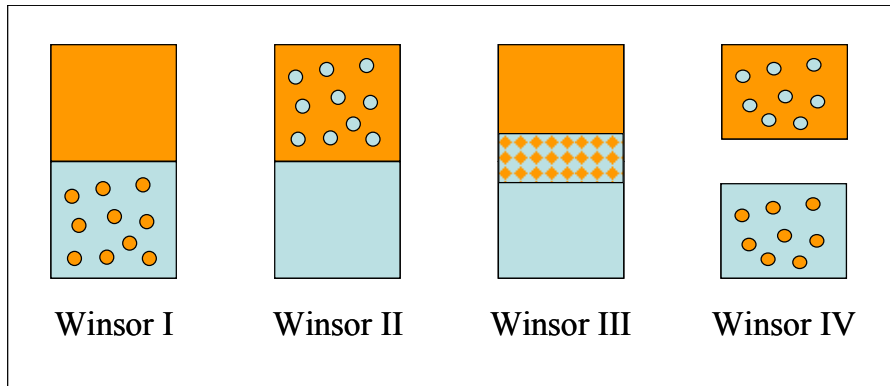


**Figure 2.5:** Picture of the four systems classified by Winsor *et al.* In the picture orange color is oil and sky blue color is water.

(o/w  $\mu$ E) or a bicontinuous phase such as the middle phase in Winsor III system. The bicontinuous phase is transparent and not viscous. Microscopic structure of the bicontinuous phase is similar to that of a sponge; both oil and water interpenetrate each other forming a disordered continuous phase. The interface between oil and water has a monolayer of surfactant (not shown in **Figure 2.5**) [47]. And also the surfactant is dissolved as a monomer in water and oil phases.

**Figure 2.6** is a sketch of the “fish” phase diagram for monodisperse ethoxylate surfactants [48], which consists of temperature versus surfactant concentration for a constant water/oil weight ratio of 1/1 g/g and a monodisperse surfactant. In the diagram is indicated the regions of 1 (W-IV), 2 (W-I and W-II) or 3 phases (W-III). Its name is due to the shape of three and one phase regions, which together resemble a fish with the “head” occurring at the lower concentrations of surfactant (W-III region) and the tail at the higher concentrations (W-IV region). The change of the microemulsion’s residence from aqueous phase to middle phase and finally to oil phase when the temperature is increased is due to the increase in hydrophobicity of the ethoxylate chain with the temperature (Section 2.2.2). The phase inversion temperature (PIT) corresponds to the horizontal line of symmetry for the fish’s body (blue line in **Figure 2.6**). At the PIT the hydrophobicity and the hydrophilicity of the surfactant mixture is balanced. The position of the “nose” is the lowest concentration at which microemulsion can be formed. It is

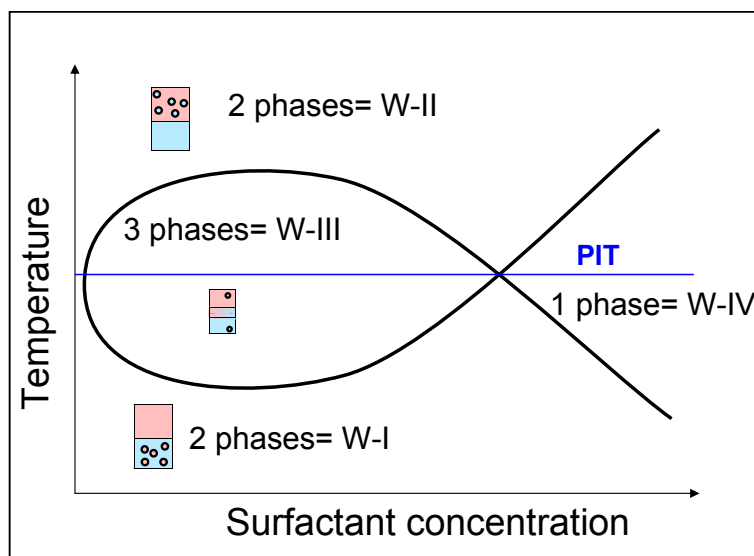


**Figure 2.6:** Conceptual model of the “fish” diagram. It represents the number of phases classified by Winsor nomenclature of an ethoxylate surfactant as a function of the temperature and surfactant concentration, with the ratio of water to oil held constant (typically at a 1:1 weight or volume ratio). Blue line: phase inverse temperature (PIT).

called critical micelle concentration (CMC). At concentrations below the CMC the surfactant is dissolved as a monomer. The body of the “fish” corresponds to Winsor-III phase region; the width (or  $\Delta T$ ) of middle phase is very small in systems near the nose of the fish and increases with the concentration of the surfactant until the “neck” is reached, where there is no excess water or excess oil remaining. At this point there is only one phase, designated by the tail of the “fish”, as indicated in **Figure 2.6**.

Ionic surfactants can also produce a fish diagram as shown in **Figure 2.6** when temperature is replaced by salt concentration. Analogous to the increase of an alkyl ethoxylate’s hydrophobicity by an increase of temperature, ionic strength reduces an ionic surfactant’s hydrophilicity through Debye shielding of its charged head group. This property is used in Section 5.3.1.3 to form Winsor-III systems used for protein extraction.

Ghoulam *et al.* studied mixtures of highly purified ethoxylate surfactants and reached the conclusion that mixtures of surfactants more soluble in oil than water have an increase in the PIT at lower concentrations of surfactant [49]. This is because at the PIT each surfactant species has a constant concentration in excess oil and excess water equal to CMC. Therefore at low concentrations of surfactant the proportion of surfactant that

dissolves in oil is larger than at high concentrations of surfactant. At high surfactant concentration most of the molecules reside at the water/oil interface and the composition of the interfacial surfactant layer is almost the same as pure surfactant. In contrast, at low concentration of surfactant the interface is enriched with the more hydrophilic components of the surfactant mixture. As a consequence the PIT is higher. **Figure 2.7** shows an example of mixtures of polyoxyethylene glycol n-dodecyl ethers ( $C_{12}E_n$ ) where  $C_{12}$  is the number of carbon atoms in the alkyl chain (12) and  $E_n$  is size, or degree of polymerization, of the ethoxylate group.

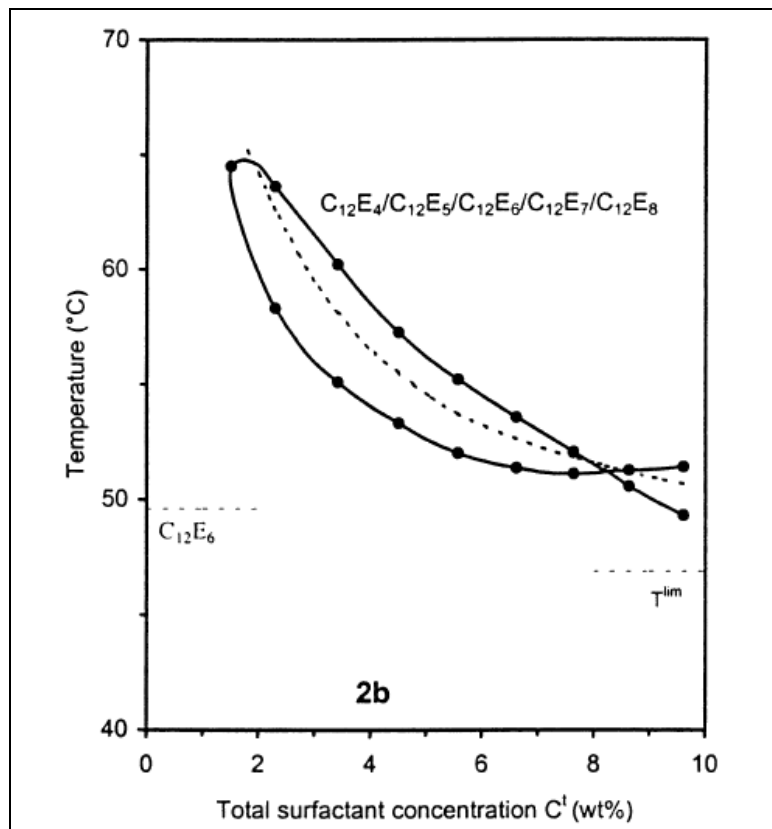


**Figure 2.7:** Increase in PIT at low concentration of a surfactant mixture which components are more soluble in oil than water observed by Ghoulam *et al.* Solid line is limit between phases. Dots line is the PIT in function of the surfactant concentration. The legend indicates the components present in the sample in the form ( $C_{12}E_n$ ) [49].

## 2.4 Microemulsion based liquid-liquid extraction-based protein purification

### 2.4.1 Description

Proteins can be extracted from the water rich phase selectively by the use of microemulsions. The driving force for protein extraction can be electrostatic, hydrophobic or biospecific based [4]. Electrostatic driving force can be used to achieve selectivity by using anionic (for example, AOT) [50] or cationic (for example, trioctylmethylammonium chloride, or TOMAC) [51] surfactants and tuning the pH in order to have the opposite-charged protein attracted to the surfactant's charge.

**Figure 2.8** shows forward extraction of proteins in a W-II system, in which the top phase consists of water in oil microemulsion (w/o- $\mu$ E), also referred to as reversed micelles. In the figure, reversed micelles with a negative-charged surfactant in the

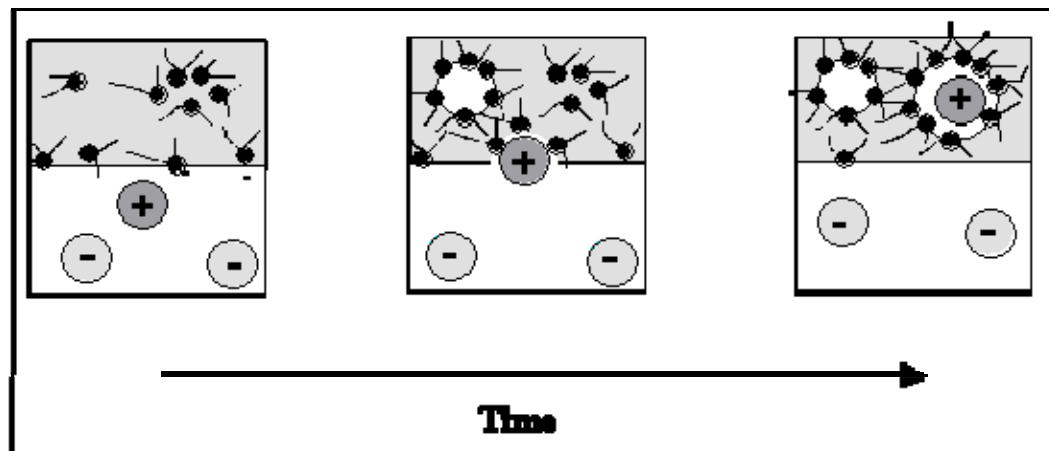


**Figure 2.8:** A diagram illustrating the *forward extraction* process in microemulsion based protein separation. The driving force in this system shown above is the electrostatic interactions between the negatively-charged surfactant head-groups and the positively-charged protein. Iyer-Raikar 2002 .

interface extract the positive-charged protein molecule but not the negatively-charged protein molecule via an electrostatic driving force.

Back extraction of a protein from the oil rich phase to the aqueous phase is much slower and less efficient than forward extraction. There are two traditional methods employed to recover encapsulated proteins [52]; but, both are around three orders of magnitude slower than forward extraction [53].

**Figure 2.9** illustrates these two traditional methods, which are increasing the ionic strength in order to reduce the electrostatic attraction or change the pH of the water solution to change the sign of the protein charge [8]. Improving back extraction is an active research field. There are many new methods to recover or extract the solute from the reverse micelles such as using a surfactant with an opposite charge of the surfactant occurring micelles to precipitate away all surfactant [52], using a degradable surfactant [52], adding cosurfactant [54] or reducing the water content of micelles by adsorption [55].

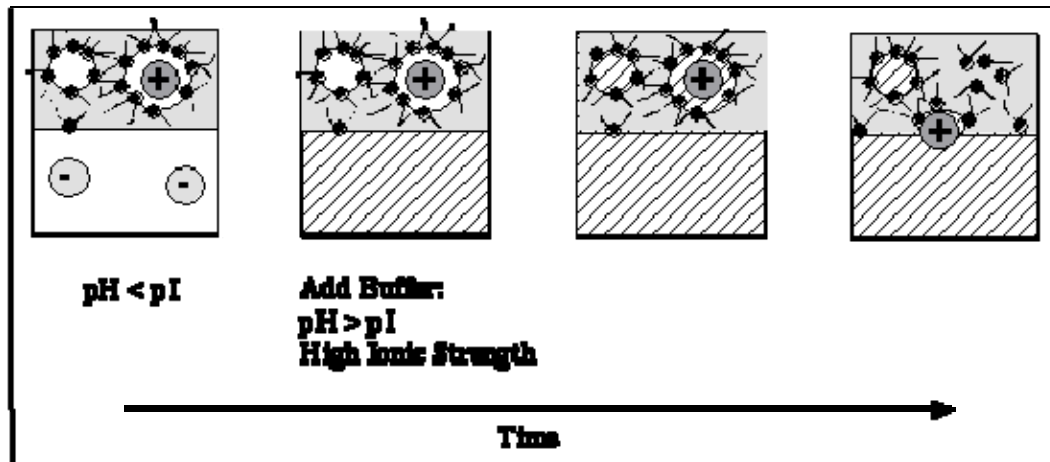


**Figure 2.9:** A diagram illustrating the *back extraction* process in microemulsion based protein separation. Iyer-Raikar 2002 .

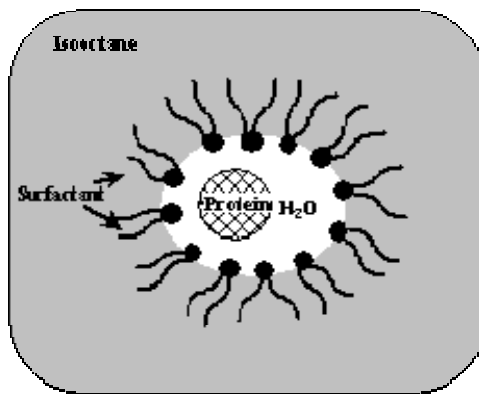


**Figure 2.10:** Diagram representing a water-in-oil microemulsion.

Reverse micelle extraction can conserve a high percentage of the protein biological activity. Different grades of protein inactivation depend on the surfactant used for extraction and the protein extracted. Activity is often conserved for proteins extracted into reverse micelles because proteins dissolve in the water pool, which is a hydrophilic environment even though the droplet is in a non-polar solvent. **Figure 2.10** is a diagram representing water-in-oil microemulsion with a protein molecule dissolved in the droplet.

Ionic surfactants interact with charged proteins more strongly than non-ionic surfactants [56]. As a consequence, ionic surfactants have stronger affinity for opposite charged proteins than non-ionic surfactants but non-ionic surfactants denature the proteins less than ionic surfactant [56]. The best situation is a mixture of ionic and non-ionic surfactant in order to have a strong driving force for the extraction but preserve the activity of the proteins as much as possible. Shioi *et al.* found that the optimal percentage of ionic surfactant, AOT in their work, is 30% and non-ionic surfactant, poly(ethylene glycol) dodecyl ether (C<sub>12</sub>E<sub>4</sub>), is 70% (**Figure 2.11**) [4].



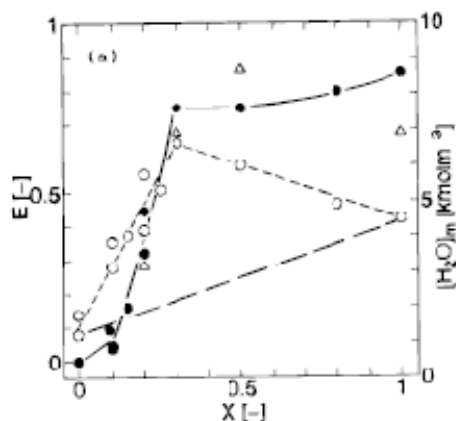


**Figure 2.11:** Dependence of the fraction of  $\alpha$ -chymotrypsinogen A (E) the concentration of water extracted from the aqueous phase on X, the fraction of AOT based on the whole surfactant.  $\Delta$ , E about 20 min after the contact;  $\bullet$ , E about 2 days after the contact;  $\circ$ ,  $[H_2O]_m$  [4]

Protein purification by reverse micelles has three advantages and two disadvantages. The first advantage is the selectivity of the extraction based on the nature of the extraction driving force. The second advantage is that the protein retains a large percentage of its activity if the surfactants and conditions are chosen correctly, such as using a non-ionic surfactant and near-neutral pH. The third advantage is that reverse micelle-based extraction is a liquid-liquid separation, so it is easy to scale up. The first disadvantage is that back extraction is slow and difficult. Second, the amount of protein that can be solubilized in reverse micelles is very small. The two disadvantages can be avoided by extracting the protein in a bicontinuous phase of a Winsor III system as it was used in this work.. The amount of water available for protein dissolution in the bicontinuous phase is around 50% so it can hold more protein than reverse micelles, which only have 5% water. The second disadvantage is also overcome by using bicontinuous phase because this phase can exist only when the hydrophobicity and hydrophilicity of the system are uniquely balanced. The balance can be easily disrupted, helping promote the recovery of the encapsulated proteins.

There are very few examples of extraction by a bicontinuous phase. To the best of the author's knowledge there is a single report for the extraction of metals [47], and

another of extraction of proteins by non-ionic surfactant [1]. Bicontinuous phase was used to extract ions from water. The ions are adsorbed at the interface. Due to the high interfacial area the amount of ion adsorbed is also high. The extraction does not involve the contact of microemulsion directly with the water solution; they intercalate a semipermeable membrane between the two phases in order to prevent transport of the surfactant and oil into the aqueous phase [47].

Vasudevan *et al.* performed protein extraction by W-III microemulsion by using non-ionic surfactants [1]. The extraction was successful only with surfactants that have a sorbitan group such as Tweens and Spans with cytochrome c dissolved in deionized water. They defined successful extraction when the partition coefficient for protein is higher than 10. Extraction of proteins by non-ionic surfactants used by Vasudevan *et al.* is not suitable for purification of proteins in most of the cases because they need an ionic strength smaller than 0.001 M to enable extraction. Normally the ionic strength in production systems is higher than .001 M [1]. One of the reasons that they used W-III system is that the disengagement between the phases is fast and the size of the water phase is larger than in reverse micelles. These two properties of W-III system are useful also when a mixture of ionic and non-ionic surfactants it is used. The phases separate faster than some W-II systems and can hold larger proteins than W-II systems. **Figure 2.12** is a scheme of the effects of the variables in the phases of a system composed of oil, water and a non-ionic surfactant. These concepts will be used for finding a W-III system. Ionic strength and surfactant HLB are the variables tuned in this work to obtain W-III system because temperature is best kept low (25°C) in order to not degrade the proteins.

**Figure 2.13** is a diagram of protein extraction by Winsor-III microemulsion. This example is for proteins extracted by electrostatic interactions. The protein is extracted under conditions that the surfactant has different charge than the protein, for example pH lower than pI (protein positive charged) and an anionic surfactant is employed. After gently mixing the proteins that have the opposite charge to the surfactant, positive in this example, are extracted in the bicontinuous middle phase and the proteins with the same charge of the surfactant are left in the water phase. Then the aqueous phase is

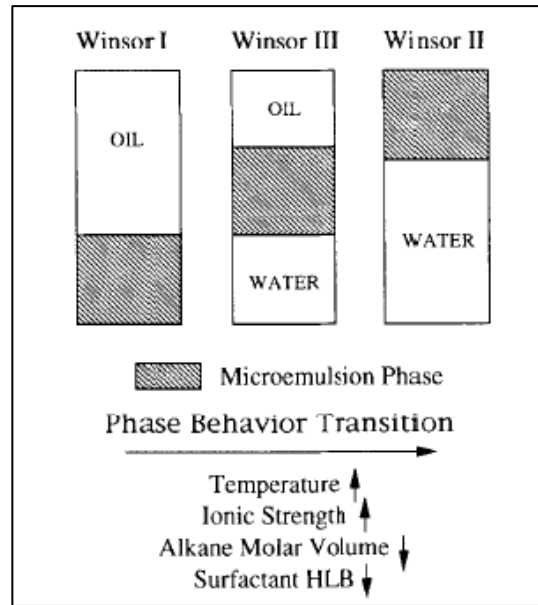


**Figure 2.12:** Diagram of effects of the variables (legend in the diagram) in the phases of a system composed of oil, water and a non-ionic surfactant [1].

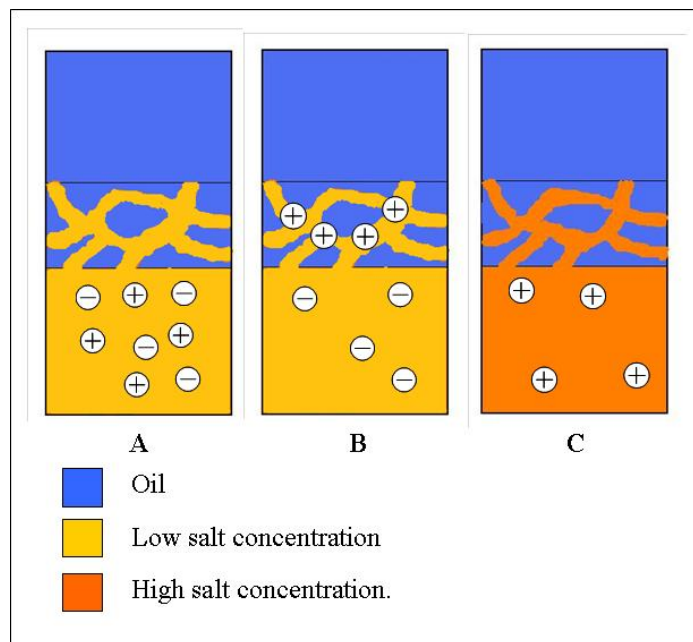


**Figure 2.13:** Diagram of protein purification by Winsor-III microemulsion system. The sequence from the left to the right is: A) Mixing oil with surfactants and water phase with proteins and low concentration of salt. B) Proteins with charge opposite to surfactant are extracted in bicontinuous phase. C) Bottom solution is replaced by a stripping solution with a concentration of salt high enough to produce Debye shielding and the proteins are released.

replaced by a solution of high concentration of salt and the positive proteins are released due to the Debye shielding, which reduces the electrostatic interaction between protein and surfactant. In this case it may be necessary to add a hydrophilic surfactant to compensate for the high concentration of salt to preserve the Winsor-III system. Another option is to replace in the last step the stripping solution by a solution with pH higher than pI. For the latter option in the same stripping solution, salt may be required to preserve the Winsor-III microemulsion system.

#### **2.4.2 Scale up and applications**

Extraction by reverse micelles can be scaled up easily because it is a liquid-liquid extraction process. One should take special care to minimize the shear force to prevent the loss of activity for the proteins. For example, a Graesser contactor consisting of a cylinder with buckets that rotate carrying one phase inside of the other has been employed. In the upper part of the contactor the dense phase is poured into the light phase; the driving force to disperse the phase is the gravitational field. And in the lower part the light phase is dispersed into the dense phase; buoyancy is the driving force that disperses the light phase [57]. Another example of equipment suitable for scaling up liquid-liquid extraction by microemulsion is a column operated in countercurrent tested successfully by Hasman *et al.* for the extraction of glucose-6-phosphate dehydrogenase [58].

#### **2.4.3 Role of microemulsion based liquid-liquid extraction in bioseparations**

Bioseparations consists of recovering and purifying products obtained from living organisms, or their components. Bioseparations in many cases has the highest percentage of the overall production costs because fermentation broths are chemically complex and some products require extremely high purity. In addition, some products are present in

the bulk liquid at very low concentration. Besides the challenges to separate the products, care must be used to maintain the biological activity of many bioproducts because this property is what has practical and economical value. Normally bioproducts are very sensitive to conditions that differ from the cell from which they were produced, such as temperature, pH, and ionic strength. **Figure 2.14** shows the most common steps used in bioseparations. The flow sheet is not comprehensive; each step can consist of substeps or include more than one variation of each step. For example, “chromatographic purification” can include ion-exchange chromatography and hydrophobic chromatography in the same process.

In **Figure 2.14**, the unit operations are divided into three stages depending on the grade of purification reached in the product. In the first stage after initial harvest and concentration, the protein is liberated from the cell and can be concentrated. In the second group, initial purification, a partial purification and concentration are achieved in order to make it easier for the chromatographic step. In the last stage, final purification, the final product is obtained. In my opinion, extraction of proteins by microemulsion is suitable for the initial purification. Purity of the protein after microemulsion extraction is not always sufficiently high. In addition, it may be necessary to eliminate surfactants and solvents after the separation of the protein. So the main use of protein extraction by microemulsion systems would be to provide a partially purified protein that is further refined by chromatography, such that the cost and time required for chromatography would be reduced. Protein extraction by microemulsion systems can be used for the concentration or replacing the chromatography in some special cases [61].

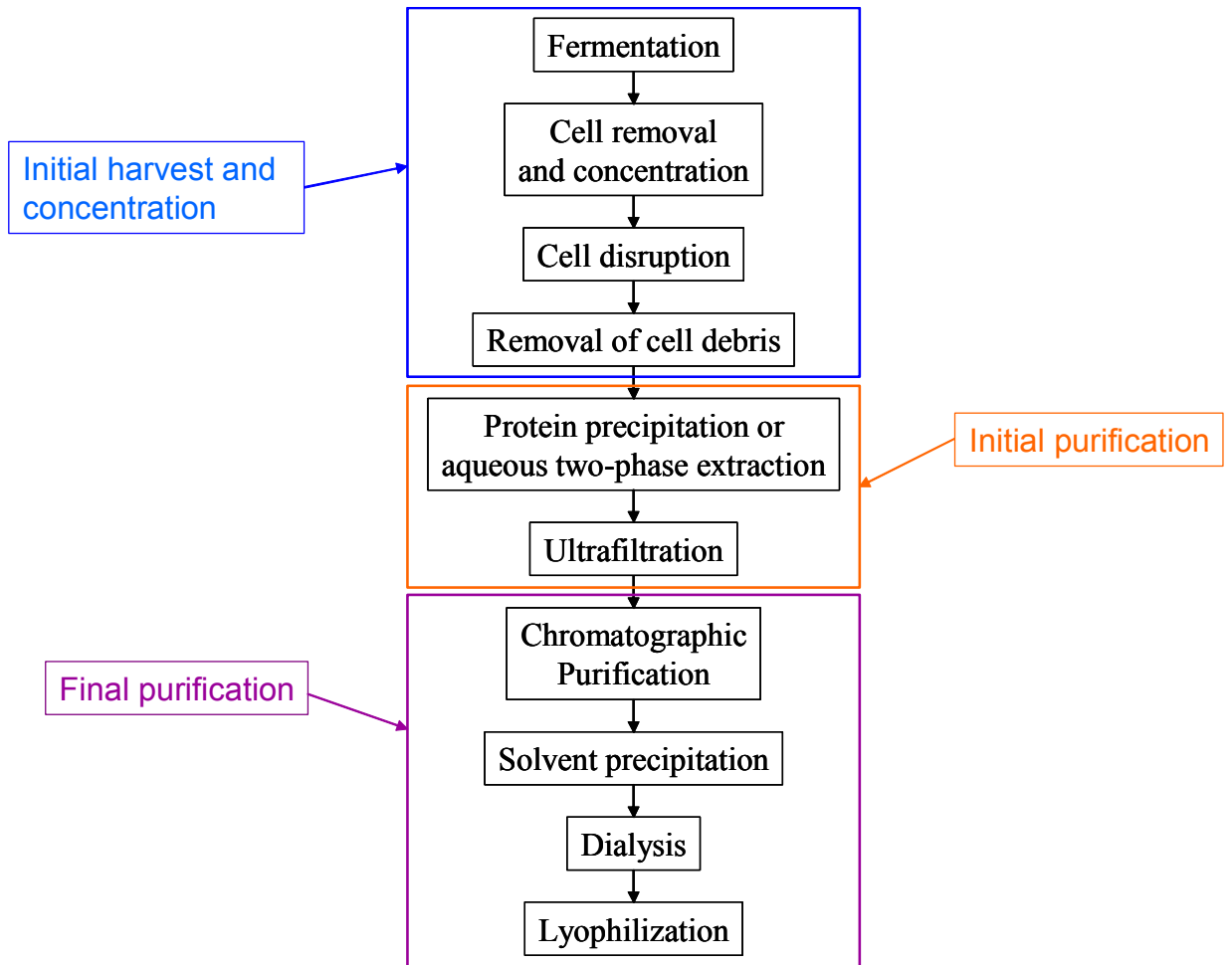


**Figure 2.14:** Common steps used to purify bioproducts [60].

# CHAPTER 3

## CHEMICAL AND MOLECULAR WEIGHT-BASED CHARACTERIZATION OF CYCLIC KETAL SURFACTANTS

### ***3.1 Introduction***

The objective described in this chapter is determining the purity of the intermediates and final product and the molecular weight of the ethoxylate starting material (MPEG 350) and final product. O-[(2-tridecyl, 2-ethyl-1,3-dioxolan-4-yl) methoxy]-O'-methoxy poly(ethylene glycol)<sub>5,45</sub>, a pH-degradable nonionic surfactant (CK7 for degree of polymerization 7.2 of the poly (ethylene glycol) used as raw material) was synthesized and analyzed in order to obtain its chemical composition because the properties of the surfactant depend on the distribution of the degree of polymerization for the poly (ethylene glycol), or ethoxylate, head group and the presence of impurities. Analyses performed upon the intermediates formed during the synthesis of CK7 and the final purified product include reverse phase High Performance Liquid Chromatography (RP-HPLC), Gel Permeation Chromatography (GPC), and Fourier Transform Infrared Spectroscopy (FTIR).

The average molecular weight and molecular weight distribution of CK7 are indicators of an alkyl ethoxylate surfactant's hydrophilicity because they reflect the length of the ethoxylate head group. The hydrophobic moiety is the same for all of the CK7 molecules. The temperature at which hydrophobicity and hydrophilicity of the ethoxylate surfactant molecules are equivalent, is called the phase inversion temperature (PIT), which is important information needed for the protein extraction experiments conducted in the dissertation because the Winsor III systems employed for the extraction occur at the PIT of a given surfactant mixture.

The molecular weight of CK7 was measured by two methods. One is (GPC), which provides the number-averaged molecular weight. The other method is (RP-HPLC),

in which CK7 molecules are separated based on the relative size of their ethoxylate groups. The average degree of polymerization and the average molecular weight can be calculated from the weighted area of HPLC peak areas of the different peaks for the CK7 molecules. Both refractive index (RI) and evaporative light scattering detectors (ELSD) were employed for RP-HPLC.

### **3.2 Materials**

Solvents used in the HPLC mobile phases were all HPLC-grade: methanol (99.9% pure), acetone (99.5% pure), tetrahydrofuran (99.9% pure) and acetic acid (96% pure) and purchased from Fisher Scientific, Pittsburgh, PA. Deionized water possessed 18 M $\Omega$  x cm of resistivity. Poly (ethylene glycol) monomethyl ether with a nominal molecular weight of 350 (MPEG-350) was purchased from Acros Organics, Fair Lawn, NJ. Triethylene glycol monomethyl ether (95% pure; MPEG<sub>3</sub>), triethylamine (99.5% pure), mesyl chloride (99.5% pure), and *p*-toluene sulfonic acid (97% pure), were purchased from Sigma–Aldrich, Milwaukee, WI. 3-Hexadecanone (97% pure) was purchased from Lancaster Synthesis, Windham, NH. Calcium hydride (90-95% pure) was purchased from Fisher Scientific.

### **3.3 Methods**

#### **3.3.1 Surfactant synthesis**

CK7 and CK3 were synthesized by the method developed by Iyer-Raikar *et al.* [5] (**Figure 3.1**), except that a new final purification step was added to eliminate unreacted



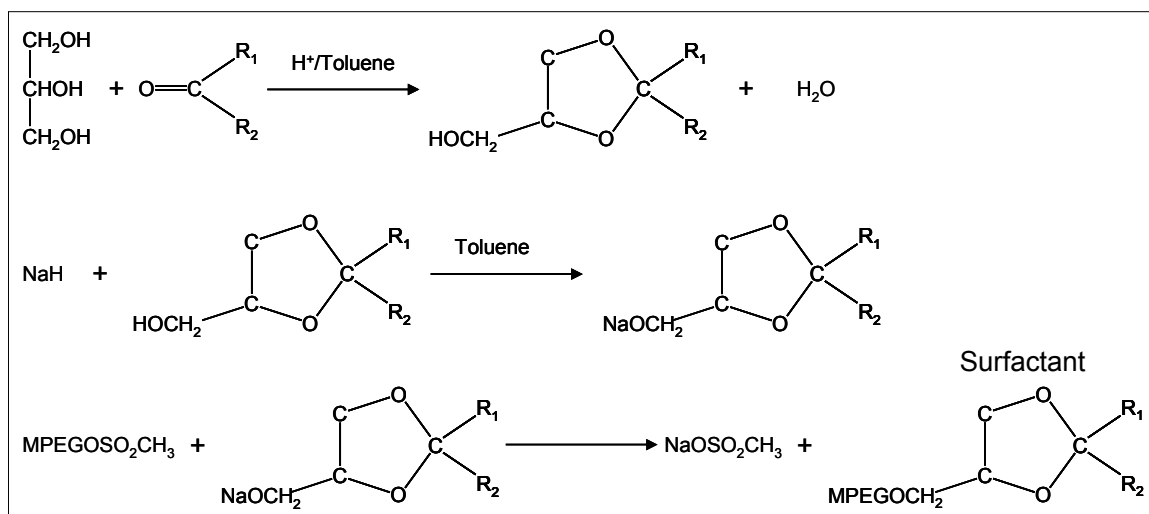


**Figure 3.1** Overview of method used to synthesize CK7 and CK3. From Iyer-Raikar *et al.* [5] MPEG refers to MPEG-350 and MPEG<sub>3</sub>, for CK7 and CK3, respectively. R<sub>1</sub> and R<sub>2</sub> refer to *n*-C<sub>13</sub>H<sub>27</sub> and CH<sub>3</sub>CH<sub>2</sub>, respectively.

MPEG, as described below. In the procedure developed by Iyer-Raikar *et al.* a molar excess of poly (ethylene glycol) monomethyl ether is used in order to have high reaction yield of the cycle ketal. The purification method developed in this work consisted of dissolving the (unpurified) surfactant (~20 g) in hexane (~ 300 mL) and then adding a small amount of water (~ 0.5 mL) to the solution, then stirring the mixture for 1 minute. Calcium hydride (~5 g) was added to the mixture; then, the mixture was stirred, and subsequently allowed to settle, during which precipitation occurred. The hexane-rich supernatant solution was filtered and then solvent removed in the rotary evaporator at 60°C. The residue, purified CK7 or CK3, was collected.

### 3.3.1.1 Qualitative Measurement of Ketone

FTIR transmittance spectra of pure CK7 were measured in a Spectrum One FTIR spectrometer from Perkin Elmer (Waltham, MA). Frequency range was from 650  $\text{cm}^{-1}$  to 4000  $\text{cm}^{-1}$ . Each sample was scanned 16 times at a resolution of 1  $\text{cm}^{-1}$  at 25°C.

Non reacted ketone also was detected by Thin Layer Chromatography (TLC). Samples were dissolved in a mixture of 3:1 volume parts of hexane/ethyl acetate. A drop of the solution is placed in a flexible TLC plate covered with silica gel 60Å, F-254, 200 micron from Selecto Scientific, Georgia, USA. Another drop of a ketone solution is placed next to the sample to serve as a standard. After drying the solvent, the TLC plates were developed in iodine vapor.

### 3.3.2 Gel permeation chromatography

The molecular weight of MPEG-350 was measured by (GPC) using a styragel HR4E, 7.8 X 300 mm column from Waters Corporation, Milford, MA, and a refractive index detector, model RI-1, from Varian (Walnut Grove, CA). The chromatography apparatus consisted of a SD-200 dual-pump analytical system from Varian Inc. (Walnut Grove, CA). The mobile phase was THF, delivered at a flow rate of 0.5 mL/min. Samples were diluted in mobile phase and analyzed immediately after sample preparation to avoid degradation. PEG standards were used to create the  $\ln(\text{MW})$  – retention time calibration depicted in **Figure 3.2**. An excellent linear relationship was obtained, as described by **Equation 3.1**.

$$M_n = 3.179 \cdot 10^{10} \cdot e^{-1.763 \cdot t_R} \quad (3.1)$$

In **Equation 3.1**  $t_R$  is the retention time and  $M_n$  is the molecular weight.

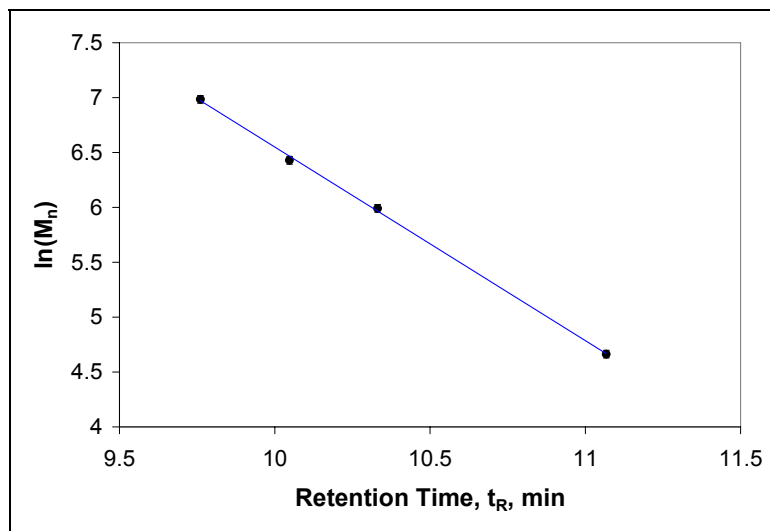


**Figure 3.2:** GPC calibration curve (natural logarithm of molecular weight vs. retention time) for poly(ethylene glycol) standards. The standard errors for the retention time values are reflected in the size of the data points.

### 3.3.3 Reverse Phase- High Performance Liquid Chromatography

The column, obtained from Varian, was of a  $C_{18}$  stationary phase, pore size  $100\text{\AA}$ , particle diameter  $5\mu\text{m}$ , column diameter  $4.6\text{ mm}$ , and column length  $250\text{ mm}$ . An evaporative light-scattering detector (model MKIII from Alltech Associates, Deerfield, IL) and Varian, Prostar 355 RI detector (Varian Inc., Walnut Creek, CA) were employed with the analytical HPLC system described in the previous subsection.

MPEG-350 was separated by its degree of polymerization using an isocratic method developed by Meyer *et al.* [62] with modification. The solvent consisted of 64 vol. % water and 35 vol. % methanol and 1 vol. % acetic acid; the flow rate was  $0.5\text{ mL/min}$ . Pure MPEG-350 dissolved in the mobile phase solvent was injected. Since the RI detector's signal is proportional to the mass of solute per unit volume [62], **Equation 3.2** was employed to convert the RI detector signal into concentration.

$$C_n = a' \cdot A_{RI,n} \quad (3.2)$$

where  $A_{RI,n}$  and  $C_n$  are the RI detector signal-derived peak area and concentration of a CK7 molecule with ethoxylate size  $n$ , respectively, and  $a'$  is a proportionality constant.

The separation of CK7 according to the ethoxylate head group size was achieved using an isocratic mobile phase of 98 vol. % acetone and 2 vol. % acetic acid at 1.0 mL/min. The samples analyzed were of purified surfactant dissolved in the mobile phase solvent system. The equation used to convert peak area from the ELSD detector to concentration [63-65] is:

$$C_n = a \cdot A_{ELSD,n}^b \quad (3.3)$$

where  $a$  and  $b$  are proportionality constants assumed to be independent of CK7's ethoxylate size and calculated using peak areas from a series of chromatograms of the same CK7 sample at different concentrations. **Figure 3.3** is a chromatogram of pure CK7 obtained by ELSD detector. Retention time is smaller for the surfactants with smaller degree of polymerization.

The mass fraction of CK7 with ethoxylate size  $n$ ,  $\omega_n$  was calculated (**Equation 3.4**) from ELSD detector data.

$$\omega_n = \frac{C_n}{\sum_{i=1}^{\infty} C_i} = \frac{A_{ELSD,n}^b}{\sum_{i=1}^{\infty} A_{ELSD,i}^b} \quad (3.4)$$

The symbol  $\infty$  in the **Equation 3.4** is a theoretical value; the practical limit in this work is 12 because CK7 molecules with ethoxylate size of  $n > 12$  were not detectable under the conditions of the experiment.

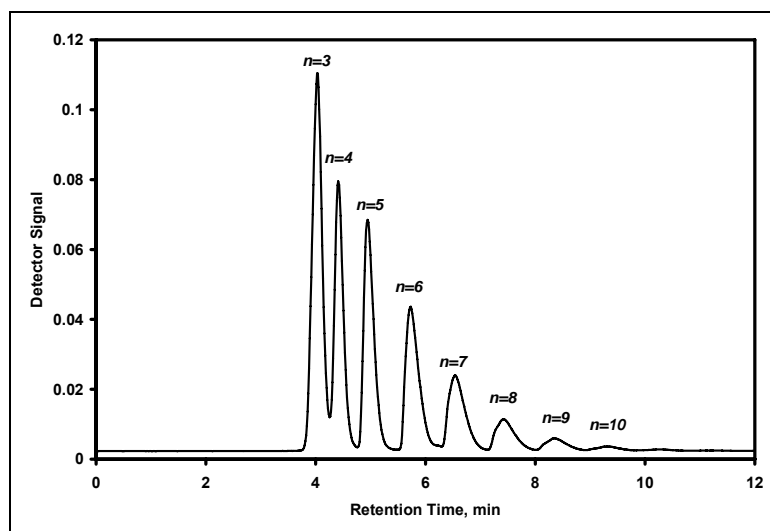


**Figure 3.3:** Chromatograms of pure CK7.  $C_{18}$  reverse phase column, isocratic mobile phase of 98 vol% acetone and 2 vol. % acetic acid at 1 mL/min. ELSD detector.  $n$  refers to the degree of polymerization of the surfactant molecule's ethoxylate group.

To assist in the calculations, CK7 was also analyzed via RP-HPLC using an RI detector. The mass fraction ( $\omega_n$ ) was also calculated from the RI detector data using **Equation 3.5:**

$$\omega_n = \frac{C_n}{\sum_{i=1}^{\infty} C_i} = \frac{A_{RI,n}}{\sum_{i=1}^{\infty} A_{RI,i}} \quad (3.5)$$

The mass fraction is used to calculate the concentration of each component of CK7 by **Equation 3.6:**

$$C_n = \omega_n \cdot C_T \quad (3.6)$$

where  $C_T$  is the total concentration of CK7 in the sample. In order to analyze RI detector data only a single parameter,  $a'$ , is needed as indicated by **Equation 3.2**.

After constants  $a$  and  $b$  are determined, they are used to calculate molar fraction ( $X_n$ ) by using **Equations 3.7** and **3.8** for ELSD and RI, respectively. **Equation 3.7** results from transforming the mass amounts of **Equation 3.3** to molar amounts.

$$X_n = \frac{\frac{C_n}{Mw_n}}{\sum_{i=1}^{\infty} \frac{C_i}{Mw_i}} = \frac{\frac{A_{ELSD,n}^b}{n \cdot 44.053 + 328.530}}{\sum_{i=1}^{\infty} \frac{A_{ELSD,i}^b}{i \cdot 44.053 + 328.530}} \quad (3.7)$$

The constant  $a'$  cancels from both numerator and denominator. Molecular weight is replaced by a linear function of the degree of polymerization obtained from the surfactant's molecular formula. By analogy, **Equation 3.8** is derived from modification of **Equation 3.5**.

$$X_n = \frac{\frac{C_n}{Mw_n}}{\sum_{i=1}^{\infty} \frac{C_i}{Mw_i}} = \frac{\frac{A_{RI,n}}{n \cdot 44.053 + 328.530}}{\sum_{i=1}^{\infty} \frac{A_{RI,i}}{i \cdot 44.053 + 328.530}} \quad (3.8)$$

There are two measures of the average molecular weight of a polymer. One uses the mass fraction of each component to obtain the weight-averaged molecular weight ( $M_w$ , **Equation 3.9**).

$$M_w = \sum_{n=1}^{\infty} \omega_n \cdot Mi_n \quad (3.9)$$

where  $Mi_n$  is the molecular weight of a monodisperse surfactant of degree of polymerization  $n$ . The other uses the mole fraction of each component to obtain the number-averaged molecular weight ( $M_n$ , **Equation 3.10**).

$$M_n = \sum_{n=1}^{\infty} X_n \cdot Mi_n \quad (3.10)$$

The ratio between  $M_w$  and  $M_n$  is called polydispersity index (PDI) and is a measure of the distribution of ethylene oxide degree of polymerization of CK7 (**Equation 3.11**).

$$PDI = \frac{M_w}{M_n} \quad (11)$$

The average number of ethoxylate units per molecule for MPEG-350 and the head groups of CK7, abbreviated “EON” (or “ethylene oxide number”), is calculated according to **Equation 3.12**.

$$EON = \sum_{n=1}^{\infty} X_n \cdot n \quad (3.12)$$

### ***3.4 Results and Discussion***

#### **3.4.1 MPEG-350 molecular weight**

The average molecular weight of MPEG-350 obtained by GPC was 350±10, which is identical to the nominal molecular weight given by the vendor. The mole and mass fractions for the components of MPEG-350, determined from RP-HPLC, are given in **Table 3.1**.

**Table 3.1:** Mole and mass fractions of the components of MPEG-350, H-(OCH<sub>2</sub>CH<sub>2</sub>)<sub>n</sub>-OCH<sub>3</sub>, according to the degree of polymerization, *n*, as determined from RP-HPLC using a refractive index detector

<b>n</b>	<b>X<sub>n</sub><sup>a</sup></b>	<b>ω<sub>n</sub><sup>b</sup></b>
2	0.004	0.001
3	0.042	0.020
4	0.081	0.049
5	0.120	0.087
6	0.156	0.132
7	0.170	0.166
8	0.137	0.151
9	0.110	0.134
10	0.078	0.105
11	0.056	0.083
12	0.045	0.072

<sup>a</sup> calculated using **Equation 3.8**. <sup>b</sup> calculated using **Equation 3.5**,

The distribution of MPEG-350 according to its degree of polymerization, *n*, is well-described by the theoretical Poisson distribution centered at *n* = 7.21, consistent with literature data for other PEG-based materials [66, 67] (**Figure 3.4**). Thus, the average EON value is 7.21, which is very near the value obtained by GPC, 7.26. *M<sub>n</sub>* calculated from RP-HPLC is 349±11, which is near the nominal *M<sub>n</sub>* (350) and the value obtained by GPC (350±10). The PDI value derived from chromatogram measured by RI detector and the data of **Table 3.1** was 1.09.

### 3.4.2 CK7 molecular weight

The distribution of molecular weight of surfactant according to the ethoxylate group size, *n*, is not coincident with the distribution for MPEG-350. Number-averaged (*M<sub>n</sub>*) and weight-averaged molecular weight (*M<sub>w</sub>*) obtained by using ELSD and RI detectors are given in **Table 3.2** and **Table 3.3**, respectively. The *M<sub>n</sub>* values contained in the tables are lower than the calculated molecular weight of CK7 using the same average



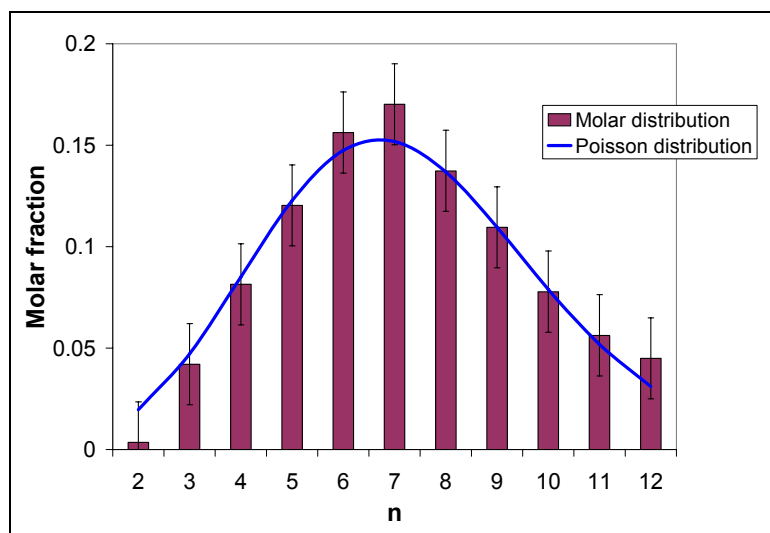


**Figure 3.4:** Molar distribution of of MPEG-350, H-(OCH<sub>2</sub>CH<sub>2</sub>)<sub>n</sub>-OCH<sub>3</sub>, versus degree of polymerization, n, as determined from RP-HPLC. Blue curve represents the Poisson distribution (Section 2.2.2) centered at n=7.21.

ethoxylate size as MPEG-350, which would be 646.5. The distribution of oligomers in the surfactant, **Figure 3.5**, also differs from the Poisson distribution of MPEG-350, **Figure 3.4**. The difference between distributions of degree of polymerization of CK7 and MPEG-350 reflects that the surfactant is more hydrophobic than would occur if the distribution of degree of polymerization for CK7 equaled that of MPEG-350. As a consequence, the reduced ethoxylate size of CK7 improves its performance because the PIT is lowered, closer to room temperature, even though it is still high (~41°C, Section 4.5.5 and 4.6.1). The PDI values calculated from data in **Table 3.2** and **Table 3.3** are both 1.03 for ELSD and RI detectors. There is a good agreement between molecular weight calculated by the RI and ELSD detectors. The PDI of CK7 is smaller than that of MPEG-350, meaning that the former is more monodisperse. The consequence of this is that a CK7 synthesized for this dissertation has a higher interfacial tension and less readily forms microemulsions compared to a CK7 possessing an ethoxylate distribution equal to that of MPEG-350. In this work the difference is not significant because CK7 forms microemulsions with a more narrow distribution of ethoxylate chain length than MPEG-350.

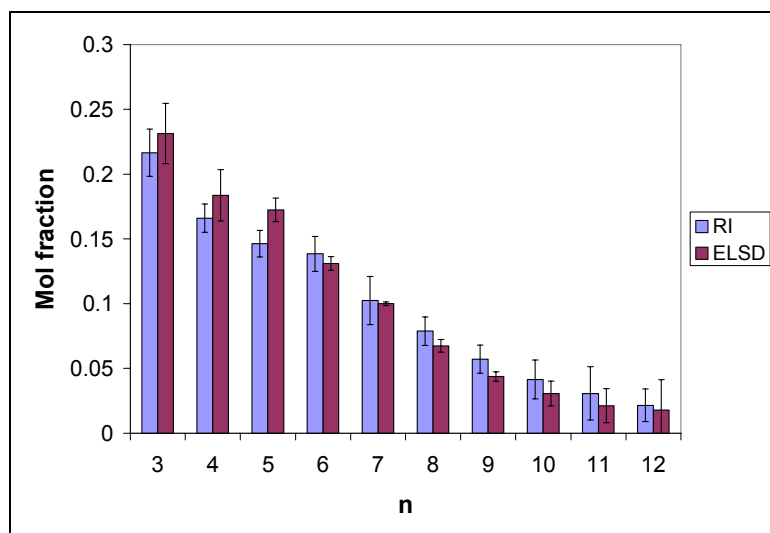


**Figure 3.5:** Mole fraction of the species present in CK7 surfactant based on the ethylene oxide number (n) of the surfactant head.

**Table 3.2:** Mole and mass fraction of CK7 molecules according to their ethoxylate group size, n, obtained by using ELSD detector.

n	$M_{i_n}^a$	$\omega_n^b$	$\omega_n \cdot M_{i_n}$	$X_n^c$	$X_n \cdot M_{i_n}$	$X_n \cdot n$
3	460.7	0.187	86.4	0.231	106.6	0.7
4	504.7	0.163	82.3	0.184	92.7	0.7
5	548.8	0.166	91.3	0.172	94.7	0.9
6	592.8	0.137	81.0	0.131	77.7	0.8
7	636.9	0.112	71.3	0.100	63.7	0.7
8	681.0	0.081	55.0	0.068	46.0	0.5
9	725.0	0.056	40.4	0.044	31.8	0.4
10	769.1	0.041	31.8	0.031	23.6	0.3
11	813.1	0.030	24.6	0.021	17.3	0.2
12	857.2	0.027	22.9	0.018	15.4	0.2
<b>Total</b>			$M_w=586.8^d$		$M_n=569.4^d$	EON=5.4

<sup>a</sup>calculated from the chemical formula, <sup>b</sup>calculated by **Equation 3.4**, <sup>c</sup>calculated by **Equation 3.7**. <sup>d</sup>Error in  $M_w$  and  $M_n$  is 12 units.

**Table 3.3:** Mole and mass fraction of CK7 molecules according to their ethoxylate group size, n obtained by using RI detector.

n	$Mi_n^a$	$\omega_n^b$	$\omega_n \cdot Mi_n$	$X_n^c$	$X_n \cdot Mi_n$	$X_n \cdot n$
3	460.7	0.172	79.0	0.217	99.8	0.6
4	504.7	0.144	72.7	0.166	83.8	0.7
5	548.8	0.138	75.8	0.146	80.3	0.7
6	592.8	0.141	83.7	0.139	82.2	0.8
7	636.9	0.112	71.5	0.103	65.3	0.7
8	681.0	0.092	62.9	0.079	53.7	0.6
9	725.0	0.071	51.6	0.057	41.5	0.5
10	769.1	0.055	42.1	0.042	31.9	0.4
11	813.1	0.043	34.8	0.031	25.0	0.3
12	857.2	0.032	27.1	0.022	18.5	0.3
<b>Total</b>			$M_w=601.3^d$		$M_n=581.9^d$	EON=5.7

<sup>a</sup>calculated from the chemical formula, <sup>b</sup>calculated by **Equation 3.5**, <sup>c</sup>calculated by **Equation 3.8**. <sup>d</sup>Error in  $M_w$  and  $M_n$  is 12 units.

### 3.4.3 Synthesis and Chemical Characterization

The synthesis of the surfactant based on the method of Iyer-Raiker *et al.* [5] employed for the experiments performed in Chapters 4-6 resulted in a yield of 70-80% for the synthesis of the intermediate MPEG mesylate derivative (MPEGOSO<sub>2</sub>CH<sub>3</sub>), 60-70% for the cyclic ketal formation step, and 60-70% for the covalent attachment of MPEG to the cyclic ketal (See **Figure 3.1**). The yields are significantly lower than the yields obtained by Iyer *et al.* which were 90-95% for the synthesis of MPEG mesylate, 80-85% for cyclic ketal formation, and 80-85% for covalent attachment of MPEG to the cyclic ketal. This difference in yields could explain the difference in EON and distribution of degree of polymerization between the surfactant synthesized by Iyer-Raiker *et al.* and employed in this work. The former possessed a Poisson distribution of degree of polymerization for its ethoxylate head group, corresponding to the source of MPEG-350 used in the synthesis [11]. For the surfactant synthesized for this dissertation, the distribution of degree of polymerization is not Poisson; it is rather experimental, skewed to low degrees of polymerization with maximum equal to 3 (discussed in Section

3.4.2). Also the EON obtained by Iyer-Raiker was 7.68, which is significantly higher than the EON obtained in this work, which was 5.6 (Section 3.4.2). The difference in purification protocol described in Section 3.3.1 cannot completely explain the difference in degree of polymerization between the two synthesized surfactants because the chromatographic analysis of the precipitate by-product obtained during the final purification step depicted an amount of surfactant just above the detection limit, with the only major chromatographic peak being for MPEG (data not shown).

After purification the surfactant possessed >95% purity. The impurities are traces of solvents not evaporated completely and ketone that did not react completely in the synthesis. Impurities can dramatically modify the surface activity of the surfactants; thus, their detection is very important. The ketone starting material was observed by thin layer chromatography and FTIR spectroscopy. As demonstrated in **Figure 3.6**, the FTIR spectrum of CK7 is consistent with its presumed chemical structure, evidenced by CH stretching ( $2700\text{-}3000\text{ cm}^{-1}$ ) and CO stretching for the ethoxylate group at  $\sim 1140\text{ cm}^{-1}$ . The carbonyl stretching region provides a clear fingerprint of the presence of unreacted ketone. As observed in **Figure 3.6**, the presence of ketone occurred for one batch of CK7 synthesized by the author of this dissertation and a second batch synthesized by a colleague, M. Alkhatib.

Ketone was also detected by TLC (**Figure 3.7**), producing a long spot at longer distance from the TLC plate's origin. This result agrees with the findings obtained by FTIR. Also it can be observed in **Figure 3.7** that the proportion of ketone is small compared to CK7 based on the relative intensity of the TLC bands. Even though it is impossible to quantify the amount of ketone. Small amount of impurities can change surface activity of surfactants.

Quantitative methods used in this dissertation, such as RP-HPLC, cannot detect ketone. Both methods used to detect ketone, FTIR and TLC, are qualitative.

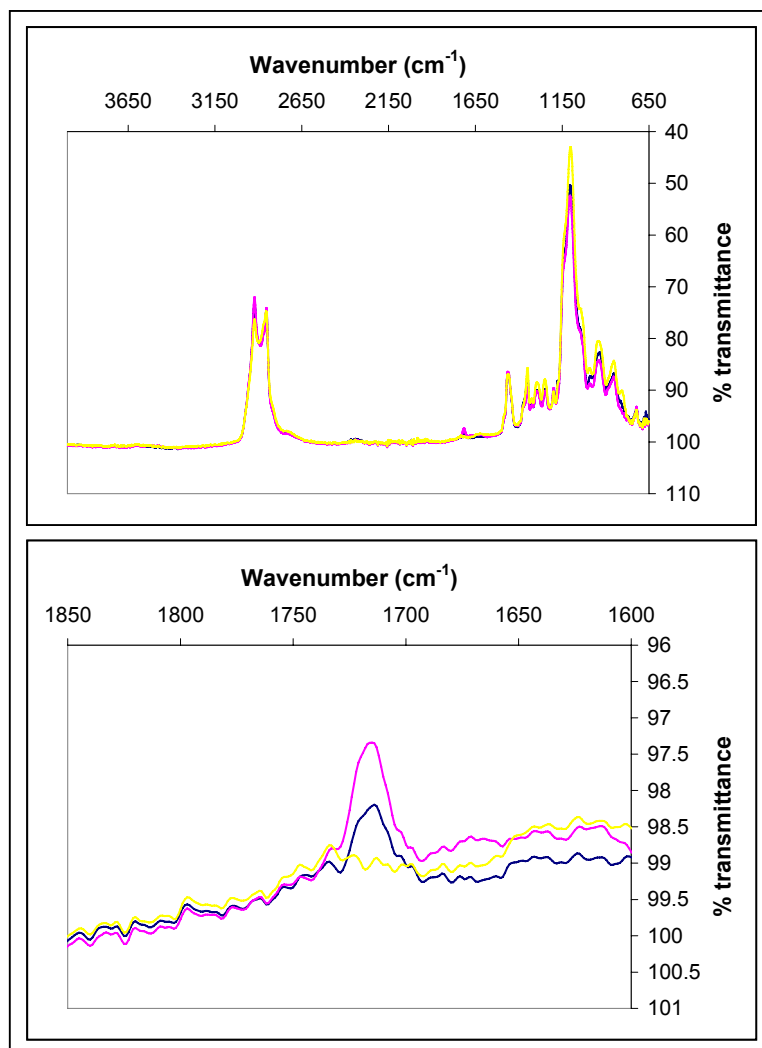


**Figure 3.6:** FTIR spectra (top: overall spectra; bottom: -carbonyl stretching region) of CK7 surfactant. Blue: CK7 surfactant synthesized by the author of this dissertation of lower purity; Magenta: highly pure CK7 surfactant synthesized by M. Alkhatib, Univ. Alabama-Huntsville, and (Yellow) CK7 surfactant synthesized by the author of this dissertation.

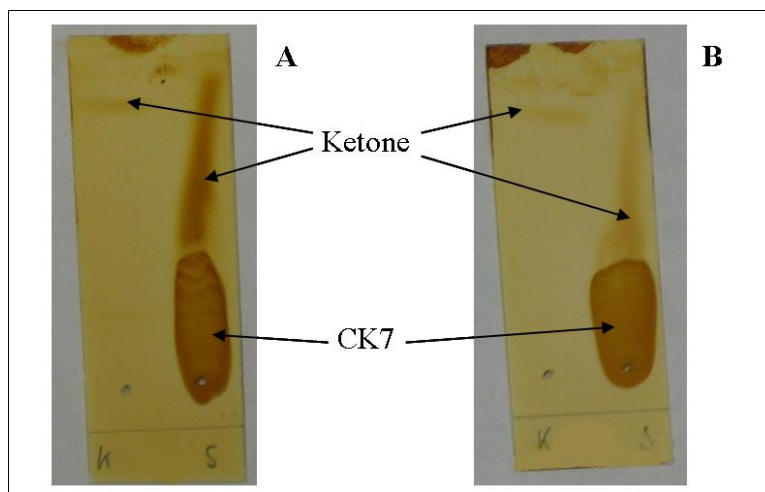


**Figure 3.7:** Thin layer chromatography of CK7 surfactant indicating the presence of ketone. The bands positions of CK7 and ketal are given in the figure. Each plate includes a band to the left for ketone standard. A) Highly pure CK7 surfactant synthesized by M. Alkhatib, Univ. Alabama-Huntsville, corresponding to magenta line in **Figure 3.6**. B) CK7 surfactant synthesized by the author of this dissertation of low purity, corresponding to blue line in **Figure 3.6**.

### 3.5 Conclusions

The molecular weight of CK7 surfactant is significantly lower than expected if one assumes that CK7 will possess the same average ethoxylate group size and size distribution as its source, MPEG-350. Also the molecular weight distribution of CK7 according to the ethoxylate group size,  $n$ , differs from that of MPEG-350. The distribution of the latter is described by a Poisson distribution (**Figure 3.4**) with an average molecular weight of 350, in agreement with the vendor's specifications, equivalent to an EON of 7.2. In contrast, CK7's distribution is centered at  $n = 5.6$  and thus is richer in molecules with lower EON values. In addition, the distribution of CK7 is not Poisson but is skewed with a maximum occurring for  $n$  equal to 3 (**Figure 3.5**). The underlying cause for the difference in ethoxylate distribution between CK7 and MPEG 350 is attributed to either an incomplete conversion for the final reaction step of the synthesis (**Figure 3.1**) or degradation of the ethoxylate chain during the synthesis, with

the final purification step developed by the author of this dissertation removing only a small amount of the high molecular weight surfactant. The consequence of the lower molecular weight is that the phase inversion temperature is to be reduced compared with a surfactant that possesses an ethoxylate group distribution equal to MPEG-350, which is desirable in this case.

# CHAPTER 4

## PARTITION OF CK7 IN 2 AND 3 PHASES MICROEMULSION SYSTEMS AS A FUNCTION OF ETHOXYLATE SIZE AND TEMPERATURE IN SINGLE AND BINARY SURFACTANT MIXTURES

### ***4.1 Introduction***

Equilibrium partitioning between water and oil determines the properties of the surfactant mixture. From observing the equilibrium partitioning behavior as a function of temperature, in conjunction with the mathematical model (Section 4.2), the phase inversion temperature (PIT) can be calculated (Section 4.6.1). PIT is a very important property for protein extraction by Winsor-III systems because at this temperature the three phases undergo disengagement very rapidly after an oil and water phase are first mixed [68].

The partitioning behavior of O-[(2-tridecyl, 2-ethyl-1,3-dioxolan-4-yl)methoxy]-O'-methoxy poly(ethylene glycol)<sub>5.2</sub> (CK7) between water and oil as a function of the molecules' ethoxylate head group size and temperature (Section 4.5.1) was investigated to compare with the partitioning of CK7 in single versus binary surfactant mixtures, the latter employed for protein extraction (Chapters 5 and 6), and with the behavior of linear alkyl ethoxylates described in the literature [69, 70]. As discussed in Chapter 3, CK7, similar to most commercial alkyl ethoxylate surfactants, possesses a broad distribution for the molecular weight of the ethoxylate head group. From these data a semi-empirical thermodynamic model was developed, which would help predict the temperature at which three phase systems would be formed. This model is useful also to fit equilibrium data of the binary surfactant system by changing the adjustable parameters of the model.

Equilibrium partitioning of CK7 was also measured in the presence of a second surfactant that will be used in protein extraction in order to know how the latter will affect CK7's equilibrium partitioning and hence the PIT (CK3: Section 4.5.2, Aerosol-



OT: Section 4.5.3, and  $C_8\beta G_1$ : Section 4.5.4). AOT is needed to induce the electrostatic attraction-based driving force for forward extraction of proteins so it is important to know how its addition would affect the hydrophobicity of the CK7/AOT surfactant mixture and the distribution of CK7 molecular sizes which controls the system's PIT. AOT is also of interest because it can affect the hydrophobicity of a surfactant mixture, enabling the formation of stable W-I or W-III microemulsion systems. Alkhatib *et al.* found that AOT mixed with CK7 makes the phase boundaries less sensitive with respect to temperature [33]. Similarly, for the partitioning of CK7 in AOT/CK7 binary systems determined herein, partition coefficients for CK7 molecules of a given ethoxylate size are independent of temperature in the range 20-50°C. Since CK3 is more hydrophobic than CK7, it is added to CK7 and AOT to shift the equilibrium partitioning to oil phase to allow for the formation of W-III phases at room temperature.

Although not employed for protein extraction in this dissertation, surfactant partitioning of the CK7 / octyl glucoside ( $C_8\beta G_1$ ) system was studied to complement an investigation within our research group by Alkhatib for use of this system as a microemulsion-based drug delivery vehicle [33], and also because of its potential use in protein extraction due to the bioaffinity driving force created by  $C_8\beta G_1$ 's head group to molecules such as the lectin concanavalin-A [71]. It was found that  $C_8\beta G_1$ , being more hydrophilic than CK7, shifts the equilibrium partitioning of CK7 to the water phase. In order to be used for protein extraction by a W-III system the  $C_8\beta G_1$ /CK7 mixture needs a third surfactant more hydrophobic than both of them to reduce the PIT to room temperature.

## 4.2 Theory

This model to calculate partitioning of CK7 between water and oil employed herein is based on the work done by Salager *et al.* [70] The group's focus was commercial ethoxylated octylphenol surfactants that form W-III systems, with the goal

being to measure the partition coefficient between water and n-heptane of the surfactant as a monomer in both solvents [70]. Commercial ethoxylated surfactants normally have a Poisson distribution of the degree of polymerization for the ethoxylate group (Section 2.2.2). The properties of these surfactants are functions of the concentration of each species in the water-oil interface. Moreover, the interfacial composition is in equilibrium with the composition in the excess water and oil phases [72]. They prepared systems with different distributions of ethoxylate chain length and investigated the partition equilibrium for W-III systems at “optimal” conditions (the maximum solubilization of water and oil in middle phase) that did not possess aggregates in the excess aqueous or oil phase [70]. One consequence of the use of “optimal” conditions is that the logarithm of the equilibrium constant vs. ethoxylate chain length is a straight line [70]. In this work Salager’s model is extended further to include systems that are not at the optimal composition and 2-phase systems.

Data were fitted to a thermodynamic model that employed enthalpy and entropy for each CK surfactant species as adjustable parameters. The main assumption in this model is that enthalpy and entropy are constant within the range of temperature investigated, 20-50°C. For each surfactant species with ethoxylate chain length  $n$ , its partition between the water and oil “excess” phases of a W-III system can be assumed to be at thermodynamic equilibrium to be described by **Equation 4.1**:

$$K_n = \frac{C_{wn}}{C_{on}} \quad (4.1)$$

where  $K_n$  is the equilibrium constant,  $C_{wn}$  is concentration of surfactant in water, and  $C_{on}$  concentration of surfactant in oil. The equilibrium constants are related to molar Gibbs free energy ( $\Delta g_n$ ) according to **Equation 4.2**.

$$-\Delta g_n = R \cdot T \cdot \ln(K_n) \quad (4.2)$$

R is the ideal gas constant, and T is the absolute temperature.  $\Delta g_n$  is the Gibbs free energy required to move a mole of surfactant of polymerization degree “n” from oil phase to water phase. **Equation 4.3** results from rearranging **Equation 4.2**, and employing the fundamental thermodynamic relationship  $\Delta g_n = \Delta h_n - T \Delta s_n$ , where  $h_n$ =enthalpy/mol and  $s_n$ =entropy/mol.

$$\ln(K_n) = -\frac{\Delta g_n}{R \cdot T} = -\frac{\Delta h_n}{R \cdot T} + \frac{\Delta s_n}{R} \quad (4.3)$$

**Equation 4.3** is an expression of the van’t Hoff equation to calculate the equilibrium constant at different temperatures.

The partitioning data were plotted for each surfactant species of a particular ethoxylate group size,  $n$ , of  $\ln(K_n)$  versus  $1/T$  to obtain  $\Delta h_n$  and  $\Delta s_n$  from the slope and intercept, respectively, of a linear fit to the data.

### 4.3 Materials

The solvents used to equilibrate the surfactants were isooctane HPLC grade Fisher Scientific, Pittsburg, PA, and deionized water 18 M $\Omega$  x cm of resistivity. Four surfactants were used. Two are nonionic surfactants with poly(ethylene glycol) monomethyl ether as the hydrophile and a cyclic ketal as the hydrophobe [5] synthesized in the lab (described in Chapter 3). The surfactants were synthesized using two different poly(ethylene glycol) (PEG) monomethyl ether reactants (Chapter 3), one with 3 units of PEG (CK3) and other with an average of 7.21 units of PEG (CK7). The third surfactant was sodium bis(2-ethylhexyl) sulfosuccinate, AOT, anhydrous, purchased from Fisher. The fourth surfactant was n-octyl- $\beta$ -D-glucopyranoside, C<sub>8</sub> $\beta$ G<sub>1</sub> (100%), purchased from Fisher.

## **4.4 Methods**

### **4.4.1 Measurement of partition coefficients**

Surfactant was dissolved into isooctane first. Then the surfactant solution was mixed with water or 1 wt% NaCl aqueous solution in a polyethylene vial sealed with parafilm. After incubation for one day at constant temperature in a thermostatic bath, model Isotemp 3028 from Fisher, the sample was centrifuged at 16,000 g for 1 minute, using an AccuSpin™ MicroR from Fisher. Overall concentrations of CK7 were 5 wt.%, 7.5 wt.% and 10 wt.% for pure CK7. The mixtures of surfactant were 3.75 wt.% CK7 and 3.75 wt.% of the second surfactant, CK3, AOT or C<sub>8</sub>βG<sub>1</sub>. Equilibration temperatures examined were 20°C, 30°C, 40°C and 50°C.

### **4.4.2 High performance liquid chromatography**

Surfactant concentration in each phase was measured by reverse-phase high-performance liquid chromatography (RP-HPLC). For samples with only CK7, a 20 μL aliquot of top or bottom phase was removed by a 25 μL graduated syringe. The aliquot was diluted with 500 μL of acetone and injected in the HPLC system. Samples from surfactant mixture experiments are less concentrated in CK7 even though the overall concentration of surfactant is 7.5 wt.%. So they required less dilution for HPLC analysis than samples with pure CK7. For mixture samples, a 50 μL aliquot of top or bottom phase is removed by a 100 μL graduated syringe. The aliquot is diluted with 400 μL of acetone and injected in the HPLC. The chromatography apparatus consists of a SD-200 analytical system from Varian Inc. (Walnut Grove, CA). The column was obtained from

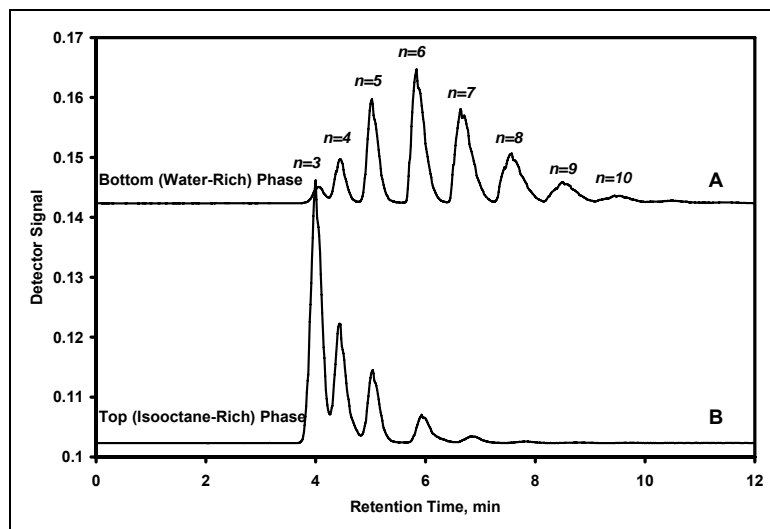


**Figure 4.1:** Example of chromatograms for the equilibrium partitioning of CK7 in a Winsor-III system obtained from reverse-phase HPLC analysis. A) Aqueous phase (bottom). B) Oil phase (top). The degree of polymerization  $n$  corresponding to each peak is indicated in the figure.

Varian,  $C_{18}$ , pore size  $100\text{\AA}$ , particle diameter  $5\mu\text{m}$ , column diameter  $4.6\text{ mm}$ , column length  $250\text{ mm}$ . An evaporative light-scattering detector (model MKIII from Alltech Associates, Deerfield, IL) was employed. The solvent system for HPLC was isocratic, consisting of 98% acetone and 2% acetic acid at a flow rate of  $1\text{ mL/min}$ . **Figure 4.1** has examples of the chromatograms obtained from bottom and top phase of CK7 at equilibrium. The retention time increases as the ethoxylate size increases.

#### 4.4.3 Phase diagram

Different concentrations of surfactants were solubilized in a mixture of water and isooctane (1:1 w/w). The mixture was centrifuged at  $16,000\text{ g}$  for 1 minute, and then placed into a constant-temperature water bath with accuracy of  $\pm 1^\circ\text{C}$  for 30 min to allow for phase separation of the two- or three-phase systems. The centrifugation and

equilibration steps were repeated until the top and the bottom phases were clear. After having a stable system the number of phases was observed visually.

## **4.5 Results**

### **4.5.1 The Partitioning of CK7 Between Water and Oil**

The equilibrium partitioning of a 1,3-dioxolane nonionic surfactant, CK7, in 2- and 3-phase microemulsion systems formed from equal mass of water and isooctane was determined as a function of temperature (20-50°C) and surfactant concentration (5-10 wt. %). This study was done in order to understand the behavior of the surfactant at different temperatures and concentrations. Properties of the microemulsion systems and its phases formed by ethoxylate surfactants that possess a wide distribution of ethoxylate molecular weight depend on the properties of surfactant molecules residing at the water-oil interface and not the original surfactant [72]. Since the liquid-liquid interfaces are in equilibrium with water and oil bulk phases, the properties of the surfactant residing at the interface can be determined indirectly through a mass balance by knowing the composition of surfactant in water and oil. The model can predict the phase inversion temperature (PIT), of importance for determining conditions required for protein extraction (Chapter 5).

In **Figure 4.2**  $\ln(K_n)$  against  $1/T$  for each surfactant species is plotted, and overlaid with a linear model based on the van't Hoff equation, **Equation 4.3**. Each set of data corresponding to an ethoxylate group size can be fitted by a straight line with most of the correlation coefficients being near 0.95. This fact implies that enthalpy and entropy nearly are constant respect to the temperature in the range 20-50°C [70]. This is the main assumption of the model. Systems of pure CK7 have 3 phases in the temperature range 30-50°C and 2 phases at 20°C.

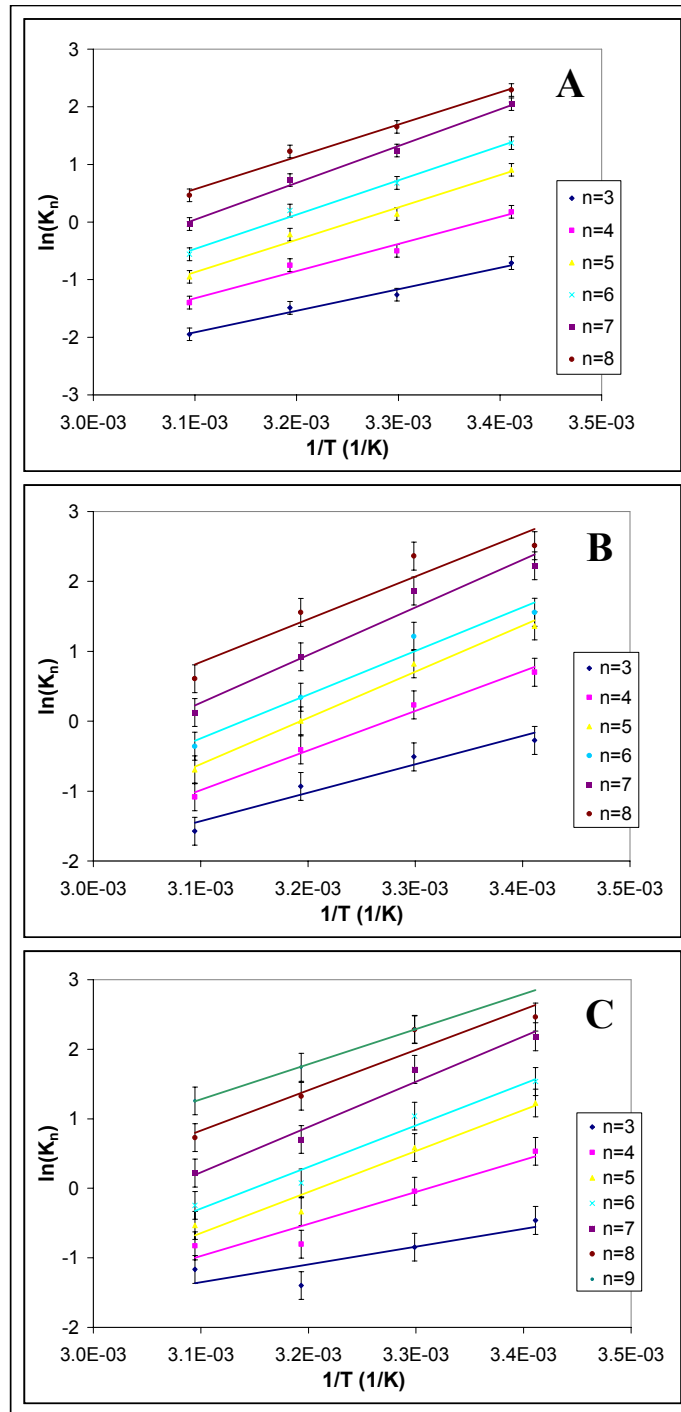


**Figure 4.2:** Fitting of van't Hoff equation (Equation 4.3) to partition coefficient data for CK7. Natural logarithm of equilibrium constant  $K_n$  ( $C_{wn}/C_{on}$ ) versus inverse of the temperature. A) 5 wt.% overall surfactant. B) 7.5 wt.% overall surfactant. C) 10 wt.% overall surfactant. Ethylene oxide degrees of polymerization, from 3 to 10 are represented as described in the legend. The lines represent the model fit (Equation 4.3) to the data.

**Figure 4.3** displays the slopes and y-intercepts of **Figure 4.2** A-C, which correspond to 5 wt. %, 7.5 wt. %, and 10 wt. % CK7, respectively, as functions of n. Slopes and intercepts versus n were fitted to second order polynomials. The equation produced when the polynomial expressions are substituted in **Equation 4.3** predicts the equilibrium constant of CK7 in function of temperature and number of ethylene glycol monomeric units. Data for pure CK7 were divided into two groups based on their concentration because the equilibrium constant is smaller for 5 wt. % of CK7 than for 7.5 wt. % and 10 wt. % of CK7 for most of the data. The two later were grouped together. Slopes and y-intercepts of fitted lines in **Figure 4.2** are proportional to the enthalpy and entropy change of bringing a surfactant molecule from oil to water, respectively. **Equations 4.4** and **4.5** are slopes and intercepts, respectively, for a concentration of 5 wt. % CK7. **Equations 4.6** and **4.7** are slopes and intercepts, respectively, for a concentration of 7.5 wt. % and 10 wt. % CK7.

Slopes for 5 wt. % CK7 from **Figure 4.2**:

$$-\frac{\Delta h_n}{R} = -190 \cdot n^2 + 2500 \cdot n - 2200 \quad (4.4)$$

Intercepts for 5 wt. % CK7 from **Figure 4.2**:

$$\frac{\Delta s_n}{R} = 0.588 \cdot n^2 - 7.27 \cdot n + 3.33 \quad (4.5)$$

Slopes for 7.5 wt. % and 10 wt. % CK7 from **Figure 4.2**:

$$-\frac{\Delta h_n}{R} = -260 \cdot n^2 + 3340 \cdot n - 4270 \quad (4.6)$$

Intercepts for 7.5 wt. % and 10 wt. % CK7 from **Figure 4.2**:

$$\frac{\Delta s_n}{R} = 0.819 \cdot n^2 - 10.2 \cdot n + 11.1 \quad (4.7)$$



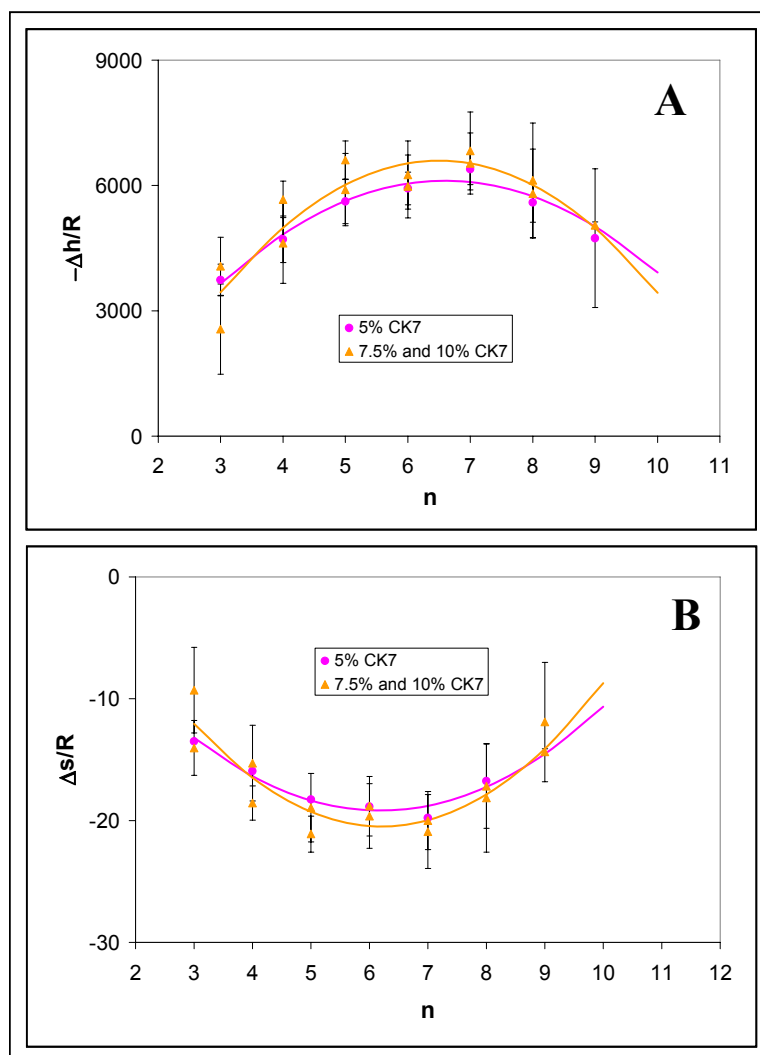


**Figure 4.3:** Enthalpy and Entropy values divided by the gas constant (R) versus ethoxylate size for CK7. Constants of van't Hoff equation obtained by fitting **Equation 4.3** to the data of **Figure 4.2**. A) Slopes of fitted lines (**Equation 4.3** in **Figure 4.2** B) Intercepts of fitted lines (**Equation 4.3**) in **Figure 4.2**. Concentrations in both figures are 5 wt. %CK7, 7.5 wt.% CK7 and 10 wt.% CK7 overall surfactant as indicated in the legend Curve represents second-order polynomial fit to the data.

**Figure 4.4** depicts the fit of **Equations 4.4, 4.5, 4.6** combined with **Equation 4.3**, to experimental data of the effect of temperature and ethylene oxide degree of polymerization,  $n$ , on the partitioning of CK7 surfactant. The partitioning of the surfactant in water decreases with increase of temperature. This trend is expected because alkyl ethoxylate surfactants are more hydrophilic at lower temperatures as described in Section 2.2.2. Moreover, the mobility of an ethoxylate chain increases with temperature so it has less water molecules attached to it, making it less hydrophilic. In addition, surfactant with higher ethoxylate degree of polymerization partitions more strongly to water. It can be observed in **Figure 4.4** that equilibrium constants from a fixed temperature have a positive slope with respect to  $n$ . The model (Section 4.2) fits very well to the data at low  $n$  and there are some “outlier” points at higher  $n$ . Partition coefficients at higher  $n$  are more difficult to measure because the equilibrium is displaced to the water phase and the concentration in oil is very small. Note that the data in **Figure 4.4** consist of both 2 phase (20°C) and 3 phase systems (30-50°C), consistent with the phase diagram in Section 4.5.5.

#### **4.5.2 Equilibrium Partitioning of CK7 in the presence of CK3**

The partial replacement of CK7 with CK3 makes the binary surfactant mixture more hydrophobic than pure CK7. **Figure 4.5** shows the fitting of van't Hoff equation (**Equation 4.3**) for each oligomer of the mixture 3.75 wt.% CK3 and 3.75 wt.% CK7. It shows that enthalpy, proportional to slopes of the model fit, is constant for a given  $n$  value in the whole range of temperatures. Likewise, the linear relationship between  $\ln(K_n)$  and  $1/T$  indicates that the entropy is constant over 20-50 °C as well. Systems of pure CK7 have 3 phases in the temperature range 30-50°C and 2 phases at 20°C.

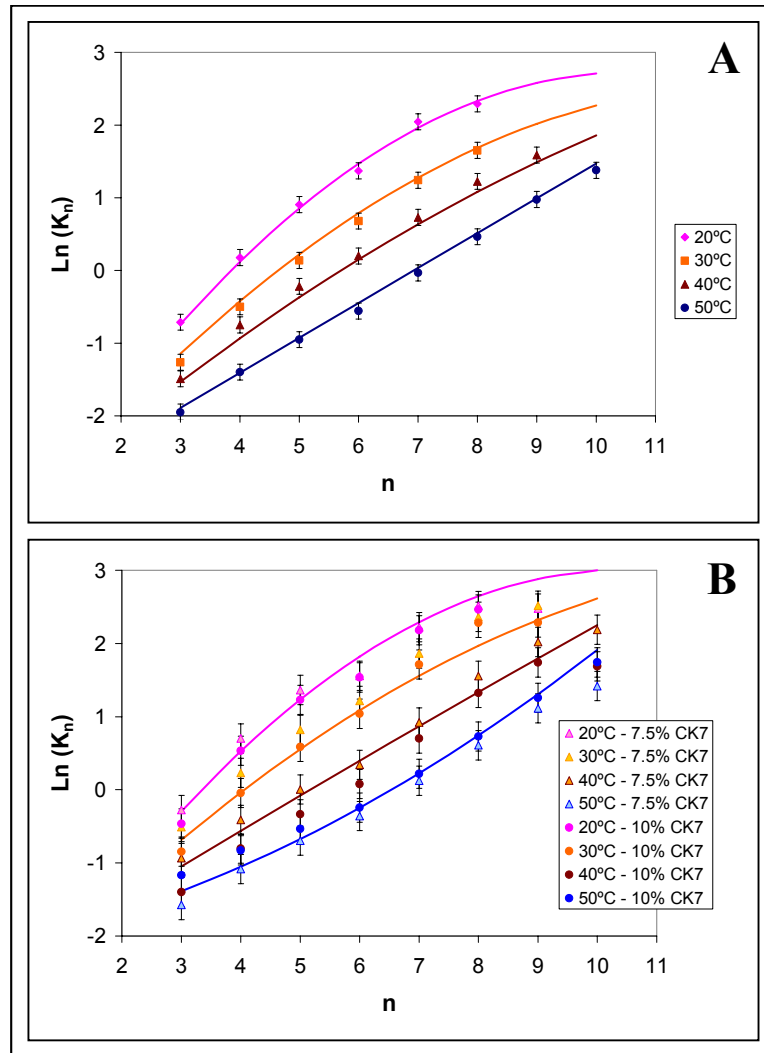


**Figure 4.4:** The effect of ethoxylate group size, surfactant concentration, and temperature on the partitioning of CK7. Data and values obtained by the semi-empirical model (Section 4.2). Natural logarithm of distribution constant ( $K_n=(C_{wn}/C_{on})$ ) for CK7 surfactant versus number of ethylene oxide unit as a function of temperature. A) 5 wt. % overall concentration of CK7. B) 7.5 wt. % and 10 wt. % overall concentration of CK7. 20°C is W-I and 30°C to 50°C are W-III system. Curves represent  $\ln(K_n)$  as predicted by the model (Section 4.2).

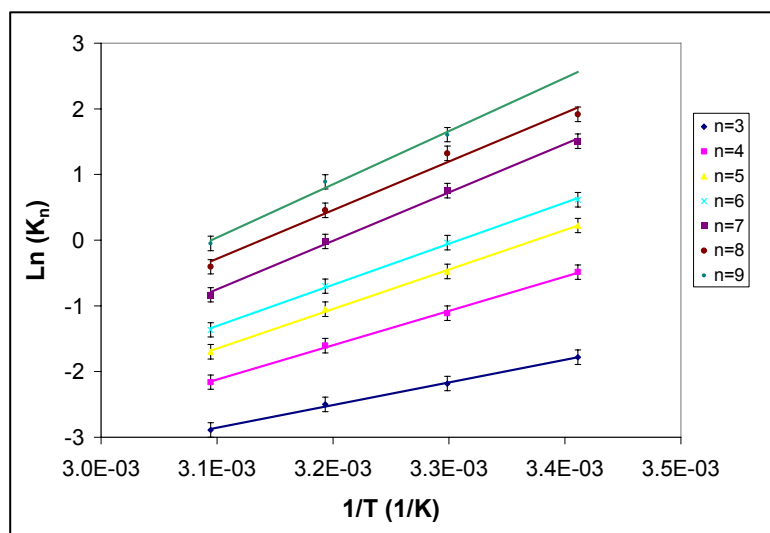


**Figure 4.5:** Fitting of van't Hoff equation (**Equation 4.3**) to the partition coefficient data obtained for the CK7 / CK3 mixed surfactant system. Natural logarithm of equilibrium constant  $K_n$  ( $C_{wn}/C_{on}$ ) versus inverse of the temperature. Concentrations are 3.75 wt.% CK7 and 3.75 wt.% CK3. Ethylene oxide degrees of polymerization, from 3 to 10 are represented as described in the legend. The lines represent the model fit (**Equation 4.3**) to the data.

Slopes and y-intercepts of **Equation 4.3** fitted in **Figure 4.5** are fitted to as a second order polynomial as function of the degree of polymerization, which is expressed by **Equations 4.8** and **4.9**, respectively.

Slopes for 3.75 wt. % CK3 and 3.75 wt. % CK7 (**Figure 4.5**):

$$-\frac{\Delta h_n}{R} = -78.2 \cdot n^2 + 1650 \cdot n - 500 \quad (4.8)$$

Intercepts for 3.75 wt. % CK3 and 3.75 wt. % CK7 (**Figure 4.5**):

$$\frac{\Delta s_n}{R} = 0.217 \cdot n^2 - 4.34 \cdot n - 3.35 \quad (4.9)$$

**Equations 4.8** and **4.9** are represented in **Figure 4.6** A and B, respectively (solid lines) together with the experimental data. The difference between these data and the previous data for pure CK7 (Figure 4.3) is that for high molecular weights the entropy and the enthalpy are larger. Enthalpy and entropy for the different single and binary surfactant systems are compared and contrasted in Section 4.6.2.

**Figure 4.7** displays the equilibrium partitioning of CK7 in presence of CK3. It can be observed when comparing the data in figures **Figure 4.4** and **Figure 4.7** that the equilibrium partitioning of the surfactant mixture is shifted by over an order of magnitude to the oil phase compared to samples composed of pure CK7. The only exception is the CK7 mixture with CK3 at 20°C and degree of polymerization higher than 8 for which equilibrium constants are in the same order of magnitude as pure CK7 at the same conditions. It means that the whole mixture is more hydrophobic after adding CK3, which would be expected. The reason of this phenomenon is because CK3 has shorter ethoxylate chain than CK7; so, it is more hydrophobic. If CK3 is added to a system composed of CK7, equilibrium exists between CK3 in excess phases (water and oil) and the interface. In other words, the concentration of CK3 will be higher in the interface than in a system with pure CK7 so that the mixture becomes more hydrophobic than pure CK7. Moreover, hydrophilicity of the surfactant mixture is a molar average of the surfactant species in the interface [72].

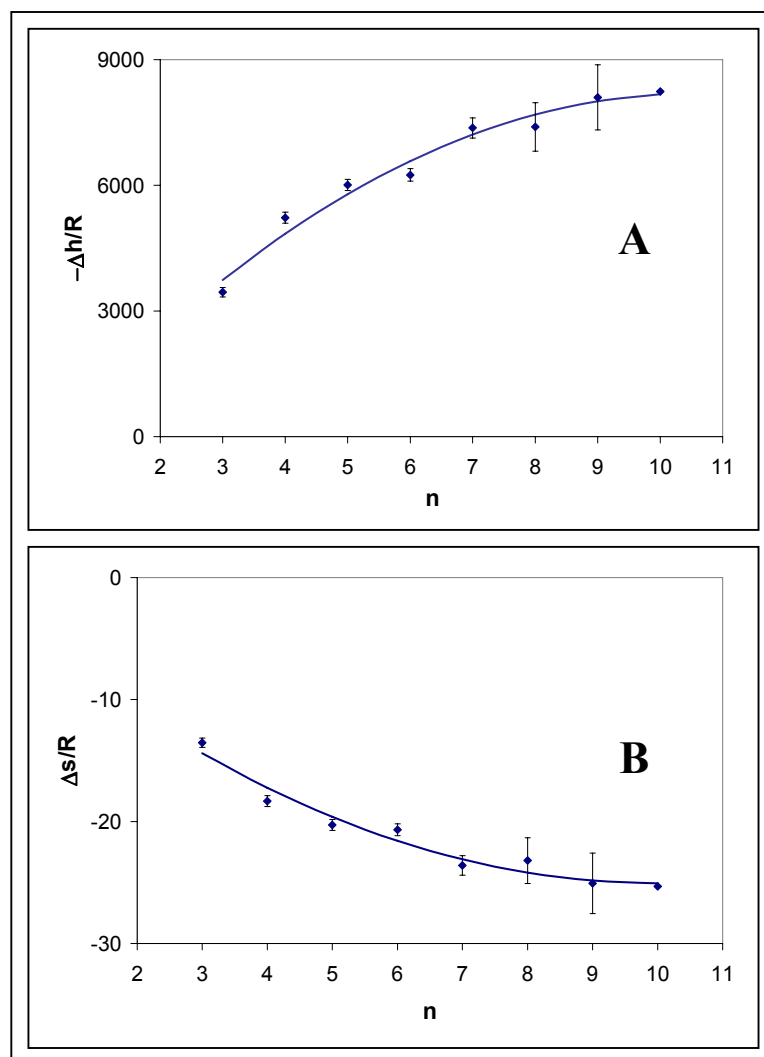


**Figure 4.6:** Enthalpy and Entropy values divided by the gas constant ( $R$ ) versus ethoxylate size for the CK7 / CK3 mixed surfactant system. Constants of van't Hoff equation obtained by fitting **Equation 4.3**. A) Slopes of fitted lines (**Equation 4.3**) in **Figure 4.5**. B) y-Intercepts of fitted lines (**Equation 4.3**) in **Figure 4.5**. Concentrations in both figures are 3.75 wt. % CK7 and 3.75 wt. % CK3 overall surfactant. Curve represents second-order polynomial fit to the data.

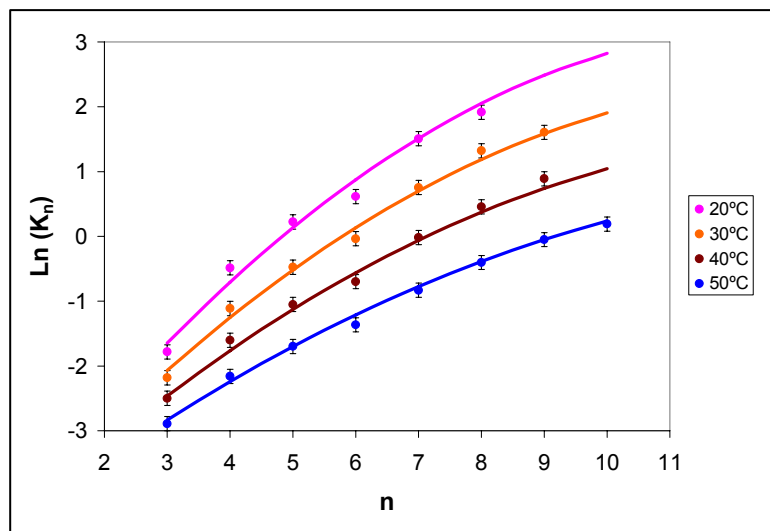


**Figure 4.7:** The effect of ethoxylate size and temperature on the partitioning data of the CK7 / CK3 mixed surfactant system. Data and values obtained by the semi-empirical model (Section 4.2). Natural logarithm of distribution constant ( $K_n=(C_{wn}/C_{on})$ ) for CK7 surfactant versus number of ethylene oxide unit as a function of temperature for a binary system of 3.75 wt.% CK7 and 3.75 wt.% CK3. Solvents are isooctane and deionized water. Solid lines are the model fitted to the data (Section 4.2).

### 4.5.3 Equilibrium of CK7 in the Presence of AOT

The effect of AOT upon the equilibrium partitioning of CK7 is a reduction of the influence of temperature on the partition coefficient and of the hydrophobicity of the surfactant mixture. **Figure 4.8** depicts the equilibrium partitioning of CK7 in samples with AOT in deionized water and isooctane utilizing 7.5 wt.% surfactant, and CK7 / AOT ratios of 1:1 and 1:4 (3.75 wt. % CK7 and 3.75 wt. % AOT, and 1.5 wt. % CK7 and 6 wt. % AOT, respectively). It can be observed in both sets of data that the equilibrium partitioning does not depend on the temperature. Data points in the graphs were collected at different temperatures between 20 and 50°C and overlap (Hence, van't Hoff plots cannot be made.) This observation is consistent with the observation of Alkhatib *et al.*

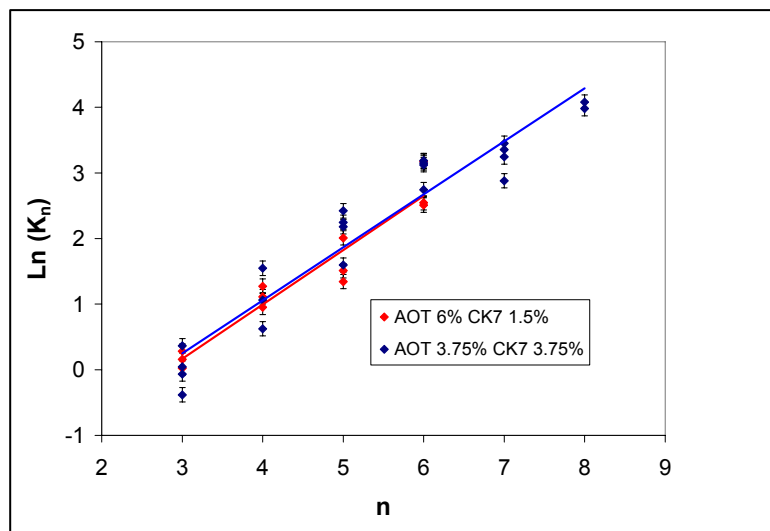


**Figure 4.8:** Natural logarithm of distribution constant ( $K_n=C_{wn}/C_{oiln}$ ) for CK7 surfactant versus number of ethylene oxide unit as a function of ethoxylate size for a binary system of (red) 6 wt. % AOT 1.5 wt. % CK7 and (blue) 3.75 wt. % AOT 3.75 wt. % CK7. Solvents are isooctane and deionized water. Lines are linear fitting to the data. Data points were obtained for temperatures from 20 °C to 50 °C.

that phase boundaries for CK7 / AOT mixed surfactant microemulsion systems are independent of the temperature [33]. Data points for a given value of  $n$  and CK/AOT ratio reflect a range of temperature of 20-50°C because the equilibrium is not a function of this variable in this particular system. Linear fitting of both sets of data nearly overlap. AOT partitioned strongly to the water phase, with the AOT content of the oil phase being below detection limits (data not shown). All the CK7-AOT systems investigated in this section have 3 phases in the temperature range 20-50°C except for one sample, 1.5 wt. % CK7, 6 wt. % AOT at 50°C, which has 2 phases.

In the presence of 1 wt. % NaCl (aq), temperature affected the equilibrium partitioning of CK7 for the CK7 / AOT binary system, but to a much smaller extent than that which occurred for pure CK7. **Figure 4.9** represents the fitting of van't Hoff equation for partition constant of CK7 in those samples. Systems of CK7 and AOT in 1.0 wt. % NaCl water solution have 2 phases in the temperature range 20-40°C and 3 phases at 50°C.



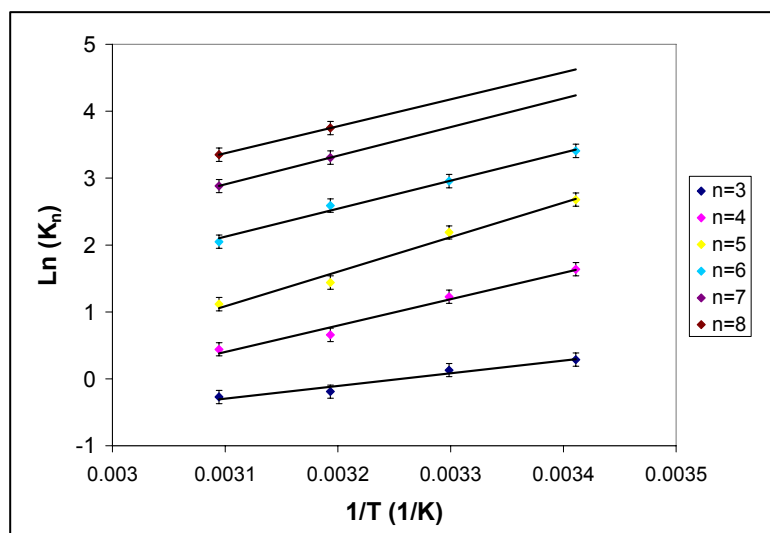


**Figure 4.9:** Fitting of van't Hoff equation (**Equation 4.3**) to the partitioning data of CK7 in the mixed CK7 / AOT system in the presence of salt. Natural logarithm of equilibrium constant  $K_n$  ( $C_{wn}/C_{on}$ ) versus inverse of the temperature is plotted. Concentrations are 3.75 wt.% CK7 and 3.75 wt.% AOT. Solvents are isooctane and 1 wt. % NaCl in water solution. Ethylene oxide degrees of polymerization, from 3 to 10 are represented as described in the legend. The lines represent the model fit (**Equation 4.3**) to the data.

Slopes derived from the fit of the van 't Hoff equation (**Equation 4.3**) applied to the data of **Figure 4.9**, displayed in **Figure 4.10**, are ~80% smaller than the  $-\Delta h/R$  values for pure CK7 (**Figure 4.3**), indicating that the addition of AOT to the system reduced the effect of the temperature on CK7 partitioning between water and oil. Values of enthalpy and entropy for this system are compared with the values obtained for other systems in Section 4.6.2.

**Figure 4.11** shows the equilibrium partitioning of CK7 in a system with AOT and 1 wt.% NaCl aqueous solution. The equilibrium partitioning is more dependent on the temperature in the presence of salt compared to salt-free systems (**Figure 4.8**), but not as much as the systems containing only CK7 (**Figure 4.4**). Solid lines in **Figure 4.11** fit data by substituting **Equations 4.10** and **4.11**, obtained empirically from **Figure 4.9** and substituted in **Equation 4.3**. AOT partitioned strongly to the oil phase, with the AOT content of the water phase being below detection limits, in contrast to the strong

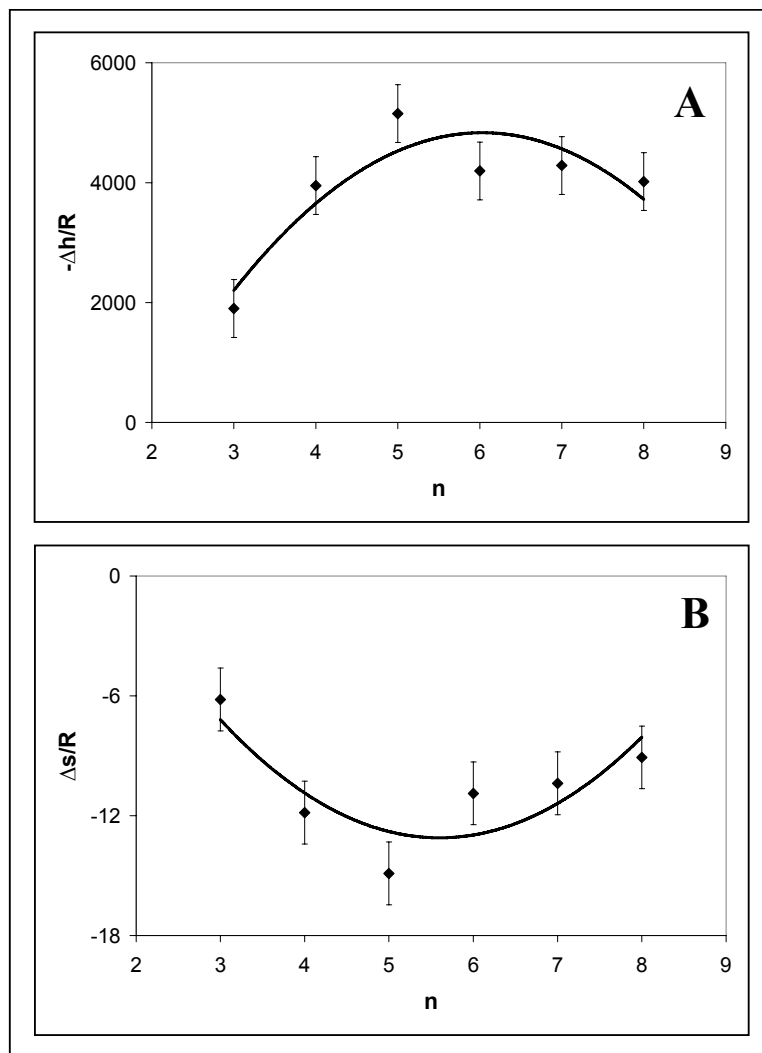


**Figure 4.10:** Enthalpy and Entropy values divided by the gas constant (R) versus ethoxylate size for the CK7 / AOT mixed surfactant system. Constants of van't Hoff equation obtained by fitting **Equation 4.3** to the partitioning data of CK7 for the mixed AOT / CK7 system in the presence of salt. A) Slopes of fitted lines (**Equation 4.3**) in **Figure 4.9**. B) Intercepts of fitted lines (**Equation 4.3**) in **Figure 4.9**. Concentrations are 3.75 wt.% CK7 and 3.75 wt.% AOT. Solvents are isooctane and 1 wt. % NaCl in water solution. Curve represents second-order polynomial fit to the data.

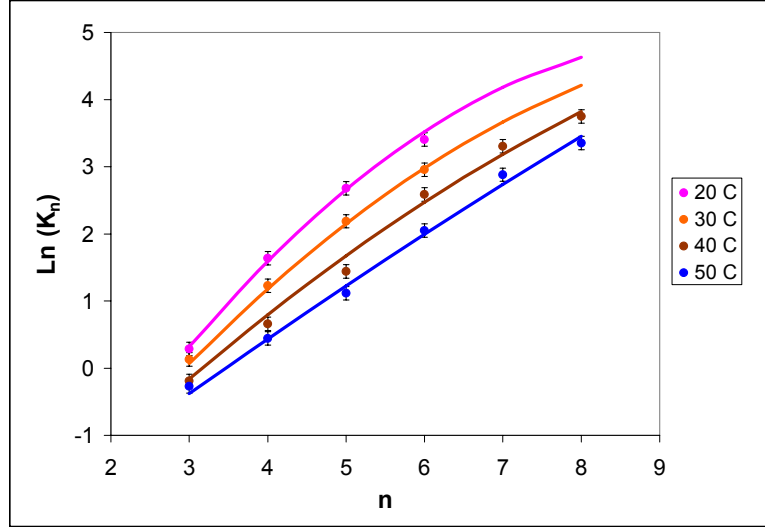


**Figure 4.11:** Effect of ethoxylate group size and temperature on the partitioning of CK7 for the AOT / CK7 mixed surfactant system in the presence of salt. Plotted are experimental data and values obtained by the semi-empirical model (Section 4.2). Natural logarithm of distribution constant ( $K_n = C_{wn}/C_{oiln}$ ) for CK7 surfactant versus number of ethylene oxide unit as a function of temperature for a binary system of 3.75 wt. %CK7 and 3.75 wt. % AOT. Solvents are isooctane and 1 wt. % NaCl in water solution. Solid lines are the model fitted to the data.

partitioning of AOT to the aqueous phase in the absence of salt (data not shown)

Slopes for 3.75 wt. % AOT and 3.75 wt. % CK7 with NaCl solution from **Figure 4.10**

$$-\frac{\Delta h_n}{R} = -286 \cdot n^2 + 3500 \cdot n - 5600 \quad (4.10)$$

Intercepts for 3.75 wt. % AOT and 3.75 wt. % CK7 with NaCl solution from **Figure 4.10:**

$$\frac{\Delta s_n}{R} = 0.875 \cdot n^2 - 9.80 \cdot n + 14.24 \quad (4.11)$$

#### 4.5.4 Equilibrium of CK7 in the presence of $C_8\beta G_1$

$C_8\beta G_1$  is a hydrophilic surfactant so is expected that it will partition to the bottom phase and also promote the partition of CK7 to the bottom phase.

**Figure 4.12** is the representation of van't Hoff equation (**Equation 4.3**) of each surfactant molecule in the mixture 3.75 wt. %  $C_8\beta G_1$  and 3.75 wt.% CK7. It shows that enthalpy, proportional to slopes of the model fit, and entropy, proportional to the intercepts of the model fit. Likewise, the linear relationship between  $\ln(K_n)$  and  $1/T$  indicates that the entropy is constant over 20-50°C for each degree of polymerization “ $n$ ” as well. Systems of CK7 and  $C_8\beta G_1$  in water have 3 phases in the temperature range 20-40°C and 2 phases at 50°C.

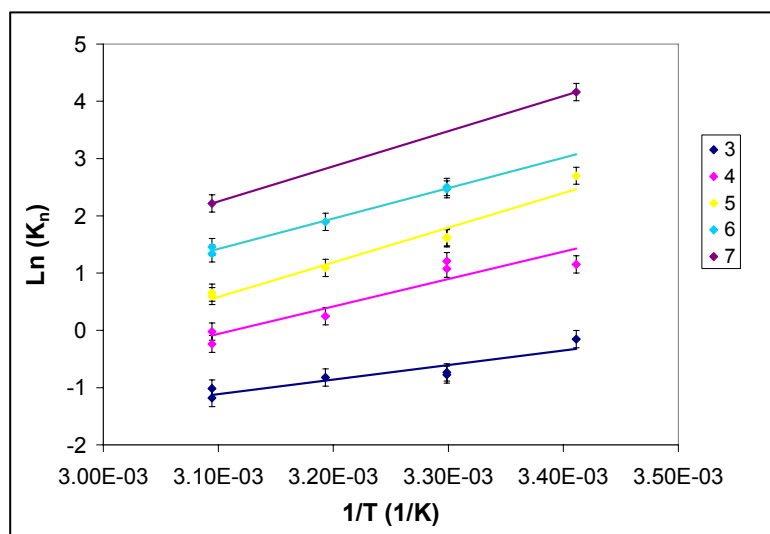


**Figure 4.12:** Fitting of van't Hoff equation (**Equation 4.3**) to the partitioning data of CK7 in the mixed CK7 /  $C_8\beta G_1$  system in the presence of salt. Natural logarithm of equilibrium constant  $K_n$  ( $C_{wn}/C_{on}$ ) versus inverse of the temperature is plotted. Concentrations are 3.75 wt. % CK7 and 3.75 wt. %  $C_8\beta G_1$ . Solvents are isooctane and deionized water. Ethylene oxide degrees of polymerization, from 3 to 10 are represented as described in the legend. The lines represent the model fit (**Equation 4.3**) to the data.

**Figure 4.13** depicts the the  $\Delta h/R$  and  $\Delta s/R$  values, obtained from the slopes and intercepts of data in **Figure 4.12**, respectively, as a function of polymerization degree “ $n$ ”. The data of **Figure 4.13** were fit with quadratic equations, expressed in **Equations 4.12** and **4.13** for  $\Delta h /R$  and  $\Delta s/R$ , respectively. Intercepts ( $\Delta s/R$  values) of van't Hoff equation (**Figure 4.12**) calculated to the system of 3.75 wt.% CK7, 3.75 wt.%  $C_8\beta G_1$ , isooctane and deionized water (**Figure 4.13**) are slightly smaller than slopes of van't Hoff equation calculated for pure CK7 (**Figure 4.3**). Enthalpy and entropy from all surfactant mixtures are compared in Section 4.6.2

Slopes for 3.75 wt. %  $C_8\beta G_1$  and 3.75 wt. % CK7 from **Figure 4.12**:

$$-\frac{\Delta h_n}{R} = -340 \cdot n^2 + 4200 \cdot n - 6800 \quad (4.12)$$

Intercepts for 3.75 wt. %  $C_8\beta G_1$  and 3.75 wt. % CK7 from **Figure 4.12**:

$$\frac{\Delta s_n}{R} = 1.05 \cdot n^2 - 12.0 \cdot n + 17.1 \quad (4.13)$$

**Figure 4.14** shows equilibrium partitioning data between water and isooctane of 3.75 wt.% CK7 in presence of 3.75 wt.%  $C_8\beta G_1$ . The equilibrium partitioning of CK7 is shifted to the aqueous phase compared to pure CK7. This is expected because  $C_8\beta G_1$  is more hydrophilic than CK7 so the whole surfactant mixture is more hydrophilic. The dependence on the temperature is slightly smaller in the mixture than for pure CK7. The slope of the  $\ln K-n$  profile is higher than that for pure CK7. Therefore, the affinity of the ethoxylate chain for the water is increased by the presence of  $C_8\beta G_1$  respect to its affinity in a system with pure CK7. Solids lines in **Figure 4.14** fit data by substituting **Equations 4.12** and **4.13**, obtained empirically from **Figure 4.12** and substituted in **Equation 4.3**.

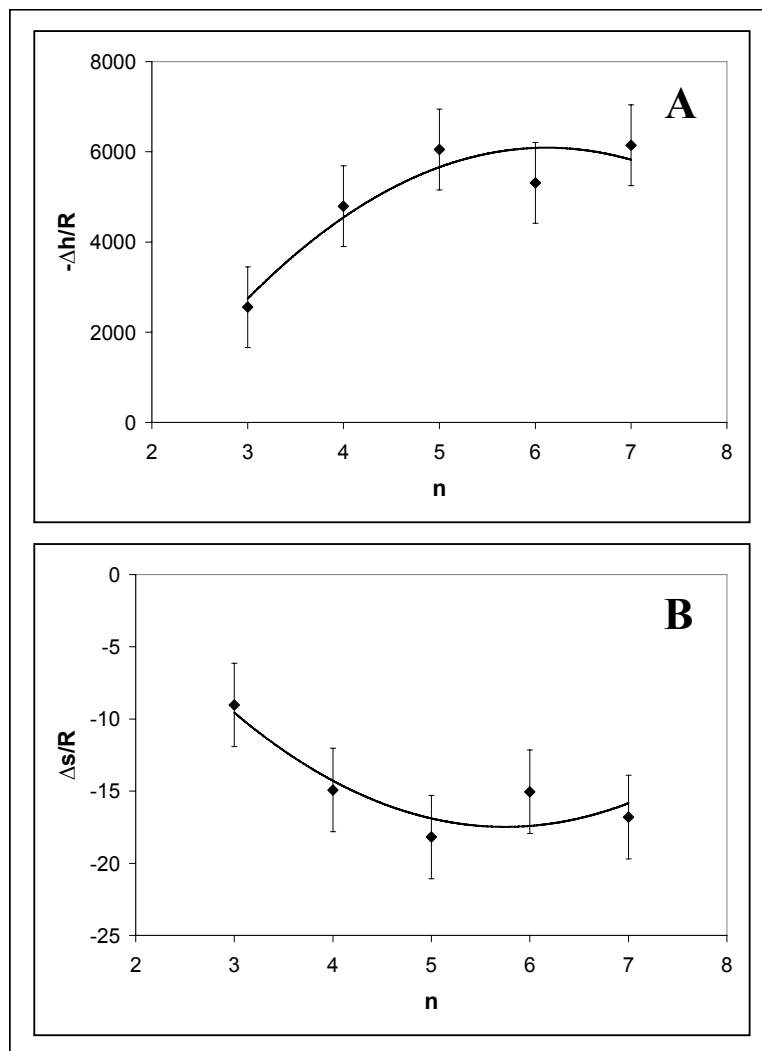


**Figure 4.13:** Enthalpy and Entropy values divided by the gas constant (R) versus ethoxylate size for the CK7 /  $C_8\beta G_1$  mixed surfactant system. Constants of van't Hoff equation obtained by fitting **Equation 4.3** to the partitioning data of CK7 for the mixed CK7 /  $C_8\beta G_1$  system. A) Slopes of fitted lines (Eq. 4.3) in **Figure 4.12**. B) Intercepts of fitted lines (Eq. 4.3) in **Figure 4.12**. Concentrations are 3.75 wt. % CK7 and 3.75 wt. %  $C_8\beta G_1$ . Solvents are isooctane and water. Curve represents second-order polynomial fit to the data.

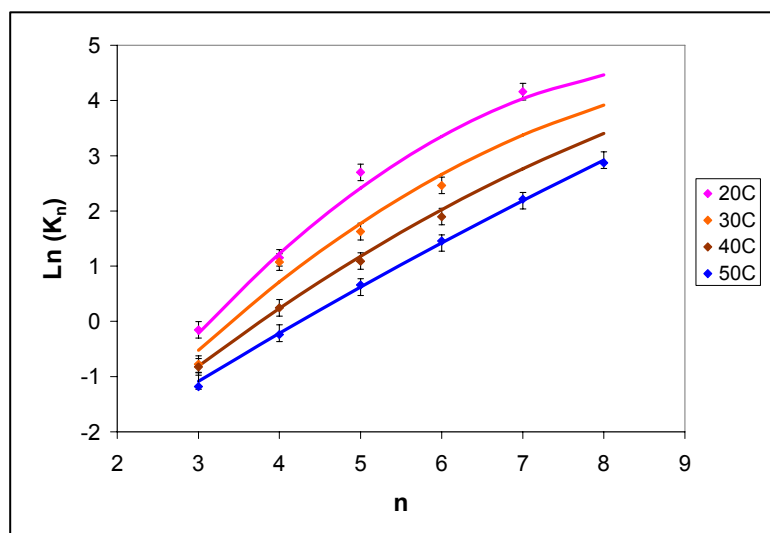


**Figure 4.14:** Effect of ethoxylate group size and temperature on the partitioning of CK7 for the AOT /  $C_8\beta G_1$  mixed surfactant system. Plotted are experimental data and values obtained by the semi-empirical model (Section 4.2). Data and values obtained by the semi-empirical model (Section 4.2). Natural logarithm of distribution constant ( $K_n=(C_{wn}/C_{on})$ ) for CK7 surfactant versus number of ethylene oxide unit as a function of temperature for a binary system of 3.75 wt. %CK7 and 3.75 wt. %  $C_8\beta G_1$ . Solvents are isooctane and water. Solid lines are the model fitted to the data.

#### 4.5.5 CK7 Phase Diagram

The phase diagram of the CK7/water/isooctane system versus temperature was conducted in order to determine the number of phases that occur for the conditions employed in the surfactant partitioning experiments, and to estimate the PIT. **Figure 4.15** shows part of the “fish” diagram [48] (Section 2.3.2), which consists of temperature versus surfactant concentration for a constant water/oil weight ratio of 1/1 g/g. The diagram indicates the regions of 1 (W-IV), 2 (W-I and W-II) or 3 phases (W-III).

The lower limit of the W-III region is 21°C, slightly higher than the minimum experimental temperature of 20°C. In other words, samples at 20°C have 2 phases and all the other samples of pure CK7 have 3 phases. In **Figure 4.15** can be observed also that PIT at high concentration of surfactant is approximately 41°C. This is in the temperature

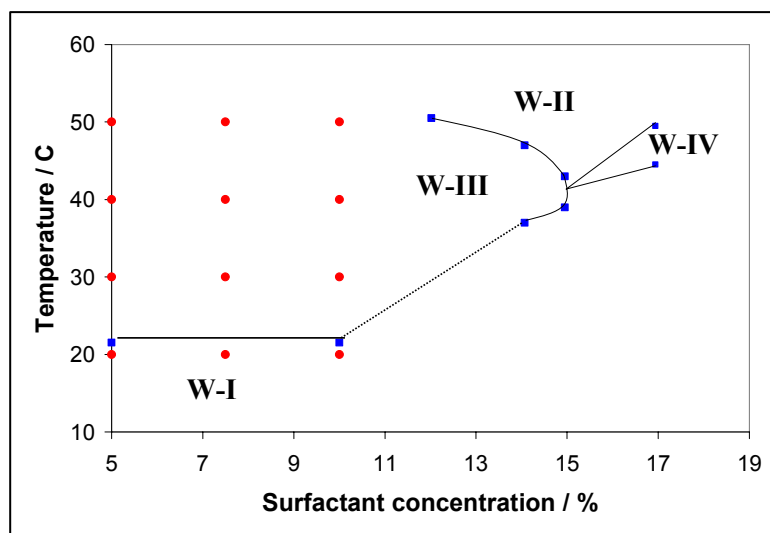


**Figure 4.15:** Part of fish diagram of CK7 in isooctane / water system. Water: isooctane ratio held constant at 1:1  $\text{g g}^{-1}$ . Blue dots are phase transition and red dots are concentration and temperature of samples used in pure CK7 equilibrium. Dotted lines represent approximate positions of phase boundaries

corresponding to the “neck” of the “fish”. The percentage of surfactant corresponding to the neck,  $\sim 14$  wt.%, is a measure of the surfactant’s efficiency.

## 4.6 Discussion

### 4.6.1 Use of Thermodynamic Model to Predict Phase Inversion Temperature

A thermodynamic model was developed that can predict equilibrium partitioning of CK7 molecules between water and oil as a function of the degree of polymerization. This model is based in part on theory developed by Marquez *et al.* [69, 70] where they use an “optimal” composition of linear and phenyl alkyl ethoxylates to calculate the equilibrium partitioning between water and oil. The optimal composition refers to the



affinity of the surfactant mixture being equal between water and oil, determined by mixing homogeneous ethoxylate surfactants of a specified ethoxylate size from the same homologous series of surfactant molecules and determining the proportion that maximizes the solubilization of water and oil in the middle phase. Moreover, the only microemulsion formation by surfactants would occur in the middle (bicontinuous microemulsion) phase; and, oil and water would have only monomeric surfactant.

**Equation 14** is the general expression of **Equations 4.4, 4.6, 4.8, 4.10** and **4.12**.

$$\frac{\Delta h_n}{R} = \frac{A}{R} \cdot n^2 + \frac{B}{R} \cdot n + \frac{C}{R} \quad (4.14)$$

**Equation 4.15** is obtained from rearranging **Equation 4.14**

$$\Delta h_n = A \cdot n^2 + B \cdot n + C \quad (4.15)$$

Coefficients of **Equation 4.15** for the systems studied in the work reported in this chapter are shown in **Table 4.1**.

**Equation 4.16** is the general expression of **Equations 4.5, 4.7, 4.9, 4.11** and **4.13**.

$$\frac{\Delta s_n}{R} = \frac{A'}{R} \cdot n^2 + \frac{B'}{R} \cdot n + \frac{C'}{R} \quad (4.16)$$

**Table 4.1:** Coefficients of second order polynomial used to calculate molar enthalpy ( $\Delta h_n$ ) in function of number of ethoxylate monomeric units for single and binary surfactant systems, Eq. 15. Units: ( $\text{J mol}^{-1}$ ).

Surfactant concentration	A	B	C
5% CK7	1500	-21000	18000
7.5% and 10% CK7	2100	-28000	36000
3.75% CK3 and 3.75% CK7	600	-14000	5000
3.75% AOT and 3.75% CK7	2300	-29000	47000
3.75% C8G1 and 3.75% CK7	2800	-36000	57000

**Table 4.2:** Coefficients of second order polynomial used to calculate molar entropy ( $\Delta s_n$ ) in function of number of ethoxylate monomeric units for single and binary surfactant systems, **Equation 4.16**. Units: ( $\text{J mol}^{-1} \text{K}^{-1}$ ).

Surfactant concentration	A'	B'	C'
5% CK7	4.9	-60	28
7.5% and 10% CK7	6.8	-85	92
3.75% CK3 and 3.75% CK7	1.8	-36	-28
3.75% AOT and 3.75% CK7	7.3	-81	119
3.75% C8G1 and 3.75% CK7	8.7	-100	142

**Equation 4.17** is obtained from rearranging **Equation 4.16**

$$\Delta s_n = A' \cdot n^2 + B' \cdot n + C' \quad (4.17)$$

Coefficients of **Equation 4.17** for the systems studied in this chapter are shown in **Table 4.2**.

The consequence of having monomers in both of the excess phases, water and oil, is that adding an ethoxylate unit to a surfactant molecule increases the latter's affinity to the aqueous excess phase. The addition of 1 ethoxylate unit to a surfactant molecule increases the energy of transferring it from oil to water [69], equal to the breakage of van der Waal's attractive forces between the surfactant molecule and oil molecules and the formation of hydrogen bonds between the surfactant's head group and water, in the absence of surfactant self-assembly aggregates. The Gibbs' free energy change for this process,  $\Delta g_n$ , is constant, given that temperature, pressure, and the number of moles of each chemical species in the system remain constant. Moreover,  $\Delta g_n$  is independent of the size of the surfactant's ethoxylate group,  $n$ , for systems where no surfactant aggregates form in the excess phases. The "optimal" conditions coincide with a system existing at its PIT. Thus, since  $\ln(K_n)$  is proportional to  $\Delta g_n$ ,  $\ln(K_n)$  increases linearly with  $n$ . In contrast, if the system is not in the "optimal" condition, the surfactant molecule can exist as a monomer in the aqueous phase or in the oil phase or as a component of a micelle or microemulsion in one of the excess phases. Therefore, the relationship between  $\ln(K_n)$  and  $n$  is more complex and is not a straight line.

The linear  $\ln(K_n)$ - $n$  relationship for systems at “optimal” conditions (i.e., at the PIT) is used in this work to calculate the PIT for CK7-based surfactant mixtures of a specified surfactant composition which is not necessarily at “optimal” conditions. Since at the PIT the  $\ln(K_n)$ - $n$  relationship is linear, the second-order terms of the equations fitted to calculate  $\Delta g$  have to equal 0. If **Equation 4.15** and **4.17** are substituted into **Equation 4.3**, **Equation 4.18** is obtained.

$$\ln(K_n) = -\frac{A \cdot n^2 + B \cdot n + C}{R \cdot T} + \frac{A' \cdot n^2 + B' \cdot n + C'}{R} \quad (4.18)$$

**Equation 4.19** is obtained by rearranging **Equation 4.18**.

$$\ln(K_n) = \left[ \left( A' - \frac{A}{T} \right) \cdot n^2 + \left( B' - \frac{B}{T} \right) \cdot n + \left( C' - \frac{C}{T} \right) \right] \cdot \frac{1}{R} \quad (4.19)$$

In order to have a straight line if  $\ln(K_n)$  is plotted versus degree of polymerization, the coefficient of the second order term has to equal 0 (**Equation 4.20**).

$$A' - \frac{A}{T} = 0 \quad (4.20)$$

This restriction leads to **Equation 4.21**, where  $T_{opt}$  is the temperature at which the surfactant mixture is the optimal composition. This temperature is approximately equal to the PIT.

$$T_{opt} = \frac{A}{A'} \quad (4.21)$$

Values of  $T_{opt}$  calculated using **Equation 4.21** are listed in **Table 4.3**

**Table 4.3:** Phase inversion temperature calculated by using the thermodynamical model fitted to data.

Surfactant concentration	K	°C
5% CK7	323	50
7.5% and 10% CK7	314	41
3.75% CK3 and 3.75% CK7	361	88
3.75% AOT and 3.75% CK7	328	54
3.75% C8G1 and 3.75% CK7	328	55

An interesting result displayed in **Table 4.3** is that the calculated PIT of pure CK7 (41°C) at 7.5 wt. % and 10 wt. %, agrees with the value suggested by the “fish” phase diagram (**Figure 4.15** in Section 4.5.5).

The PIT of a given water/oil/alkyl ethoxylate-based surfactant mixture system is not constant with respect to surfactant concentration, particularly when the ethoxylate surfactants possess a broad distribution of degree of polymerization. Moreover, the PIT increases as the ethoxylate surfactant concentration decreases. In other words, the PIT temperature is higher for the “nose” of the “fish” diagram than for its “neck” (Ghoulam *et al.* [49], and Section 2.3.2). This phenomenon can be observed for CK7. At 5 wt. % CK7, the PIT is approximately 9°C higher than the PIT for 7.5 wt. % and 10 wt.% CK7 (**Table 4.3**). The increase of PIT with a decrease of surfactant concentration may serve as the underlying reason for the high value of PIT obtained for the mixture 3.75 wt.% CK3 (81°C) compared to low concentrations of CK7 (50°C for 5 wt. % CK3; **Table 4.3**). A lowering of the PIT by the replacement of 3.75 wt. % CK7 by CK3 was expected due to the increase of hydrophobicity that occurs. The replacement of CK7 by CK3 reduces the CK7 concentration by 50%, which would increase the PIT according to the above-mentioned principle. So the dilution effect that occurs when replacing a portion of CK7 by CK3 seems to be a stronger determinant of the change of PIT than the effect of increasing the hydrophobicity of the surfactant mixture.

The lowering of the PIT by increasing the hydrophobicity of the surfactant mixture is more evident for the replacement of 50 wt. % CK7 by AOT in the presence of 1 wt. % NaCl in water. The increase of ionic strength reduces the strength of AOT's

**Table 4.4:** Effect of surfactant characteristics present in the interface on the PIT.

Mixture characteristic	Effect on PIT
Decreasing the concentration of CK7	Increase
Hydrophilicity	Increase
Hydrophobicity	Reduce

sulfonate head group through Debye shielding. Therefore AOT becomes more hydrophobic. For these systems, AOT is more hydrophobic than CK3, inferred from the fact that AOT is not detectable in water phase (Section 4.5.3) but CK3 at a similar concentration is present in water phase (Section 4.5.2). In agreement, the PIT calculated from the data using CK7 / AOT in the presence of NaCl (54°C) is lower than the value for CK7 / CK3 (88°C; **Table 4.3**). The PIT of CK7-AOT and CK3-AOT mixtures are higher than pure CK7 at 7.5 wt. % or 10 wt. % CK7 (41°C) because of the dilution effect, moreover, the increase of PIT with a decrease of ethoxylate surfactant concentration. The increase of PIT 55°C, **Table 4.3**) by replacing part of CK7 by C<sub>8</sub>βG<sub>1</sub>, approximately 14°C, is consistent with the dilution of the CK7 concentration, as discussed above, and the increase of hydrophilicity imparted by the glucoside surfactant. **Table 4.4** is a summary of the effect of the characteristics of the interface mixture of surfactants. Surfactants more hydrophobic than CK7, such as CK3 or AOT with NaCl, reduce the PIT; surfactants more hydrophilic than CK7, such as C<sub>8</sub>βG<sub>1</sub> and AOT in the absence of salt increase the PIT, and a reduction of the concentration of CK7, such as comparing the 7.5 wt. % data to the 5 wt. %, increases the PIT.

#### 4.6.2 Thermodynamic properties

**Figure 4.16** displays the enthalpy and entropy of transferring a mole of CK7 with ethoxylate size “n” from oil to water calculated in this work. It can be observed that for CK7 molecules with lower ethoxylate molecular weight,  $3 \leq n \leq 6$ , the enthalpies are very similar to each other for the single and binary surfactant systems. It means that the

forces involved in transferring the molecules are similar. The exception to this statement is for the CK7 / AOT system in the presence of 1 wt. % NaCl(aq), which is a more hydrophobic surfactant mixture than all the others used in this work. Smaller values of the absolute value of  $\Delta h_n$  for the CK7/AOT mixture could be explained by formation of micelles and/or microemulsions in the top phase which would decrease the energy of transferring a molecule from oil phase to water phase. For degrees of polymerization larger than 6 the mixture 3.75 wt. % CK3 and 3.75 wt. % CK7 has a significantly higher absolute value of  $\Delta s_n$ , which probably means that there are fewer micelles and/or microemulsions in the aqueous excess phase and surfactant molecules dissolve predominantly in water as monomers.

In order to analyze the thermodynamic behavior of the systems studied the following situation was considered: a molecule of CK7 dissolved in oil is transferred to a micelle or microemulsion in water. This assumption is based on the fact that most of the systems studied are below the PIT. De Maeyer *et al.* reach to the conclusion that the two main changes in entropy for the aggregation of surfactants in micelles are due to the “hydration of a hydrophobic hydrocarbon”, which drives the formation of micelles, and the “translational degrees of freedom”, which opposes to the formation of micelles[73]. The molecules lose translational degrees of freedom when they move from oil (monomer) to water (micelles) because the molecules are constricted to the micelle volume instead of free solvent volume. Hydration of a hydrophobic hydrocarbon does not exist in this analysis because the monomeric molecules are dissolved in isooctane. Therefore, the entropy reduction due to translational degrees of freedom is compensated by the enthalpy reduction due to the hydrogen bonds that form between water and the ethoxylate chain. The addition of  $C_8\beta G_1$  can have two effects, to modify the structure of the water molecules of hydration for CK7's ethoxylate groups and in that way increase the affinity of the ethoxylate chain to the water, and to increase the number of micelles or microemulsions in aqueous phase. If the number of micelles or microemulsions is increased, it would drive the partitioning of surfactant molecules to the self-assembly state and thus the entropy reduction would be smaller. It would explain the smaller absolute value of  $\Delta s_n$  of the CK7 molecules in the mixture with  $C_8\beta G_1$  that can be observed in **Figure 4.16**.

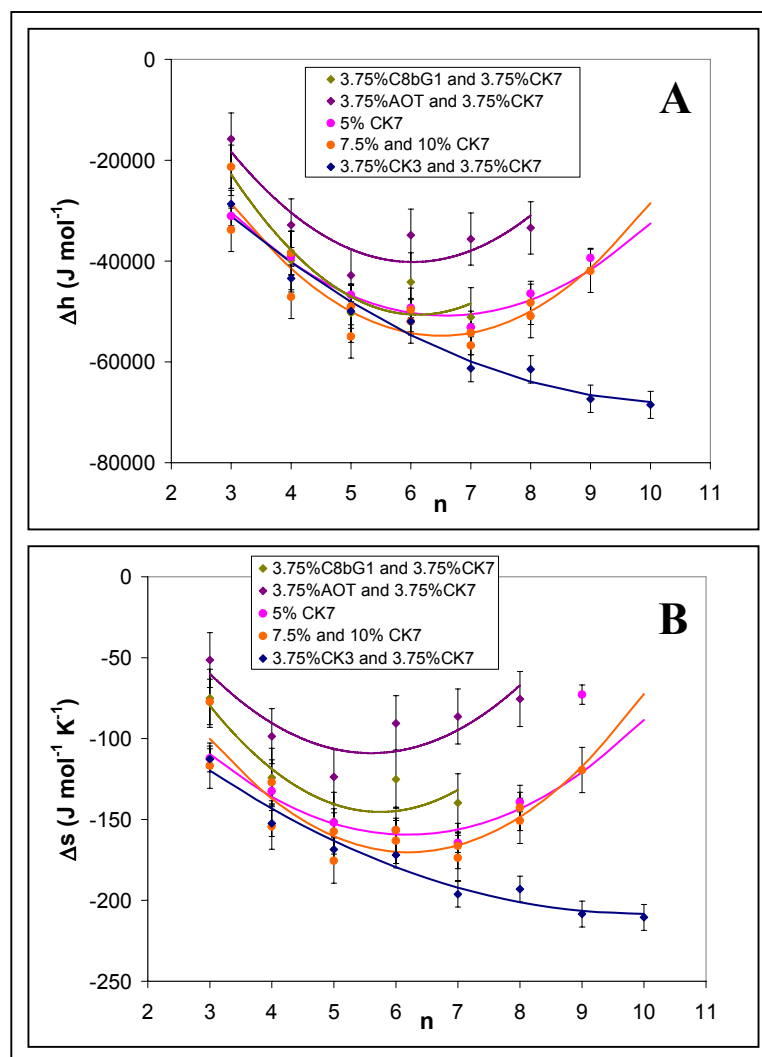


**Figure 4.16:** A) Enthalpy and B) entropy of transferring a molecule from oil to water. Dots are calculated from measured data and solid lines are second order polynomial fitted to the data. Each color corresponds to the concentration of surfactants described in the legend.

**Table 4.5:** Root mean square error (RMSE) of the  $\ln(K_n)$ ,  $\Delta h$  ( $\text{J mol}^{-1}$ ) and  $\Delta s$  ( $\text{J mol}^{-1} \text{K}^{-1}$ ) calculated for each surfactant mixture.

Surfactant concentration	$\ln(K)$	$\Delta h$ ( $\text{J mol}^{-1}$ )	$\Delta s$ ( $\text{J mol}^{-1} \text{K}^{-1}$ )
5% CK7	0.11	1869	6.0
7.5% and 10% CK7	0.20	4292	13.3
3.75% CK3 and 3.75% CK7	0.11	2665	7.9
3.75% AOT and 3.75% CK7	0.10	5133	17.2
3.75% C8G1 and 3.75% CK7	0.15	5745	17.5

### 4.6.3 Model Validation

Validation of the model was done by calculating the root mean square error (RMSE) (**Equation 4.21**), provided in **Table 4.5**.

$$RMSE = \sqrt{\frac{1}{N} \sum_{i=1}^N (x_i - x_{mi})^2} \quad (21)$$

In **Equation 4.21**  $N$  is the number of samples,  $x_i$  is measured value and  $x_{mi}$  is the value calculated by the model. The error was calculated for each mixture of surfactant because they were fitted with different constants.

There is a very good agreement between the semi-empirical model and the data. The root mean square error of  $\ln(K)$  represents 5% percent of the range of data in the worst case (**Figure 4.4**, **Figure 4.7**, **Figure 4.11** and **Figure 4.14**). The root mean square error of  $\Delta h$  and  $\Delta s$  is approximately 10% of the value calculated and measured.

## 4.7 Conclusions

Equilibrium partitioning data of CK7 between water and oil in single surfactant systems can be described by **Equation 4.3** after determining empirical relationships



between enthalpy/mol ( $h_n$ ) and entropy/mol ( $s_n$ ) versus  $n$ . The models developed can fit data well for the whole range of the temperatures (20-50°C) and CK7 concentration (5-10 wt. %) for pure CK7. Trends found in these experiments are consistent with theory. The partitioning is more favorable to the water at higher ethoxylate size and lower temperature because the head group of the surfactant becomes more hydrophilic. Also the PIT can be calculated from partition data.

The addition of a second surfactant to CK7 changes the equilibrium partitioning in an expected way in the mixtures tested in this work. CK3, which is more hydrophobic than CK7, shifts the equilibrium partitioning of CK7 to the oil phase. In contrast, C<sub>8</sub>βG<sub>1</sub>, which is more hydrophilic, shifts the equilibrium partitioning to the water phase, which is not desired if the goal is formation of 3-phase systems. AOT has the desired property of reducing the sensitivity to the temperature of the ethoxylated surfactant.

## CHAPTER 5

### PROTEIN FORWARD EXTRACTION

#### *5.1 Introduction*

Protein extraction using Winsor III (W-III) systems is used in this work as an improvement of traditional Winsor II-based extraction in which proteins are encapsulated into reverse micelles because the former system's bicontinuous microemulsion phase possesses larger interfacial area [47] and water solubilization capacity [1], therefore, leading to higher protein capacity.

Protein extraction was conducted using W-III systems formed by equal volumes of water and oil, and 1 wt.% of a binary or ternary surfactant mixture of CK7, AOT, and CK3. The extraction and disengagement of the phases were fast, less than 30 seconds, and the partition coefficient for protein solubilization in the middle phase was high. More than 95 % of the protein was recovered in the middle phase, and the latter's protein concentration was 5 times higher than the concentration of the original solution. The increase in the concentration is due to the small size of the middle phase, approximately 15% of the whole system volume, with the exact percentage tuned by selecting the relative proportions of the surfactants. The middle phase volume also depends on the protein type and concentration extracted.

Stable W-III systems used for protein extraction, formed using equal volume amounts of water and isooctane and 1 wt.% of a CK7/AOT surfactant mixture, did not occur at room temperature due to the surfactant mixture's relatively strong hydrophilicity. However, by using three different approaches to increase hydrophobicity, stable W-III systems occurred. The first was employing a temperature higher than ambient, e.g., 40°C, near CK7's PIT, 41°C (Section 4.5.5 and 4.6.1). The second was adding CK3, which is a surfactant more hydrophobic than CK7, to the previous system to reduce the phase

inversion temperature (PIT) to near 25°C. The third was increasing the hydrophobicity of AOT by using NaCl in the aqueous phase. The last method induced a PIT of near 25°C without requiring the addition of CK3 or the elevation of the temperature. Adding CK3 to the system complicates the phase behavior making it difficult to predict the PIT and raising the temperature can deactivate the protein.

Most of the samples were prepared with an aqueous protein solution of a concentration 1 g/l. Only for the third method, AOT hydrophobicity tuned by NaCl, were different concentrations of proteins employed, with the goal being to find the highest concentration achievable in the middle phase and the highest partitioning of protein to the middle phase. Knowing the level of protein saturation for the middle phase is useful in order to have the highest recovery of activity after back extraction. When the middle phase reaches saturation protein-surfactant complex forms and then precipitates and has reduced biological activity (Chapter 6).

## **5.2 *Materials***

The solvents used to equilibrate the surfactant were isooctane Fisher HPLC grade and deionized water 18 M $\Omega$  x cm of resistivity. The alkyl ethoxylate surfactants employed contained poly(ethylene glycol) monomethyl ether as the hydrophile and a cyclic ketal as the hydrophobe [5] synthesized in the lab (Chapter 3). Sodium bis(2-ethylhexyl) sulfosuccinate, AOT, anhydrous, was purchased from Fisher Scientific, Fair Lawn, NJ. All the proteins: lysozyme from chicken egg white (three times crystallized, dialyzed and lyophilized, containing approximately 95% protein with the balance being primarily buffer salts),  $\alpha$ -chymotrypsin from bovine pancreas (three times crystallized from four times crystallized chymotrypsinogen; dialyzed, essentially salt free and lyophilized powder), pepsin from porcine stomach mucosa (purified by crystallization followed by chromatography, essentially salt free and lyophilized powder), cytochrome c

from horse heart (dialyzed and lyophilized), bovine serum albumin (BSA, lyophilized) were from Sigma, St. Louis, MO.

### **5.3 *Methods***

#### **5.3.1 Forward Extraction of Protein**

##### **5.3.1.1 CK7/AOT Surfactant System, Using Super-Ambient Temperature**

Extraction of proteins by using W-III system obtained by the first method mentioned, which is tuning the hydrophobicity of the surfactants by temperature, was done at 40°C. Concentration of surfactants was between 6.45 wt. % and 3.03 wt. % of overall mass. Surfactants were dissolved in isooctane, and proteins dissolved in a pH 7 0.1 M phosphate buffer. Equal volumes of each solution were gently mixed manually in 2 mL plastic vials. After a few minutes the phases were completely separated but samples were equilibrated in a thermostatic bath, model Isotemp 3028 from Fisher Scientific at 40°C for 24 hours to assure thermodynamic equilibrium.

##### **5.3.1.2 CK7/AOT/CK3 Surfactant System at 25°C**

The second method of forward extraction consisted of replacing part of CK7 by CK3 in order to reduce the PIT. Lysozyme,  $\alpha$ -chymotrypsin, cytochrome c, and pepsin

were extracted at 25°C. Concentration of surfactants were 0.3 wt. % CK7, 0.4 wt. % CK3 and 0.3 wt. % AOT with respect to whole system. These consist of mild conditions for the protein and the chemo-labile surfactants CK7 and CK3. Other conditions and procedures are identical to those of Section 5.3.1.1.

### **5.3.1.3 CK7/AOT/ Surfactant System at 25°C, Addition of Salt**

The third method consisted of using NaCl to increase the AOT hydrophobicity. Lysozyme,  $\alpha$ -chymotrypsin, cytochrome c, and BSA were extracted in the middle phase of a system composed by 0.5 wt. % CK7, 0.5 wt. % AOT, isooctane and 1.5 wt. % NaCl water solution. The aqueous feed solution was not used a buffer as occurred for the two previous methods; but, the pH was within 0.2 units of pH=7. Samples were prepared in the same way as described in Sections 5.3.1.1 and 5.3.1.2. Then they were equilibrated for one day and observed to see if an opaque precipitate separated from the transparent middle phase, particularly for samples containing high protein concentrations. Protein concentration was measured for each phase of the W-III system.

In order to determine the solubilization limit of proteins in the middle phase of W-III systems, the initial aqueous phase protein concentration was varied. Original concentrations of protein in the water phase were 0.0, 0.4, 0.8, 1.2, 1.6, 1.8 and 2.0 mg/mL for lysozyme, cytochrome-c and BSA. Original concentrations of  $\alpha$ -chymotrypsin were 0.0, 0.2, 0.4, 0.6, 0.8 and 1.0 mg/mL, lower than other three proteins because the saturation of the middle phase was reached at an original concentration in water lower than 1 mg/mL. Three replicates were performed for each experimental result given in this chapter.

## **5.3.2 Quantitative Analysis of Forward Extraction Experiments**

### **5.3.2.1 Protein Quantification**

Protein concentration was measured by a Coomassie Blue G-250 colorimetric assay that measured absorbance at 595 nm [74]. A method to prepare the sample before measuring the protein concentration was developed because surfactant also changes the color of Coomassie Blue G-250 dye. An aliquot of 50  $\mu\text{L}$  is taken from the sample and mixed with acetone in a 2 mL vial. The mixture is centrifuged and the acetone-rich top phase is removed and discarded. The precipitated protein in the bottom is retained. The procedure was performed twice. The remaining acetone wetting the protein was evaporated in vacuum. The dry protein is dissolved in Coomassie Blue G-250 solution and the absorbance at 595 nm is measured.

### **5.3.2.2 Surfactant Quantification**

Surfactant concentration in each phase was measured by reverse-phase high-performance liquid chromatography (RP-HPLC). A 50  $\mu\text{L}$  aliquot of top, middle or bottom phase was removed by a 100  $\mu\text{L}$  graduated syringe. The aliquot was diluted with 400  $\mu\text{L}$  of acetone and injected in the HPLC. The chromatography apparatus consisted of a SD-200 analytical system from Varian Inc. (Walnut Grove, CA). The column was obtained from Varian,  $\text{C}_{18}$ , pore size 100 $\text{\AA}$ , particle diameter 5 $\mu\text{m}$ , column diameter 4.6 mm, column length 250 mm. An evaporative light-scattering detector (model MKIII from Alltech Associates, Deerfield, IL) was employed. The solvent system for HPLC was isocratic, consisting of 98% acetone and 2% acetic acid at a flow rate of 1 mL/min.

### 5.3.2.3 Volume Calibration of Vial

Volumes of the phases in the vial were measured by taking a photograph and then comparing the level of the liquid-liquid or liquid-air interfaces with a calibration curve (**Figure 5.2**). Calibration was done by filling the vial to different levels with deionized water and measuring the weight, assumed to be equivalent to the volume in milliliters. The level of the water is measured by using a dimensionless length ( $L$ ) calculated by dividing the level “ $s$ ” by length “ $a$ ” as is indicated in **Figure 5.1** and **Equation 5.1**.

$$L = \frac{s}{a} \quad (5.1)$$

The calibration curve of **Figure 5.2** was fitted to a cubic expression indicated in **Equation 5.2** and shown in **Figure 5.2**.

$$Volume(mL) = (0.229 \cdot L^3 + 0.1375 \cdot L^2 + 1.5002 \cdot L + 0.0927) \quad (5.2)$$

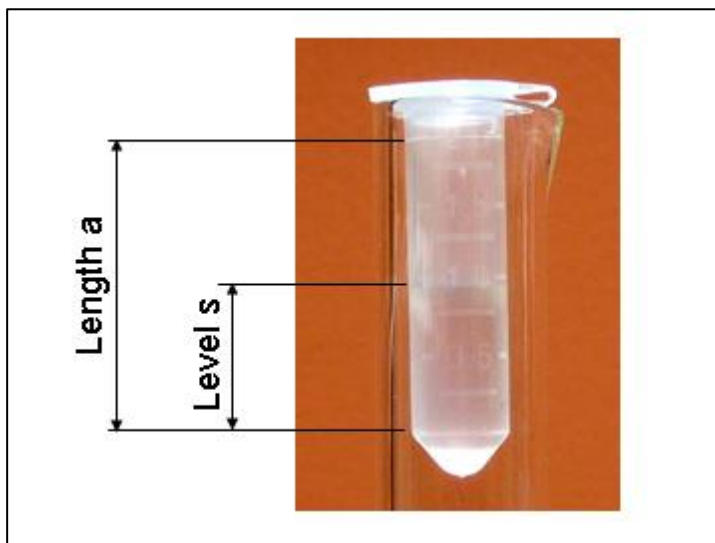


**Figure 5.1:** Vial with indication of the lengths used for volume calculation.  $a$  is a distance between the two marks in the vial as indicated in the figure and  $s$  is the level of the liquid of which volume is measured.

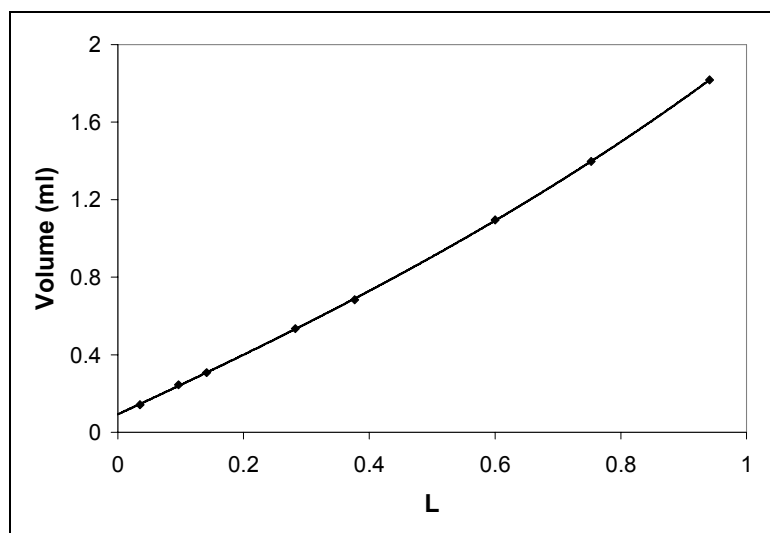


**Figure 5.2:** Calibration curve of volume of liquid related to the level “L” calculated in **Equation 5.1**.

## 5.4 Results

Forward extraction of proteins was performed under three different conditions with excellent results achieved. At 40°C it was observed that proteins and AOT anionic surfactant partition together, mostly into the middle phase, and into the top phase in some cases. The necessary concentration of AOT for extraction into the middle phase was very small; larger concentrations can lead to extraction in the top + middle phases. The coupled partitioning of AOT and protein demonstrates the importance of the electrostatic interaction-based driving force. Extraction of proteins at 25°C was successfully achieved through either the addition of CK3 or NaCl. For the W-III systems formed using NaCl, the protein BSA was extracted through a hydrophobic interaction-based driving force since electrostatic repulsion existed between BSA and AOT under the conditions employed (Section 0).



#### 5.4.1 W-III-Based Extraction Using AOT/CK7 at 40°C

A super-ambient temperature for the AOT/CK system is required for W-III formation to decrease the hydrophilicity of CK7; moreover the PIT for the Water/CK7/Isooctane system is  $\sim 41^{\circ}\text{C}$  (Section 4.5.5 and 4.6.1). The addition of AOT causes only a slight change on the PIT, as evidenced by the slight increase of hydrophilicity noted for the surfactant partitioning experiments (Chapter 4) Therefore, its concentration can be changed significantly without a inducing a phase change. The main function of AOT in this case is only to induce an electrostatic driving force. The employment of  $40^{\circ}\text{C}$ , near the PIT of CK7 ( $41^{\circ}\text{C}$ ), is sufficiently high to allow for W-III formation for pure CK7, but is sufficiently low to prevent the unfolding of many proteins. **Figure 5.3** and **Figure 5.4** display the distribution of lysozyme and AOT between each phase of W-III systems, respectively. If **Figure 5.3** is compared with **Figure 5.4** it is observed that proteins extract to the phase most enriched in AOT. **Figure 5.4** also indicates that the smaller the AOT proportion among the surfactants, the larger its partition to the middle phase instead of the top phase. The sample described in **Figure 5.3** without AOT did not extract lysozyme into the middle phase even though the pH was 7, and thus a favorable electrostatic driving force between lysozyme and AOT existed. This confirms that proteins will partition to the phase richest in AOT for this set of conditions.

Partition coefficients for lysozyme, the mass of lysozyme in the top + middle phase divided by the amount present in the bottom phase, are higher than 10 in all the studied cases at  $40^{\circ}\text{C}$  and pH 7 (**Figure 5.5**). When the proportion of AOT among the surfactants is  $\geq 50$  wt. %, most of the protein is extracted to the top phase; otherwise, if the AOT proportion is  $\leq 14\%$ , most of the protein partitions to the middle phase. Partition coefficients based on concentration are much higher than coefficients based on total mass because the volume of the middle phase is between 9% and 25% of the whole volume, significantly smaller than the initial aqueous phase, which is more than 50% of the whole volume. Volumes fractions of each phase are shown in **Figure 5.7** for the W- III systems undergoing extraction of lysozyme. **Figure 5.6** shows the partition

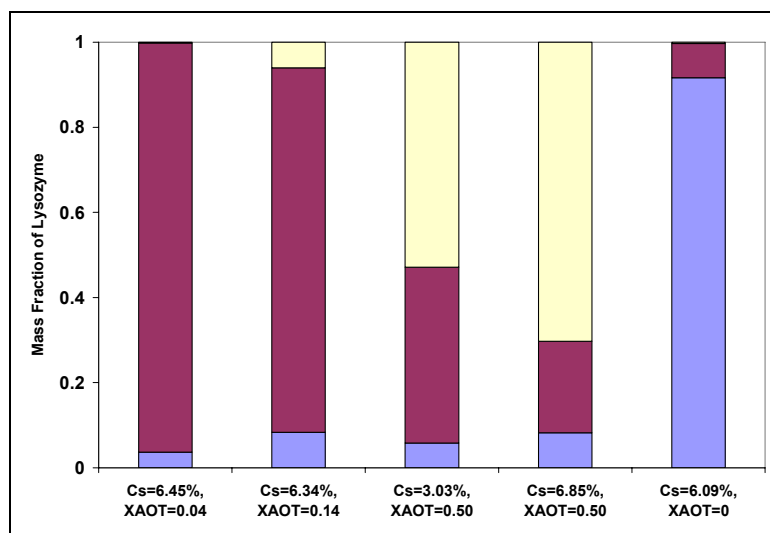


**Figure 5.3:** Distribution of lysozyme in the bottom (blue), middle (red), and top phase (yellow) of a Winsor III system formed by AOT, CK7, water, and isooctane. Volumes of water and isooctane are the same. Aqueous solution consists of a 0.1 M pH 7 phosphate buffer and contains 1 mg/mL of protein. Cs is overall weight percentage of surfactant and XAOT is the mass fraction of AOT among the surfactants. Temperature = 40°C.

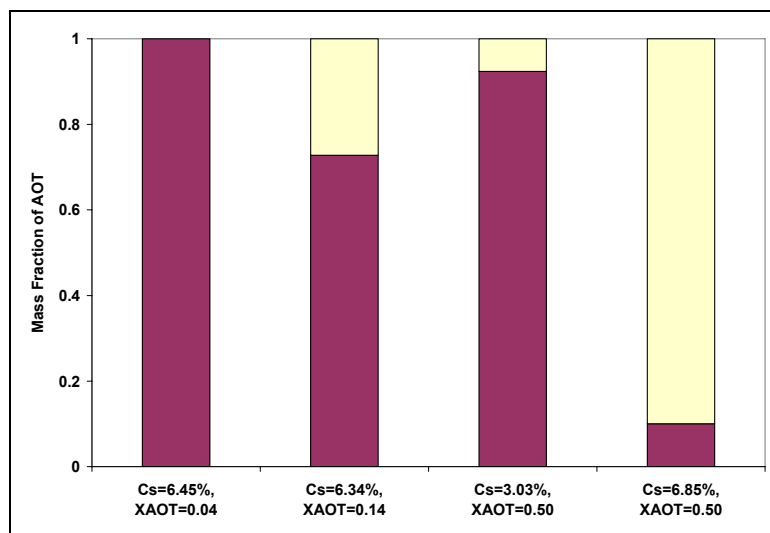


**Figure 5.4:** Distribution of AOT present in the bottom (blue), middle (red), and top phase (yellow) of W-III systems for the experiments described in **Figure 5.3**. Conditions for extraction are given in **Figure 5.3**.

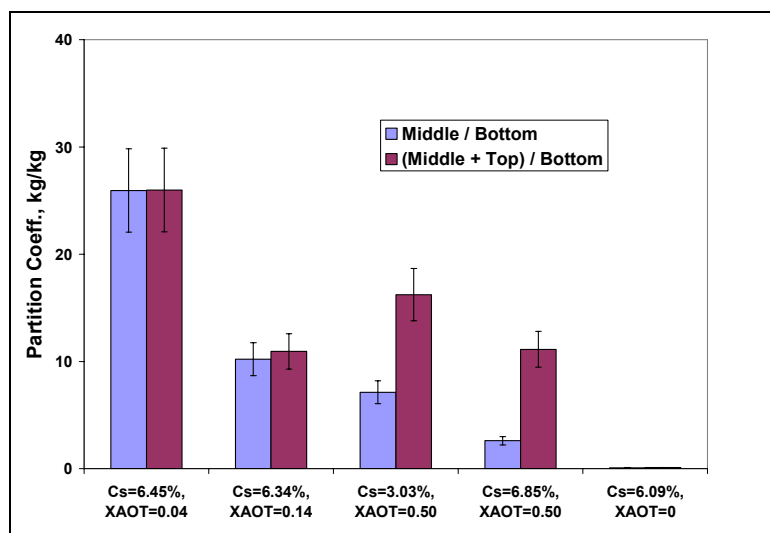


**Figure 5.5:** Partition coefficients for lysozyme based on mass amounts corresponding to the systems in **Figure 5.3**. Conditions for extraction are given in **Figure 5.3**.

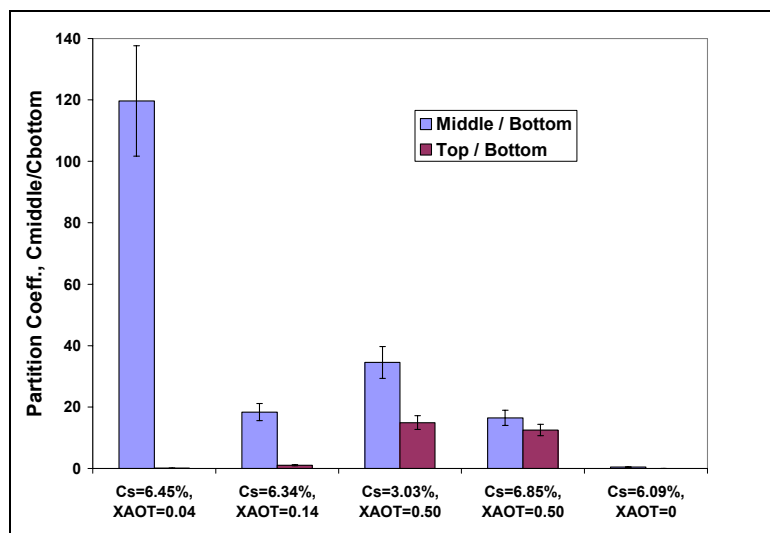


**Figure 5.6:** Partition coefficients for lysozyme based on relative concentrations corresponding to the systems in **Figure 5.3**. Conditions for extraction are given in **Figure 5.3**.  $C_{\text{middle}}$  is concentration of protein in the middle phase ( $\text{g}_{\text{prot}} \cdot \text{mL}_{\text{middle phase}}^{-1}$ ) and  $C_{\text{bottom}}$  is concentration of protein in the bottom phase ( $\text{g}_{\text{prot}} \cdot \text{mL}_{\text{bottom phase}}^{-1}$ )

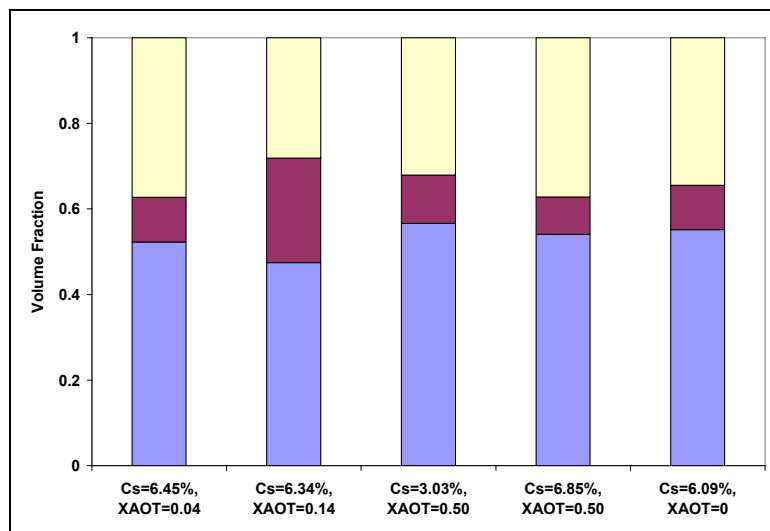


**Figure 5.7:** Volume fraction of bottom (blue), middle (red), and top phase (yellow) of W-III system composed by CK7, AOT, isooctane and 0.1 M pH7 phosphate buffer at 40°C, corresponding to the experiments of **Figure 5.3-Figure 5.6**. Conditions for extraction are given in **Figure 5.3**.

coefficients for lysozyme based on relative concentrations. It can be observed that the coefficients are larger than mass partition because the volume of the middle phase (**Figure 5.7**) is approximately 5 times smaller than bottom phase.

**Figure 5.8** depicts the extraction of BSA at pH 2, lower than its pI (4.7; **Table 5.1**), and pH 7, higher than its pI. This experiment shows that for the CK7/AOT surfactant system at 40°C, the driving force for BSA's extraction is by electrostatic interactions. If the pH of the aqueous solution is lower than pI the charge of the protein is positive, producing a strong electrostatic driving force for extraction with the negative charged AOT. Consistent with the domination of the electrostatic driving force, BSA is strongly extracted at pH 2 (**Figure 5.8**). In contrast, at pH 7, both the protein and AOT have a negative charge and the protein is not extracted (**Figure 5.8**). This experiment indicated that proteins can be extracted selectively by W-III system by utilization of the electrostatic driving force. Lysozyme was successfully extracted using the AOT/CK7 system at 40°C (**Figure 5.3, Figure 5.5, and Figure 5.6**). However, it is better to reduce the temperature because enzymes deactivate following an Arrhenius law [75]. Therefore, in subsequent work, two different approaches were employed to enable the use of 25°C, to lessen the extent of enzyme inactivation: the addition of CK3 and of NaCl.

**Table 5.1:** Isoelectric point and molecular weight of the proteins used in this work<sup>1</sup>.

Protein	pI	M <sub>w</sub>
Cytochrome C	10.6	66000
Lysosyme	9.3	12300
α-chymotrypsin	8.3	14400
Pepsin	3.3	25000
BSA	4.7	34600

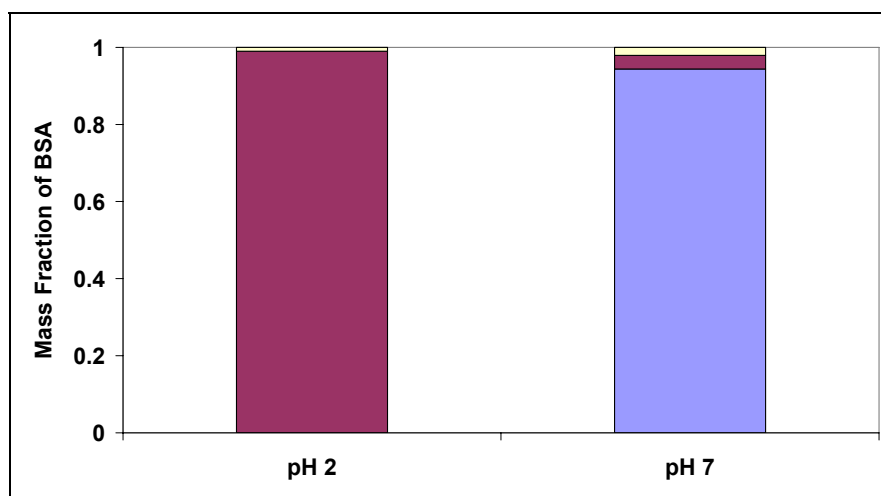


**Figure 5.8:** Distribution of BSA mass in the bottom (blue), middle (red), and top phase (yellow) of Winsor III system. Volumes of water and isooctane are the same and overall surfactant is 1 wt.%. Percentage of each surfactant among the surfactants is 0.7 wt. % CK7; 0.3 wt. % AOT. Temperature 40°C

<sup>1</sup> Data obtained from the website of Sigma-Aldrich, Inc. (St. Louis, MO): [www.sigmaaldrich.com](http://www.sigmaaldrich.com)

#### 5.4.2 Hydrophobicity Tuned by a Third Surfactant

Proteins were extracted by W-III microemulsion systems at 25°C using a ternary surfactant mixture containing AOT, CK7, and CK3 at a weight ratio of 4:3:3 and an overall concentration of 1 wt.%. Equal volumes of isooctane and 0.1 M pH 7 phosphate buffer containing 1 g/L of protein were mixed together. More than 95% of proteins (lysozyme,  $\alpha$ -chymotrypsin, and cytochrome c) partitioned to the middle phase (**Figure 5.9**). At pH 7, all of the listed proteins were positively charged since their pI values were  $> 7$  (**Table 5.1**); hence, the main driving force for these proteins appears to be electrostatic, since AOT is completely solubilized in the middle phase according to the HPLC analysis. The partition coefficients are coincident with the difference between the pH and pI. Moreover, lysozyme has the highest pI and has the highest partition coefficient. Partition coefficients for the other proteins decrease as their pI values decrease. The concentration of the proteins in the middle phase was  $\sim 5$  times higher than that of the original aqueous solution because of the high percent extraction (**Figure 5.10**) and the smaller volume of the middle phase (**Figure 5.11**). In contrast, the partition coefficient of pepsin is 0.7; moreover, it partitions more favorably to the remaining aqueous phase (and/or the surfactant layer present at the liquid-liquid interface) than into the bicontinuous microemulsion phase, with a small amount solubilized in the top, isooctane-rich, excess phase (**Figure 5.9** and **Figure 5.10**). Pepsin has pI lower than the pH of the system (**Table 5.1**), meaning that protein and surfactant both have a net negative charge; hence, the electrostatic attractive driving force is weak. **Figure 5.12** vividly shows that the red-colored protein cytochrome c is strongly extracted in the middle phase of the W-III system, consistent with the discussion of this paragraph. Another observation in **Figure 5.11** is that middle phase with high concentration of proteins has a smaller volume than middle phase with low concentration extracted such as pepsin or a control experiment without protein. Partition coefficients calculated based on the relative weights of protein in the middle versus the bottom phase reflect the same

trends as depicted in **Figure 5.13** for concentration-based partition coefficients (**Figure 5.10**).

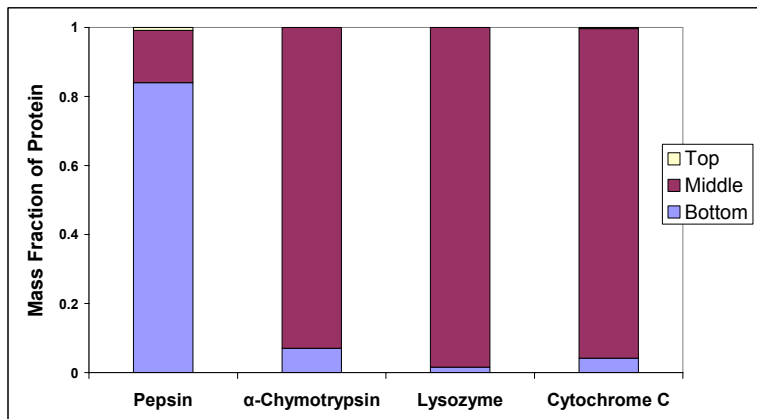


**Figure 5.9:** Distribution of protein mass in the bottom (blue), middle (red), and top phase (yellow) of W-III system. Volumes of 0.1 M pH 7 phosphate buffer and isooctane are the same and overall surfactant is 1 wt. %. Percentage of each surfactant among the surfactants were 0.30 wt. % CK7; 0.3 wt.% CK3, and 0.4 wt.% AOT. Temperature 25°C

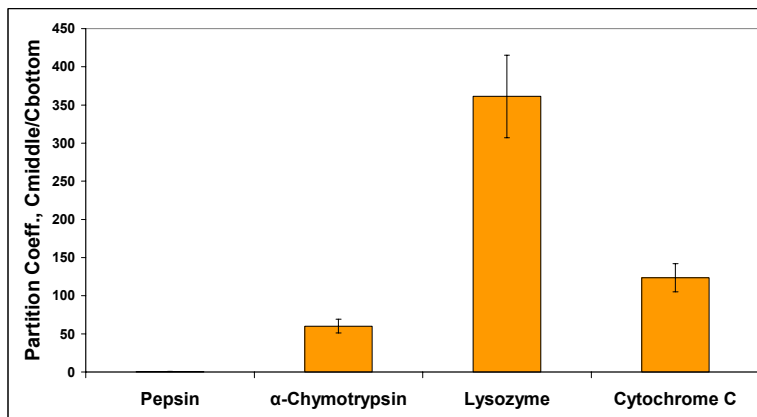


**Figure 5.10:** Concentration partition coefficient between middle and bottom phase of the proteins during W-III-based protein extraction, displayed in **Figure 5.9**. Conditions listed in **Figure 5.9**. Cmiddle is concentration of protein in the middle phase ( $g_{\text{prot}} \cdot \text{mL}_{\text{middle phase}}^{-1}$ ) and Cbottom is concentration of protein in the bottom phase ( $g_{\text{prot}} \cdot \text{mL}_{\text{bottom phase}}^{-1}$ )

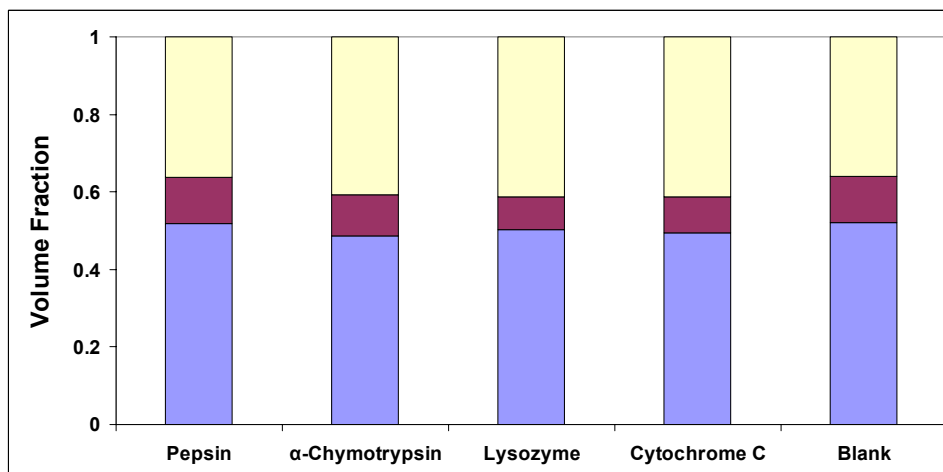


**Figure 5.11:** Volume fraction of the bottom (blue), middle (red), and top phase (yellow) of W-III-based protein extraction, displayed in **Figure 5.9**. Conditions listed in **Figure 5.9**.



**Figure 5.12:** Forward extraction of cytochrome c by 1 wt.% of overall surfactant at 25°C using the conditions listed in **Figure 5.9**.

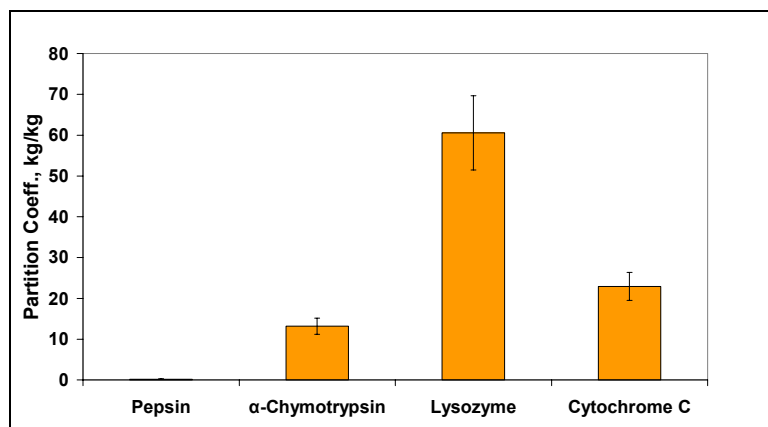




**Figure 5.13:** Mass partition coefficient between middle and bottom phase of the proteins during W-III-based protein extraction for data displayed in **Figure 5.9**. Conditions listed in **Figure 5.9**.

### 5.4.3 Hydrophobicity Tuned by NaCl

#### 5.4.3.1 Forward Extraction for 1.0 mg/mL Protein Solution

Forward extraction performed using the CK7 / AOT surfactant system at room temperature with NaCl added to increase the hydrophobicity of AOT, thus allowing for formation of Winsor-III systems, led to the successful partitioning of the proteins from the bottom phase to the middle phase (**Figure 5.14**, data plotted for  $x = 1.0$  g/L). The protein concentration remaining in the bottom phase was below detection limits with exception of BSA, which at pH 7 does not possess a favorable electrostatic driving force for extraction. BSA concentration is approximately 0.2 mg/mL in aqueous phase (**Figure 5.15**) after the extraction from an original solution 1 mg/mL of protein. BSA's partition coefficient based on concentration is 19 at 1 mg/mL. Partition coefficients for lysozyme,  $\alpha$ -chymotrypsin, and cytochrome-c cannot be calculated due to the undetectable concentration in the bottom phase. Partition coefficient for systems that were treated by NaCl to increase hydrophobicity at 25°C are at least equally high as those obtained in systems where hydrophobicity was tuned by CK3 at 25°C (**Figure 5.10** and **Figure 5.13**). In both systems when the electrostatic driving force is favorable, more than 90% of the protein is in the middle phase and for most of the cases the protein is undetected in water and oil excess phases. This is different for systems where hydrophobicity was tuned by temperature, for which protein partitioned into the oil and water excess phases. The ethoxylate surfactant is more hydrophobic if the temperature increases; therefore, microemulsion can occur in the top phase also. Relative volumes of middle phase are in the same range (10%) for all the samples, tuned by temperature, CK3 or NaCl.

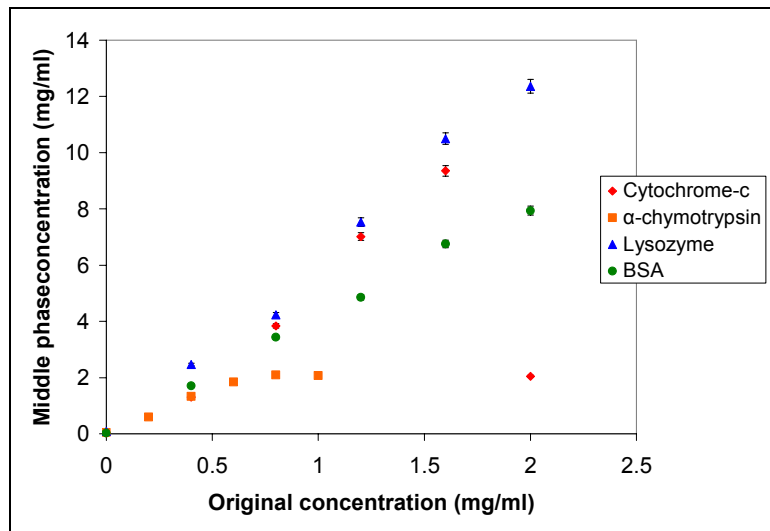


**Figure 5.14:** Equilibrium concentration of cytochrome-c,  $\alpha$ -chymotrypsin, lysozyme and BSA in the middle phase versus original concentration in the aqueous phase. Volumes of 1.5 wt.% NaCl aqueous solution and isooctane are the same and overall surfactant is 1 wt. %. Percentage of each surfactant among the surfactants were 50 wt. % CK7, and 50 wt % AOT. Protein concentrations are mass per volume of the whole phase. Temperature 25°C. Standard errors were less than 2% in all the cases.

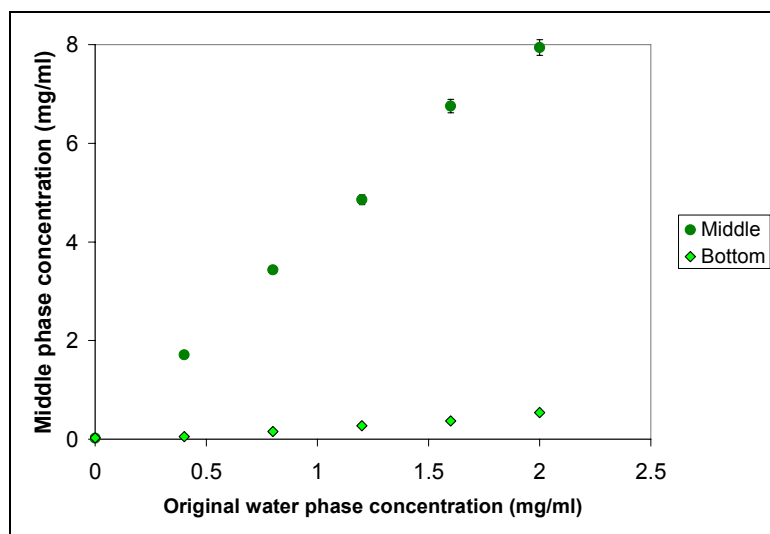


**Figure 5.15:** Equilibrium concentration of BSA in the middle and bottom phase versus original concentration in the water phase. Conditions listed in **Figure 5.14**. Errors were less than 2% in all the cases.

### 5.4.3.2 Saturation of the Middle Phase

In order to determine the maximum solubilization of proteins, the effect of the initial aqueous protein concentration was varied, with concentrations larger than 1 mg/mL employed, using salt to increase the hydrophobicity as per Section 5.4.3.1. **Figure 5.14** depicts the concentration of cytochrome-c,  $\alpha$ -chymotrypsin, lysozyme and BSA in the middle phase versus the original concentration in the aqueous phase. Saturation of the middle phase with proteins was not achieved for concentrations up to 2 g/L, with the exception of cytochrome-c that saturates at 1.6 mg/ml and  $\alpha$ -chymotrypsin that saturates near 0.8 mg/mL. For cytochrome c, lysozyme, and BSA, >75% extraction was achieved at all concentrations.

Once the middle phase is saturated, the excess protein is precipitated and resides at the liquid-liquid interface formed by the bottom and middle phase but does not dissolve in water [76-78]. In most of the experiments used to create **Figure 5.14**, protein in the bottom phase was undetected after extraction with exception of BSA

BSA is extracted into the middle phase from the 1.5 wt. % NaCl solution even though the pH is higher than pI=4.7, implying the driving force for extraction is mainly hydrophobic interactions. If the pH is lower than pI, the protein precipitates at 1 mg/mL of original solution when it is in contact with the surfactant solution. If unbuffered 1.5 wt. % NaCl solution is employed, BSA is extracted in middle phase and less than 7% remains in the excess aqueous phase.

**Figure 5.15** represents the equilibrium concentration of BSA in middle and bottom phase versus the original concentration of protein in the water phase. The concentration in the middle phase is more than 15 times higher than the concentration in the bottom phase. Comparing with the experiment at 40°C (**Figure 5.8**) it seems that they have different mechanism of extraction because at 40°C the protein is not extracted at pH > pI. At 25°C and 1.5 wt.%NaCl solution, BSA is extracted at pH higher than pI. This difference suggests that the extraction at 40°C is due to electrostatic interactions and extraction at 25°C is due to hydrophobic interactions. Proteins' hydrophobicity increases

with the concentration of salt [79]; therefore, BSA should be more hydrophobic at 1.5 wt.% (0.256 M) NaCl (aq) than in 0.1 M of pH 7 phosphate buffer solution used for the 40°C experiments. The lower temperature at 25°C makes the protein more hydrophilic [80] but it seems that the effect of the salt is stronger than the effect of the temperature in this case.

The volume of the middle phase is reduced as the middle phase's protein concentration is increased (**Figure 5.16**). The reduction in volume is a small contribution to the increased concentration of the protein in the middle phase depicted in **Figure 5.14** and **Figure 5.15**.

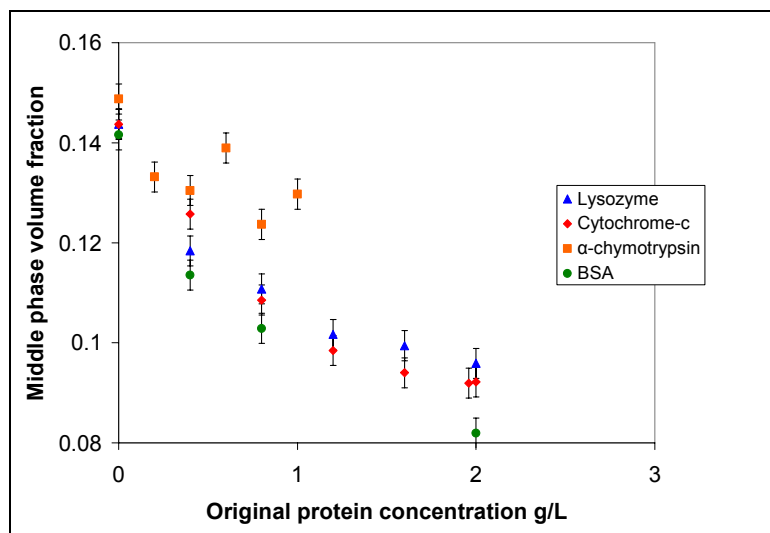


**Figure 5.16:** Effect of original protein concentration on the volume fraction of the middle phase for the experiments plotted in **Figure 5.14**.

## 5.5 Discussion

### 5.5.1 Comparison of the Three Approaches Used to Form Winsor-III Systems

Systems using 50% CK3, 50% AOT and 1.5 wt.% NaCl solution have the advantage that they can be formed at room temperature without the addition of a third surfactant. Comparing with W-III system formed at 40°C, the concentration of surfactant needed to form a middle phase of the same size (10% of the volume) is 6 times lower. Also for most of the NaCl-based systems there is no occurrence of extraction to the top phase. In contrast, at 40°C there is extraction in top phase at high proportions of AOT among the surfactants ( $\geq 50$  wt. %). Also there is a difference in the extraction of BSA, which is extracted at 40°C and pH lower than pI (pH 4.7) but not at pH higher than pI. This observation suggests that BSA is extracted by an electrostatic attractive driving force. This concept is reinforced by the fact that lysozyme is not extracted to the middle or top phase at 40°C and pH 7 in the system that the only surfactant is CK7, for which no electrostatic driving force exists (**Figure 5.3, 5.5, and 5.6**). On the other hand at 25°C and 1.5 wt.% NaCl BSA is extracted at pH 7, even though both BSA and AOT are negatively charged (**Figure 5.14, and 5.15**).

Comparing the system tuned by NaCl with system tuned using CK3 at 25°C, forward extraction is more complete for the former system. For the former system the protein in the excess aqueous phase is below detection limits, but for the latter a small but measurable aqueous phase protein concentration occurs. The volumes of the middle phase are in the same range for systems with NaCl and systems with CK3. Also the total concentration of surfactant is 1 wt. % in both systems, even though there are small differences depending on the protein extracted. In the system tuned by NaCl most of the extractions performed using an initial protein concentration of 1 mg/mL yielded a volume

fraction for the middle phase of 10% except for  $\alpha$ -chymotrypsin, which yielded a larger volume but contained a lower concentration of proteins because of the precipitate that forms. This is consistent with **Figure 5.16**, which shows that the middle phase volume decreases with an increase of middle phase protein concentration. In systems with CK3 the volume is more variable. In samples with pepsin the middle phase volume fraction is around 12% of the total volume and in samples with lysozyme and cytochrome c the volume fraction is 8.4% and 9.2%.

Nearly-complete separation into three phases for all the systems takes only a few minutes with a small amount of a macroemulsion existent at the liquid-liquid interfaces. In order to obtain a completely clear middle phase it takes a few hours. Therefore for this work the samples were equilibrated for one day to assure complete separation. The rapid phase separation is due to the low viscosity of the phases at the PIT (optimal condition to have W-III systems) [68, 81]. Moreover, the curvature of interface is 0 so it does not form macroemulsions that make difficult the separation [81].

### **5.5.2 Comparison of protein extraction and solubilization capacity using W-III versus W-II systems**

Extraction of proteins by W-III is faster and the protein solubilization capacity of the microemulsion phase is higher than the traditional method, using a W-II system. The latter difference is due in part to the higher water content for bicontinuous microemulsions 50% [82], compared to water-in-oil microemulsions, less than 6% [76, 77].

Comparing the difference in solubilization capacity between the reverse micellar phase of a W-II system and the bicontinuous microemulsion phase of a W-III system, Matzke *et al.* achieved a reverse micellar solution that contained 0.22 mg/mL  $\alpha$ -chymotrypsin from a “traditional” Winsor-II based extraction using an original aqueous solution of 2.0 mg enzyme /mL [83]. In contrast, the bicontinuous microemulsion phase of a W-III system used in this work became saturated using an initial aqueous phase

containing 0.6 mg/mL, yielding a bicontinuous microemulsion phase concentration of 1.84 mg/mL almost one order of magnitude larger than the concentration obtained by Matzke et. al [83].

Shin et. al. found the solubilization limit for lysozyme in reverse micelles using a cationic surfactant, dioctyldimethyl ammonium chloride (DODMAC) was 1.2 mg/mL [77]. When attempting to surpass this limit they observed the formation of a surfactant-protein precipitate. The avoidance of precipitate formation is also a criterion used in this work to determine the solubilization limit. Herein, for W-III system at 25°C and 1.5 wt. % of NaCl and 0.5 wt. % CK7 and 0.5 wt. % AOT the solubilization limit for lysozyme in the bicontinuous phase is 12 mg/mL (**Figure 5.14**), one order de magnitude higher than the value obtained by Shin *et. al.* The water content of the reversed micelles employed by Shin *et al.* was 1% v/v [77], much less than the water content of the bicontinuous phase, approximately 50% [82].

Adachi et. al. extracted cytochrome-c using a Winsor-II system formed by AOT in n-heptane using an initial aqueous phase concentration of 0.12 mg/mL or less without precipitation occurring. The percentage of water in the water-in-oil microemulsions was 3.5% [76]. Shioi *et al.* extracted cytochrome-c with a mixture of alkyl ethoxylate surfactant (C<sub>12</sub>E<sub>4</sub>) and AOT in Winsor II-based extraction. At the optimal molar ratio between AOT and C<sub>12</sub>E<sub>4</sub>, equal to the ratio employed in this work (0.44) Shioi *et al.* extracted approximately 80% of the protein from a 0.12 mg/mL aqueous solution. Since they used equal volumes of oil and water, the concentration in the water-in-oil microemulsions is approximately 0.1 mg/mL [4]. Although an increase of surfactant concentration could theoretically result in an increase of extraction into reverse micelles for Winsor-III –based protein extraction, a practical limit on the amount of AOT exists because AOT concentrations higher than 100 mM lead to formation of a macroemulsion and/or precipitation of a surfactant-protein complex [50, 84]. Extraction of cytochrome-c using a W-III system at 25°C and 1.5 wt. % of NaCl is complete from an original concentration of 1.2 mg/mL (**Figure 5.14**). The saturation of the microemulsion phase obtained herein using a W-III system occurred using a 1.6 mg/mL original aqueous

solution and the concentration of the protein in the bicontinuous microemulsion phase is 9 mg/mL, more than an order of magnitude higher than the values reported by Adachi and Shioi.

Iyer-Rairkar *et al.* saturated a system with reverse micelles using CK7 by the “injection method” [32]. This method for water-in-oil microemulsion (reverse micelle) formation consists of adding a microliter amount of concentrated aqueous protein solution (40-66 mg/mL) to a mL-sized solution of surfactant in isooctane. Then the mixture is shaken until the protein solution is dissolved in the surfactant solution, i.e., until microemulsion formation occurs. The highest concentration of lysozyme obtained was 11.2 mg/mL, slightly smaller than saturation in W-III system, which was 12.3 mg/mL. Iyer-Rairkar *et al.* obtained larger concentration of  $\alpha$ -chymotrypsin in the reverse micelles (10 mg/mL) [32] than W-III system in this work (1.84 mg/mL). The “injection method” for introducing proteins into microemulsions can induce a reverse micelles system to hold higher concentration than by other means because there is not a competition between a surfactant self-assembly structure and water (in the aqueous phase) to interact with protein. Of note, Iyer-Rairkar’s use of the “injection method” negated the need for ionic surfactants, which strongly interact with the protein and can make the protein precipitate. So for Iyer-Rairkar’s reverse micellar system the microemulsion dissolves the protein until saturation of the dispersed aqueous phase occurs and not until precipitation of the complex surfactant-protein occurs.

## **5.6 Conclusions**

Protein extraction using W-III systems led to high partition coefficient and high saturation concentration compared to extraction by Winsor II systems, which is the traditional approach employed. Other advantages are that the phases separate rapidly because they are near the PIT, where the interfacial tension is at a minimum value.



Moreover, the viscosity of the microemulsion-containing phase is low and the natural curvature of the surfactant monolayer is 0, reducing the formation of macroemulsions.

The three methods employed for forming suitable CK7 / AOT Winsor-III systems were described in chronological order. The first one, using a super-ambient temperature, 40°C, proved that proteins can be completely extracted in the middle phase of a Winsor III system composed by a non-ionic and an anionic surfactant. It shows also that in this case the main driving force is electrostatic because the protein is extracted only when the pH is lower than the pI. Extracted proteins partitioned to the phases where the AOT is present. The underlying reason for this may be that proteins form a complex with AOT before being extracted. This method can be used to extract proteins that are thermostable at 40°C. It has the advantage that the concentration of AOT can be very low because it is not needed to induce W-III formation, but is required only to provide a driving force for extraction.

Once it was proven that proteins can be extracted into the middle, bicontinuous microemulsion phase of a W-III system the effort was directed to obtain W-III systems that extract proteins at near-ambient temperatures. The two successful approaches that achieved this goal were replacing part of CK7 by CK3 or adding NaCl to the aqueous phase. Both approaches have the goal to make the surfactant mixture more hydrophobic, in order to induce W-III formation at 25°C. CK3 is more hydrophobic than CK7 which increases the hydrophobicity of the surfactant system for the former and salt makes AOT become more hydrophobic due to Debye shielding, which results in the reduced dissociation of AOT's sulfonate head group and Na<sup>+</sup> counterion, as described in Chapter 4. The system that contains CK3 extracts by an electrostatic attractive driving force as its underlying mechanism. In contrast, systems with 1.5 wt. % of NaCl extract proteins in part by a hydrophobic interaction-based driving force. The strength of the proteins' charged surface groups and AOT's anionic head groups are reduced by Debye shielding, thus reducing the electrostatic driving force.

Extraction of proteins by a system with 1.5 wt. % of NaCl showed that the middle phase can achieve a higher solubilization of proteins than reverse micelles and >95% extraction from aqueous solutions containing 1-2 mg/mL of protein.

In **Table 5.2** is summarized the characteristics of the three approaches used in this dissertation.

**Table 5.2:** Summary of the characteristics of the three approaches of forward extraction by Winsor-III microemulsion systems.

Approach	Surfactant	Temperature	Highest Mass partition coefficient achieved	Driving force	Overall surfactant concentration (wt. %)	Observations
Super-Ambient Temperature	AOT and CK7 at different concentrations	40°C	25	Electrostatic	6.3	1)High mass partition 2)High AOT fraction among the surfactants.
Hydrophobicity tuned by a third surfactant	0.4 wt.% AOT, 0.3 wt.% CK3, and 0.3 wt.% CK7	25°C	350	Electrostatic	1	1)High mass partition. 2)Low concentration of surfactant. 3)Low temperature. 4)Inconvenient of using 3 surfactants instead of 2.
Hydrophobicity tuned by NaCl	0.5 wt.% AOT, and 0.5 wt.% CK7	25°C	$\infty$	Electrostatic and hydrophobic	1	1)Very high mass partition. 2)Low concentration of surfactant. 3)Low temperature. 4)Less selectivity due to hydrophobic interactions.

## CHAPTER 6

### BACK EXTRACTION

#### ***6.1 Introduction***

After forward extraction (Chapter 5), proteins need to be recovered from the bicontinuous microemulsion (middle) phase of the Winsor-III system employed into an aqueous phase to be useful unless the approach employed is to remove undesired proteins from the aqueous broth through forward extraction. The recovery process, “backward extraction,” needs to be as complete as possible and must yield protein that is fully active after the process.

Backward extraction is achieved by reducing the electrostatic attractive driving force between the protein’s positively charged surface groups and the negatively charged sulfonate head group of AOT, most readily achieved by removing the aqueous phase of the resultant Winsor-III system and replacing it with an aqueous “stripping” solution with a higher concentration of NaCl and/or a  $\text{pH} > \text{pI}$ .

Back-extraction from W-II microemulsion systems, the traditional method of extraction of proteins by microemulsion, is slow and does not recover the whole mass or activity of biomolecules, especially for those which solubilize or interact with the microemulsion’s interfacial region (Section 2.4.1). The original hypothesis of this work was the use of a surfactant mixture consisting of an acid cleavable surfactant (CK7) and AOT, with the latter providing the electrostatic driving force of the extraction, would result in successful back-extraction through the cleavage of the former, leading to disruption of microemulsion formation. A W-III system can extract a higher concentration of proteins than a W-II system (Section 0). However, during preliminary experiments, it was observed that adding an acidic aqueous buffer stripping solution to the W-III system resulted in a changing of phases to produce a W-I system and the

protein was released almost instantaneously into the aqueous phase. The rapid release of protein is inconsistent with the relatively slow rate of hydrolysis of CK7 observed in separate experiments (data not shown). In contrast, Iyer-Raikar observed that CK7 underwent a zeroth-order hydrolysis in Winsor-III system formed by Water / CK7 / Isoooctane [11]. The relatively low extent of hydrolysis observed in this work may be attributed to the lower ethoxylate chain length of the CK7 surfactant synthesized for this dissertation compared to Iyer-Raikar's work (discussed in Chapter 3), and/or to the presence of an additional surfactant, AOT. Moreover, Holmberg and co-workers demonstrated that the hydrolysis of a cleavable surfactant in a self-assembled structure is strongly affected by the presence of additional amphiphiles [85]. Therefore, it is believed that the release of proteins in this case is attributable to the increased Debye shielding of AOT by the increase of ionic strength, resulting in an increase of AOT's hydrophobicity (discussed in Section 2.2.1).

Although back-extraction was successfully achieved by adding a stripping solution with high ionic strength (NaCl concentration) at various different values, this approach introduced a new problem: surfactants partitioned to the aqueous stripping solution, thus introducing new challenges for the further downstream purification of the proteins. In addition, the presence of surfactant made it very difficult to measure the activity of the  $\alpha$ -chymotrypsin recovered in the stripping solution. To overcome these problems, the above-mentioned approach was modified by employing conditions that allowed for the use of aqueous stripping solutions that contained a high concentration of NaCl (5 wt.%) or pH > pI (12), but that also retained the W-III microemulsion system. This was most readily achieved by adding a small amount of an isooctane solution highly concentrated in CK7. The modified approach achieved the successful back-extraction of proteins, producing a rapid process that yielded a high recovery of protein mass and biological activity.

## **6.2 Materials**

The solvents used to equilibrate the surfactant were isooctane (HPLC grade, Fisher Scientific, Pittsburgh, PA) and deionized water, 18 M $\Omega$  x cm of resistivity. The alkyl ethoxylate surfactants CK7 and CK3 contained poly(ethylene glycol) monomethyl ether as the hydrophile and a cyclic ketal as the hydrophobe [5] and were synthesized in the lab (Chapter 3). Sodium bis(2-ethylhexyl) sulfosuccinate, AOT, anhydrous, was purchased from Fisher Scientific, Fair Lawn, NJ. All the proteins: lysozyme from chicken egg white (three times crystallized, dialyzed and lyophilized, containing approximately 95% protein with the balance being primarily buffer salts),  $\alpha$ -chymotrypsin from bovine pancreas (three times crystallized from four times crystallized chymotrypsinogen; dialyzed, essentially salt free and lyophilized powder), cytochrome c from horse heart (dialyzed and lyophilized), were from Sigma, St. Louis, MO. N-glutaryl-L-phenylalanine p-nitroanilide (GNPNA) was purchased from Sigma. Dimethyl sulfoxide used was molecular biology grade and was purchased from Fisher. Coomassie Brilliant Blue G-250<sup>®</sup> was purchased from Pierce (Rockford, IL) [86].

## **6.3 Methods**

### **6.3.1 Backward Extraction Using 5 wt. % NaCl Stripping Solution**

Proteins were forward extracted from a 1.5 wt.% NaCl aqueous solution to the middle phase of a W-III system, for which the overall surfactant concentrations were 0.5 wt. % AOT and 0.5 wt.% CK7 (Section 5.3.1.3). An aqueous feed containing protein (lysozyme, cytochrome-c or  $\alpha$ -chymotrypsin) at 1 mg/mL was added to an equal volume

of surfactants dissolved in isooctane in 2 mL polypropylene microcentrifuge tubes and gently mixed through manual reciprocation for a few minutes, then allowed to equilibrate. Although only a few minutes were required for phase separation, samples were equilibrated at room temperature for 1 hour to ensure clear phase separation.

Backward extraction was applied to the systems obtained by the method described in the previous paragraph. Two approaches to backward extraction were used. One consisted of removing the majority of the bottom, aqueous excess phase (600  $\mu\text{L}$ ) of the Winsor-III system and adding a nearly-equal volume (760  $\mu\text{L}$ ) of an aqueous stripping solution highly concentrated in NaCl (5 wt. %). Subsequently, the vial is shaken gently by hand until the contents are completely mixed. In order to form a W-III system for the higher concentration of salt at room temperature, 160  $\mu\text{L}$  of a solution of 9.28 wt. % CK7 in isooctane was added. The vial is shaken gently by hand until completely mixing was achieved. As a result, it yielded a system with 0.3 wt. % AOT and 0.7 wt. % CK7; and, the aqueous bottom phase contained 5 wt. % NaCl. If the three phases did not disengage rapidly, it was because the PIT was shifted by a few  $^{\circ}\text{C}$  below room temperature. For these cases, the sample was cooled by placement in a cold water bath for approximately 5 seconds, after which the phases began to separate. Then the sample was equilibrated at room temperature for 10 minutes to achieve complete phase separation.

The second back-extraction method was identical to the first, except the aqueous stripping solution contained a pH higher than pI (0.33 M pH 12 phosphate buffer + 1.75 wt. % NaCl). However in this case, the addition of 9.28 wt. % CK7 in isooctane was not needed to achieve formation of a Winsor-III system at room temperature.

### **6.3.2 Mass Quantification**

Protein concentration was measured by a Coomassie Blue G-250 colorimetric assay that measured absorbance at 595 nm [74]. A sample preparation method was required and developed because surfactant also changes the color of Coomassie Blue G-

250 dye. An aliquot of 50  $\mu\text{L}$  is taken from the sample and mixed with acetone in a 2 mL vial. The mixture is centrifuged and the acetone-rich top phase is removed and discarded. The precipitated protein at the bottom is retained. The procedure was performed twice. The remaining acetone wetting the precipitated protein was evaporated in vacuum. The dry protein is dissolved in Coomassie Blue G-250 solution and the absorbance at 595 nm is measured.

### 6.3.3 Activity

The relative activity of  $\alpha$ -chymotrypsin comparing with the original protein was measured by a modified method as suggested by Mao *et al* [87]. In this method N-glutaryl-L-phenylalanine p-nitroanilide (GNPNA), the substrate, is hydrolyzed by  $\alpha$ -chymotrypsin, releasing the product *p*-nitroaniline which absorbs at  $\lambda = 410$  nm. The substrate solution is 80 mg/L of GNPNA in 0.1 M of tris buffer solution and 2.3 mg/L of dimethyl sulfoxide (DMSO). Samples of 50  $\mu\text{L}$  were extracted from the bottom phase of a Winsor-III system resulting from back extraction and mixed with 700  $\mu\text{L}$  of substrate solution. Then the absorbance at 410 nm was recorded at room temperature in quartz cuvettes of 1.0 cm path length in the course of 15 minutes at intervals of 1.0 s and collected in a Microsoft Excel spreadsheet through the system's data acquisition system. The slope of the straight line obtained is divided by the slope of the standard to calculate the relative activity.

**Figure 6.1** shows the absorbance of light at  $\lambda = 410$  nm versus time of a biochemical reaction performed under standard conditions: 50  $\mu\text{L}$  of 0.5 mg/mL of untreated  $\alpha$ -chymotrypsin dissolved in 5 wt. % NaCl aqueous solution and mixed with 700  $\mu\text{L}$  of the substrate solution described above. The slope of the fitted line, indicated in the graph (**Figure 6.1**), is used as denominator (“St” in **Equation 6.1**) to calculate the percent relative activity (%A) remaining in the protein after backward extraction.



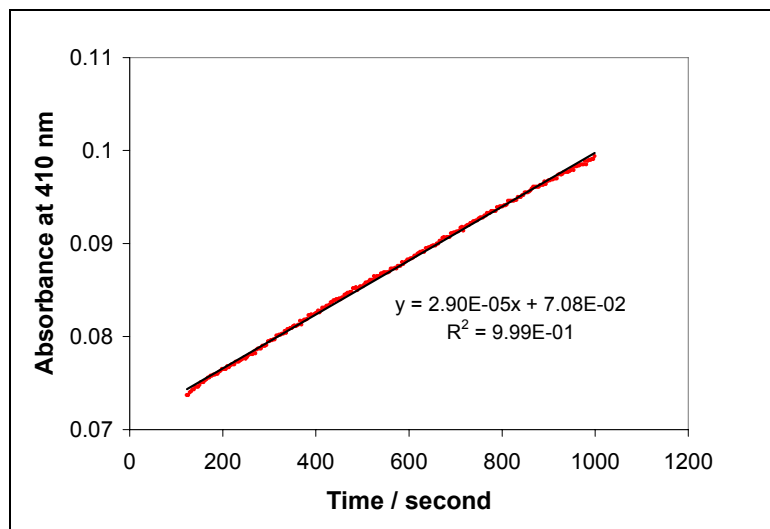


**Figure 6.1:** Absorbance of light at  $\lambda=410\text{nm}$  versus time of the hydrolysis of GNPNA catalyzed by  $\alpha$ -chymotrypsin under standard conditions, used to calculate the “standard” activity of  $\alpha$ -chymotrypsin (“St” in Eq. 1). 50  $\mu\text{L}$  of 0.5 mg/mL  $\alpha$ -chymotrypsin in 5 wt. % NaCl aqueous solution was mixed with 700  $\mu\text{L}$  of GNPNA substrate solution, as described in the Experimental section. (red circles): experimental data; (black line): straight-line fit to the data.

$$\%A = \frac{Sl}{St} \quad (6.1)$$

The numerator is the slope (“Sl”) of a graph similar to **Figure 6.1** obtained using 50  $\mu\text{L}$  of the bottom solution of the W-III system after backward extraction of  $\alpha$ -chymotrypsin.

## 6.4 Results

### 6.4.1 Back Extraction Using a 5 wt. % NaCl(aq) Stripping Solution

The mass recovery of cytochrome-c, lysozyme and  $\alpha$ -chymotrypsin through addition of a 5 wt. % aqueous NaCl solution was measured as described in Section 6.3.

**Figure 6.2** shows that cytochrome-c, lysozyme, and  $\alpha$ -chymotrypsin were recovered at 78%, 18%, and 57%, respectively.  $\alpha$ -Chymotrypsin had an incomplete recovery because precipitation occurred, as observed by the presence of solid at the liquid-liquid interface between the middle and bottom phases. Moreover, the initial aqueous phase concentration of chymotrypsin employed, 1 mg/mL, is higher than the concentration that produced a saturated middle phase, between 0.6 and 0.8 mg/mL as indicated in Section 5.4.3.2. Therefore the protein that is precipitated does not re-dissolve into the bottom phase under conditions of back extraction employed. Lysozyme had low yield of backward extraction compared to the other two proteins. Probably the low yield is due to hydrophobic interactions between the protein and the AOT molecules residing at the interface because the concentration of NaCl is high, which increases the hydrophobicity of AOT.

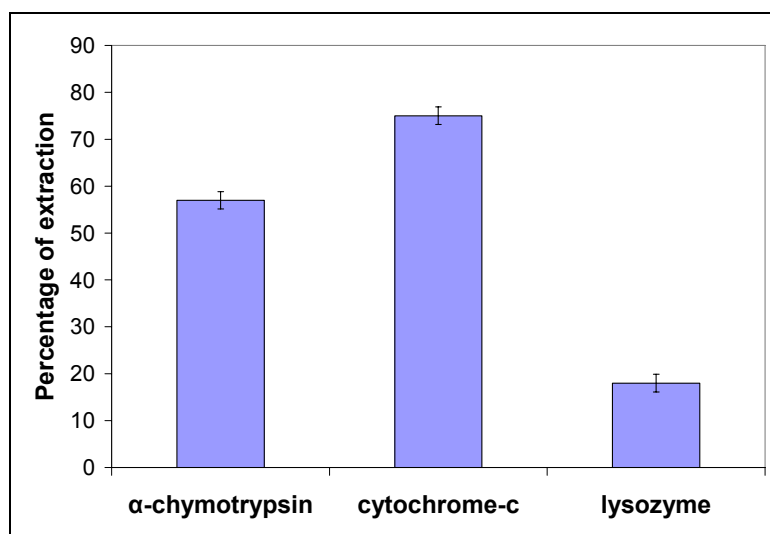


**Figure 6.2:** Mass percentage of back extracted protein based in the original protein solution using a 5 wt.% NaCl aqueous stripping solution. The distribution of surfactant consists of 30 wt. % AOT and 70% CK7. Cytochrome-c, lysozyme, and  $\alpha$ -chymotrypsin were present at 1 mg/mL in the initial aqueous solution used for forward extraction. Other conditions are listed in the Experimental section.

## 6.4.2 Enzymatic Activity

**Table 6.1** displays the level of activity for  $\alpha$ -chymotrypsin recovered from a W-III system by different back-extraction methods. The best method was removing the aqueous or “bottom” phase and then adding an aqueous stripping solution of 5 wt. % NaCl. After that a concentrated solution of CK7 in isoctane was added to obtain a weight ratio of 7:3 of CK7/AOT for the overall system to retain the presence of a Winsor-III system, as described in the Methods section. For this method the percentage of activity recovery was 99% for a system that employed 0.5 mg/mL of  $\alpha$ -chymotrypsin in the aqueous feed used for forward extraction. The data for mass recovery in the bottom phase after backward extraction was not measured, but should be very near 100% because the total activity recovered is 99%. The same method applied to a sample produced from forward extraction using 1.0 mg/mL  $\alpha$ -chymotrypsin in the aqueous feed had a lower mass recovery, 57%; and, the specific activity of the recovered protein was 89% of the original, due to the precipitated protein that formed during forward extraction, as described in Subsection 6.4.1.

Backward extraction of chymotrypsin using a pH 12 stripping solution, which imposed unfavorable electrostatic interactions between the enzyme and AOT (since pH > pI), provided interesting results (

**Table 6.1).** Even though the percent recovery of protein mass backward extraction was only 78%, the specific activity of the backward extracted protein is equal to that of the original protein prior to its treatment by forward and back-extraction. In future work, it is recommended that the equilibrium partitioning of chymotrypsin between the middle phase and the stripping solution (i.e., bottom phase) be measured because since the three phases are completely clear without any precipitate, it is theoretically possible to extract 100% of protein by this method using multiple steps of back-extraction.

**Table 6.1:** Mass percent and relative activity of backward extracted  $\alpha$ -chymotrypsin by three methods<sup>a</sup>

Backward extraction method <sup>b</sup>	Chymotrypsin Concentration (mg/ml) <sup>c</sup>	% of mass recovery	% Recovery of Activity	% of Original Specific Activity Retained <sup>d</sup>
5% NaCl, 160uL CK7 2.98%	1	57±1.9	51±1.5	89±5.6
5% NaCl, 160uL CK7 2.98%	0.5	N/D	99±1.5	N/D
0.33M pH 12 buffer, 1.75% NaCl	0.5	78±1.9	78±1.5	100±4.4

<sup>a</sup> Forward extraction conditions: equal volume proportions of 0.25 wt. % CK7 and 0.25 wt. % AOT in isooctane and aqueous protein feed containing 1.5 wt. % NaCl and chymotrypsin concentrations listed in the table were mixed at room temperature; <sup>b</sup> a more detailed description of the back-extraction conditions are listed in the Experimental section; <sup>c</sup> concentration of chymotrypsin in the aqueous feed used for forward extraction; <sup>d</sup> estimated by dividing the % recovery of activity by the % recovery of mass

## 6.5 Discussion

Shin *et al.* performed backward extraction of lysozyme from 1 mg/mL of protein in AOT microemulsions [88]. The method that they used was increasing the concentration of NaCl and the pH to 12. Shin *et al.* achieved the backward extraction; but, the protein did not dissolve into the aqueous phase of the Winsor-II system but instead precipitated as a solid that resided at the liquid-liquid interface. The concentration of protein in the bottom phase was below detection limits. The difference between Shin *et al.* and the work contained in this chapter is that they used pure AOT, which denature the proteins, and herein a mixture of AOT with non-ionic surfactant was employed, which would minimize the inactivating effect of ionic surfactants on proteins.

Dungan *et al.* examined the time course of back extraction of 1 mg/mL of  $\alpha$ -chymotrypsin and cytochrome-c from a reverse micellar phase formed in isooctane that contained 0.2 M AOT. The stripping solution was at pH 9.9 and contained a Na<sup>+</sup> concentration of 0.6 M [53]. They recovered only 7% of the protein for the microemulsion after 9 hours. The time required for back-extraction was several orders of magnitude higher than the time needed for back extraction by W-III systems (1-2 minutes) [53].

The percent recovery of activity for microemulsion-encapsulated  $\alpha$ -chymotrypsin  
obtained in this dissertation (

**Table 6.1)** is approximately the same as that obtained by Iyer-Raikar *et al.* from a water in oil microemulsion of the same ethoxylated surfactant as used in this work, 90% [32]. Iyer-Raikar *et al.* used only CK7 as surfactant and solubilization was achieved by the “injection” method, as described in Section **Error! Reference source not found.**, not by liquid-liquid extraction [32]. In this work more than 90% of specific activity was recovered using a 5 wt. % NaCl aqueous stripping solution (and the addition of a concentrated CK7 / isooctane solution to maintain a Winsor-III system at room temperature) and a protein concentration < 1% as the feed for forward extraction. The shorter time needed by Iyer-Raikar *et al.* to extract 90% of lysozyme or  $\alpha$ -chymotrypsin was 60 minutes [32], which is much higher than the 1-2 minutes needed to disengage the three phases of a W-III microemulsion system.

## 6.6 Conclusions

Back extraction from W-III system was done successfully with high percentage of recovery of mass and activity compared to backward extraction from a W-II system, which is the traditional method of microemulsion-based protein extraction. If the original concentration of protein of the aqueous feed employed for forward extraction is sufficiently small to remain under the saturation limit for the bicontinuous microemulsion, or middle, phase, the recovery can be 100%. Otherwise the mass of protein is not completely recovered, due to the formation of precipitate during forward extraction; and, the recovered enzyme had a slightly lower specific activity (



**Table 6.1).**

Backward extraction of  $\alpha$ -chymotrypsin achieved by using an aqueous stripping solution of pH 12 resulted in a high mass yield and 100% recovery of specific activity. The yield of mass recovery is lower than that achieved using a 5 wt. % NaCl aqueous stripping solution. Therefore the latter method is more convenient than the first one.

## CHAPTER 7 CONCLUSIONS AND RECOMMENDATIONS

### *7.1 Conclusions*

Results reported in this dissertation demonstrate that proteins can be forward extracted by a Winsor-III (W-III) system and backward extracted by high NaCl concentration or pH higher than pI without loss of biological activity. This method has the advantage that backward extraction is faster than methods that used W-II microemulsions (Section 6.5) and the yield is higher. Also the middle, bicontinuous microemulsion, phase of W-III system can contain more than 10 times higher concentration of protein than the w/o-microemulsion (reverse micellar) phase of a Winsor-II system, the traditional method of protein extraction by microemulsions. The level of protein solubilization achieved through Winsor-III-based protein extraction in this dissertation is equivalent to the level obtained in reverse micelles using the “injection” method, which yields the largest concentrations reported in the literature.

Three successful approaches were employed to obtain W-III systems based on an equal volume fraction of aqueous protein solutions and isooctane, and the AOT / CK7 surfactant mixture, useful for protein extraction. The first was employment of a temperature near the phase inversion temperature ( $\sim 41^\circ\text{C}$ ). Using this method, it was

shown that proteins were extracted by electrostatic interactions, and even at low proportion of AOT among the surfactant, the extraction can be achieved if a pH is employed which yields a favorable electrostatic attraction-based driving force between AOT's sulfonate anionic head group and the protein's charged surface groups ( $\text{pH} > \text{pI}$ ). Also it was demonstrated that extraction will not occur if the charge of the surfactant and protein are the same or if AOT is absent. The second approach was adding the surfactant CK3, which is a non-ionic surfactant more hydrophobic than CK7, to the AOT / CK7 - based system to reduce the phase inversion temperature (PIT) to near 25°C. This approach has the advantage that the temperature is lower so the extracted proteins have less probability of being thermally inactivated. The extraction was also controlled by an electrostatic attraction-based driving force. An important advantage comparing with the 40°C approach is that the concentration of surfactant needed to form the W-III system was 6 times lower, which will reduce materials costs. The third approach was to tune the hydrophobicity of the surfactant mixture by increasing the ionic strength of the aqueous protein solution fed to the process, which increases the hydrophobicity of AOT by Debye shielding, which in turn reduces the phase inversion temperature (PIT) to near 25°C. As a result of the Debye shielding, the electrostatic attraction-based driving force was lowered; thus, unlike the two approaches described above for Winsor-III –based extraction, it was shown that proteins with the same charge as AOT can be extracted, presumably due to a hydrophobic interaction- based driving force. For this system, the protein concentrations of the aqueous feed which produced a saturation concentration of  $\alpha$ -chymotrypsin, cytochrome-c, BSA and lysozyme in the middle phase were determined. In order to have high yield of protein recovered from the middle phase by back-extraction, the middle phase's protein concentration has to be under the saturation limit. Otherwise, part of the protein precipitates as a solid and does not redissolve in the stripping solution. Back extraction was tested in  $\alpha$ -chymotrypsin, cytochrome-c, and lysozyme. It was fast and total recovery of the activity for  $\alpha$ -chymotrypsin was achieved. Other proteins have smaller percentage of mass recovery in the conditions tested but comparable with yields

of water in oil microemulsion. The activity of back extracted protein was measured only for  $\alpha$ -chymotrypsin. For all the cases back extraction was very fast

From the experiments of CK7 partitioning between the aqueous and oil phases was found the effect in the hydrophobicity of other surfactants in the mixture with CK7. It was observed that CK3 shift the whole mixture to hydrophobic properties, in other words it the equilibrium is shifted to oil phase comparing with CK7. AOT make the mixture more hydrophobic in presence of 1 wt.% NaCl aqueous solution or independent of the temperature in water. Finally,  $C_8\beta G_1$  make the mixture more hydrophilic.  $C_8\beta G_1$ . Also a semi-empirical model was developed to calculate the partition coefficient of CK7 between aqueous and oil phase. The model was useful to estimate the PIT. The most useful W-III systems for protein extraction are those near of the PIT to allow for rapid disengagement of the three phases (due to minimization of the interfacial tension at the liquid-liquid interface), which accelerates the process productivity and reduces the denaturation of proteins at the liquid-liquid interface.

If one were to apply the technology developed in this dissertation, protein purification by a Winsor-III microemulsion system, to a specific protein separation, the following method should be used. First, the physical properties of the protein to be recovered (pI, molecular weight, degree of hydrophobicity), and the other proteins present in solution, need to be determined. Also, the pH and ionic strength of the aqueous protein solution needs to be known. Second, assuming the best means of separation is through an electrostatic driving force, the pH has to be adjusted to be lower than the pI of the targeted protein. (Alternatively, if hydrophobic interaction is deemed to be the most useful driving force, the concentration of salt may need to be adjusted to a higher level.) Third, the conditions required to form a Winsor-III system at room temperature need to be determined. The model developed in Chapter 4 will be used first to estimate approximate conditions required for Winsor-III formation. Next, the model's prediction will be utilized in experimental work to determine the PIT. The aqueous protein solution is contacted with a surfactant solution in isooctane (e.g., 1.21 wt. % AOT and 1.21 wt. % CK7, isooctane based; the resultant mixture will contain 0.5 wt. % AOT and 0.5 wt. %

CK7). The system should be equilibrated for 1 hour and centrifuged if is necessary in order to have the phases separated. Then a chromatogram of top and bottom phase should be performed to calculate the equilibrium constant ( $K_n$ ) of each component of CK7. When the plot of  $\ln(K_n)$  versus degree of polymerization ( $n$ ) is made, the curve obtained could be convex or concave. The goal is to have straight line, which corresponds to the PIT; so, either salt or CK3 should be added to reach the PIT if the curve is concave-down. Alternatively, the proportion of AOT, or the removal of salt by dialysis, will take place if the  $\ln(K_n)$ - $n$  profile is concave-down. If the curve is convex is because the mixture is too hydrophilic. Fourth, when the resultant conditions are employed for protein extraction, as described in Chapters 5 and 6.

## ***7.2 Recommendations***

My recommendations for the next phase of this investigation are as follows:

In order be purified, a protein have to be separated from the other proteins. In this dissertation was demonstrated that some proteins can be extracted and other proteins cannot under the same conditions. However, to complete the study it should to be proven that if two proteins with different individual partition coefficient can be separated when they are together in the same solution. To prove the latter statement it is proposed to fractionate proteins from a mixture in aqueous solution via W-III-based extraction.

The non-ionic surfactant CK7 was used in this dissertation with the original goal being its degradation under acidic conditions to achieve the back-extraction. Since this process step is not necessary to achieve back-extraction from Winsor-III systems, it would be good to test commercial non-ionic surfactants as components of a mixed surfactant system in extraction of proteins by W-III microemulsion systems. The

important property of non-ionic surfactants in this method is that they reduce the degradation of the proteins promoted by the ionic surfactants.

In this dissertation was tested extraction by electrostatic interactions and hydrophobic interactions. It would be interesting test the third possible interactions between microemulsions and proteins, which is biospecific interactions. In order to achieve this goal we suggest to find a W-III system with CK7, AOT and C<sub>8</sub>βG<sub>1</sub> that can extract the lectin concanavalin-A by a bioaffinity-based driving force.

Back-extraction did not achieve 100% recovery of the protein in all the cases but also the formation of solid precipitate was not observed. Therefore, it is possible that the remaining protein in the middle phase can be back-extracted through a second stage of stripping solution addition. The most probable underlying cause for < 100% recovery is that the protein solubilization is in equilibrium between middle and bottom phase. Therefore, if the original stripping solution is replaced with fresh stripping solution, the equilibrium would form again, back-extracting additional protein. It is proposed to repeat the back-extraction several times to prove if the mentioned hypothesis is true. If it is true the equilibrium partitioning of proteins between aqueous phase and middle phase in W-III systems used in backward extraction should be determined. This data would be useful to calculate the number of steps needed to achieve near 100% recovery of proteins by backward extraction.

Proteins can reach a very high concentration in the middle phase (12 mg/ml) and water and oil are in very near contact in the bicontinuous microemulsion so an enzymatic reaction which has a substrate soluble in water and the other soluble in oil should perform very well in a Winsor-III system. It is proposed to test enzymatic reactions between hydrophobic and hydrophilic substrates using an enzyme encapsulated at high concentration in the middle (bicontinuous microemulsion) phase. The substrates have to be dissolved in oil phase and aqueous phase.



## LIST OF REFERENCES

## List of References

1. Vasudevan, M., K. Tahan, and J.M. Wienczek, *Surfactant structure effects in protein separations using nonionic microemulsions*. Biotechnology and Bioengineering, 1995. **46**(2): p. 99-108.
2. Singh, A., J.D. Van Hamme, and O.P. Ward, *Surfactants in microbiology and biotechnology: part 2. Application aspects*. Biotechnology Advances, 2007. **25**(1): p. 99-121.
3. Kahlweit, M., *Microemulsions*. Annual Reports on the Progress of Chemistry, Section C: Physical Chemistry, 1999. **95**: p. 89-115.
4. Shioi, A., et al., *Protein Extraction in a Tailored Reversed Micellar System Containing Nonionic Surfactants*. Langmuir, 1997. **13**(4): p. 609-616.
5. Iyer, M., D.G. Hayes, and J.M. Harris, *Synthesis of pH-degradable nonionic surfactants and their applications in microemulsions*. Langmuir, 2001. **17**(22): p. 6816-6821.
6. Leser, M.E., et al., *Application of reverse micelles for the extraction of proteins*. Biochemical and Biophysical Research Communications, 1986. **135**(2): p. 629-35.
7. Wolbert, R.B.G., et al., *Protein transfer from an aqueous phase into reversed micelles. The effect of protein size and charge distribution*. European Journal of Biochemistry, 1989. **184**(3): p. 627-33.
8. Goklen, K.E. and T.A. Hatton, *Liquid-liquid extraction of low molecular-weight proteins by selective solubilization in reversed micelles*. Separation Science and Technology, 1987. **22**(2-3): p. 831-41.
9. Adamson, A.W., A.P. Gast, and Editors, *Physical Chemistry of Surfaces, Sixth Edition*. 1997. 784 pp.
10. Marquez, N., et al., *Partitioning of Ethoxylated Alkylphenol Surfactants in Microemulsion-Oil-Water Systems: Influence of Physicochemical Formulation Variables*. Langmuir, 2002. **18**(16): p. 6021-6024.
11. Iyer, M.A., *Synthesis and characterization of pH-degradable nonionic surfactants and their applications in microemulsions*. 2002. p. 154 pp.
12. Hellberg, P.-E., K. Bergstrom, and K. Holmberg, *Cleavable surfactants*. Journal of Surfactants and Detergents, 2000. **3**(1): p. 81-91.
13. Bientiecki, A. and K.A. Wilk, *Oil-in-water microemulsions based on chemodegradable surfactants as reaction media*. Journal of Physical Organic Chemistry, 1995. **8**(2): p. 71-6.
14. Ono, D., et al., *Biodegradation of different carboxylate types of cleavable surfactants bearing a 1,3-dioxolane ring*. Journal of the American Oil Chemists' Society, 1995. **72**(7): p. 853-6.
15. Epstein, W.W., et al., *The synthesis of a photolabile detergent and its use in the isolation and characterization of protein*. Analytical Biochemistry, 1982. **119**(2): p. 304-12.



16. Eastoe, J., et al., *Photoresponsive Microemulsions*. Langmuir, 2003. **19**(17): p. 6579-6581.
17. Gallardo, B.S., M.J. Hwa, and N.L. Abbott, *In Situ and Reversible Control of the Surface Activity of Ferrocenyl Surfactants in Aqueous Solutions*. Langmuir, 1995. **11**(11): p. 4209-12.
18. Hayashi, Y., et al., *Synthesis and properties of 2-alkoxy-N,N-dimethylethylamine N-oxides*. JAOCS, J. Am. Oil Chem. Soc., 1985. **62**(3): p. 555-7.
19. Von Rybinski, W. and K. Hill, *Alkyl polyglycosides*. Surfactant Science Series, 1998. **74**(Novel Surfactants): p. 31-85.
20. Jaeger, D.A. and M.R. Frey, *Preparation and characterization of destructible surfactants*. Journal of Organic Chemistry, 1982. **47**(2): p. 311-15.
21. Bieniecki, A., K.A. Wilk, and J. Gapinski, *Micellar Aggregation Behavior at Low Ionic Strength of Cyclic Acetal-Type Cationic Surfactants Containing the 1,3-Dioxolane Moiety*. Journal of Physical Chemistry B, 1997. **101**(6): p. 871-875.
22. Wang, G.-W., et al., *Synthesis and characterization of cleavable cationic surfactants with a 1,3-dioxane ring*. Journal of the American Oil Chemists' Society, 1995. **72**(1): p. 83-7.
23. Wang, G.-W., et al., *Preparation, properties, and applications of vesicle-forming cleavable surfactants with a 1,3-dioxane ring*. Journal of Colloid and Interface Science, 1995. **173**(1): p. 49-54.
24. Yue, C., et al., *Synthesis and characterization of cleavable surfactants derived from poly(ethylene glycol) monomethyl ether*. Journal of the American Oil Chemists' Society, 1996. **73**(7): p. 841-845.
25. By, K. and M.H. Nantz, *Dioxazocinium ortho esters: a class of highly pH-vulnerable amphiphiles*. Angewandte Chemie, International Edition, 2004. **43**(9): p. 1117-1120.
26. Mohlin, K. and K. Holmberg, *Nonionic ortho ester surfactants as cleavable emulsifiers*. Journal of Colloid and Interface Science, 2006. **299**(1): p. 435-442.
27. Eliason, R. and M.M. Kreevoy, *Kinetic hydrogen isotope effects in the concerted mechanism for the hydrolysis of acetals, ketals, and ortho esters*. Journal of the American Chemical Society, 1978. **100**(22): p. 7037-41.
28. Gallardo, B.S. and N.L. Abbott, *Active Control of Interfacial Properties: A Comparison of Dimeric and Monomeric Ferrocenyl Surfactants at the Surface of Aqueous Solutions*. Langmuir, 1997. **13**(2): p. 203-208.
29. McElhanon, J.R., et al., *Thermally Cleavable Surfactants Based on Furan-Maleimide Diels-Alder Adducts*. Langmuir, 2005. **21**(8): p. 3259-3266.
30. Sokolowski, A., et al., *Surface activity and micelle formation of chemodegradable cationic surfactants containing the 1,3-dioxolane moiety*. Colloids and Surfaces, A: Physicochemical and Engineering Aspects, 1995. **98**(1/2): p. 73-82.
31. Sokolowski, A., B. Burczyk, and J. Oles, *Acetals and ethers. 11. Solubility of alkyl-substituted 1,3-dioxolanes and 1,3-dioxanes in water*. Journal of Physical Chemistry, 1984. **88**(4): p. 807-9.

32. Rairkar, M.E., D.G. Hayes, and J.M. Harris, *Solubilization of enzymes in water-in-oil microemulsions and their rapid and efficient release through use of a pH-degradable surfactant*. Biotechnology Letters, 2007. **29**(5): p. 767-771.
33. Alkhatib, M.H., *pH-Degradable 1, 3-dioxolane surfactants: synthesis and application in mixed surfactant systems*. 2006: p. 172 pp.
34. Kunieda, H. and K. Shinoda, *Solution behavior and hydrophile-lipophile balance temperature in the aerosol OT-isooctane-brine system: correlation between microemulsions and ultralow interfacial tensions*. Journal of Colloid and Interface Science, 1980. **75**(2): p. 601-6.
35. Nave, S., et al., *What Is So Special about Aerosol-OT? 2. Microemulsion Systems*. Langmuir, 2000. **16**(23): p. 8741-8748.
36. Rahaman, R.S. and T.A. Hatton, *Structural characterization of  $\alpha$ -chymotrypsin-containing AOT reversed micelles*. Journal of Physical Chemistry, 1991. **95**(4): p. 1799-811.
37. Schulman, J.H., W. Stoeckenius, and L.M. Price, *Mechanism of formation and structure of micro emulsions by electron microscopy*. Journal of Physical Chemistry, 1959. **63**: p. 1677-80.
38. Flanagan, J. and H. Singh, *Microemulsions: A potential delivery system for bioactives in food*. Critical Reviews in Food Science and Nutrition, 2006. **46**(3): p. 221-237.
39. Solans, C., et al., *Nano-emulsions*. Current Opinion in Colloid & Interface Science, 2005. **10**(3,4): p. 102-110.
40. Kim, B.J., et al., *Nanoparticle Surfactants as a Route to Bicontinuous Block Copolymer Morphologies*. Langmuir, 2007. **23**(14): p. 7804-7809.
41. Eastoe, J., et al., *Ionic Liquid-in-Oil Microemulsions*. Journal of the American Chemical Society, 2005. **127**(20): p. 7302-7303.
42. Paul, B.K. and S.P. Moulik, *Uses and applications of microemulsions*. Current Science, 2001. **80**(8): p. 990-1001.
43. Lawrence, M.J. and G.D. Rees, *Microemulsion-based media as novel drug delivery systems*. Advanced Drug Delivery Reviews, 2000. **45**(1): p. 89-121.
44. Malmsten, M., *Soft drug delivery systems*. Soft Matter, 2006. **2**(9): p. 760-769.
45. Schwuger, M.-J., K. Stickdorn, and R. Schomaecker, *Microemulsions in Technical Processes*. Chemical Reviews (Washington, D. C.), 1995. **95**(4): p. 849-64.
46. Winsor, P.A., *Hydrotropy, solubilization, and related emulsification processes. I*. Transactions of the Faraday Society, 1948. **44**: p. 376-82.
47. Tricoli, V., M. Farnesi, and C. Nicoletta, *Bicontinuous microemulsions as adsorbents for liquid-phase separation/purification*. AIChE Journal, 2006. **52**(8): p. 2767-2773.
48. Olsson, U. and H. Wennerström, *Globular and bicontinuous phases of nonionic surfactant films*. Advances in Colloid and Interface Science, 1994. **49**: p. 113-146.
49. Ben Ghoulam, M., et al., *Quantitative Effect of Nonionic Surfactant Partitioning on the Hydrophile-Lipophile Balance Temperature*. Langmuir, 2004. **20**(7): p. 2584-2589.

50. Kawakami, K., et al., *Mechanism of protein solubilization in sodium bis(2-ethylhexyl) sulfosuccinate water-in-oil microemulsion*. Colloids and Surfaces, A: Physicochemical and Engineering Aspects, 1996. **109**: p. 217-33.
51. Forney, C.E. and C.E. Glatz, *Extraction of Charged Fusion Proteins in Reversed Micelles: Comparison between Different Surfactant Systems*. Biotechnology Progress, 1995. **11**(3): p. 260-4.
52. Jarudilokkul, S., L.H. Poppenborg, and D.C. Stuckey, *Backward extraction of reverse micellar encapsulated proteins using a counterionic surfactant*. Biotechnology and Bioengineering, 1999. **62**(5): p. 593-601.
53. Dungan, S.R., et al., *Interfacial transport processes in the reversed micellar extraction of proteins*. Journal of Colloid and Interface Science, 1991. **145**(1): p. 33-50.
54. Hayes, D.G. and C. Marchio, *Expulsion of proteins from water-in-oil microemulsions by treatment with cosurfactant*. Biotechnology and Bioengineering, 1998. **59**(5): p. 557-566.
55. Gupta, R.B., C.J. Han, and K.P. Johnston, *Recovery of proteins and amino acids from reverse micelles by dehydration with molecular sieves*. Biotechnology and Bioengineering, 1994. **44**(7): p. 830-6.
56. Ono, T. and M. Goto, *Bioseparation through liquid-liquid interfaces*. Interfacial Nanochemistry, 2005: p. 287-302.
57. Jarudilokkul, S., E. Paulsen, and D.C. Stuckey, *The hydrodynamics of a Graesser ("raining bucket") contactor with a reverse micellar phase*. Biotechnology progress, 2000. **16**(6): p. 1071-8.
58. Hasmann, F.A., et al., *Continuous counter-current purification of glucose-6-phosphate dehydrogenase using liquid-liquid extraction by reverse micelles*. Biochemical Engineering Journal, 2007. **34**(3): p. 236-241.
59. Lightfoot, E.N. and J.S. Moscariello, *Bioseparations*. Biotechnology and Bioengineering, 2004. **87**(3): p. 259-273.
60. Shuler, M. and F. Kargi, *Bioprocess engineering - Basic Concepts, 2nd Ed.* 2005: p. 576 pp.
61. Noh, K.-H. and J.-Y. Imm, *One-step separation of lysozyme by reverse micelles formed by the cationic surfactant, cetyltrimethylammonium bromide*. Food Chemistry, 2005. **93**(1): p. 95-101.
62. Meyer, T., D. Harms, and J. Gmehling, *Analysis of polyethylene glycols with respect to their oligomer distribution by high-performance liquid chromatography*. Journal of Chromatography, 1993. **645**(1): p. 135-9.
63. Mourey, T.H. and L.E. Oppenheimer, *Principles of operation of an evaporative light-scattering detector for liquid chromatography*. Analytical Chemistry, 1984. **56**(13): p. 2427-34.
64. Li, W. and J.F. Fitzloff, *Determination of 24(R)-pseudoginsenoside F(11) in North American ginseng using high performance liquid chromatography with evaporative light scattering detection*. J Pharm Biomed Anal FIELD Full Journal Title:Journal of pharmaceutical and biomedical analysis, 2001. **25**(2): p. 257-65.

65. Kimball, B.A., W.M. Arjo, and J.J. Johnston, *Single-Point Calibration with a Non-linear Detector: Carbohydrate Analysis of Conifer Needles by Hydrophobic Interaction Chromatography-Evaporative Light-Scattering Detection (HIC-ELSD)*. Journal of Liquid Chromatography & Related Technologies, 2004. **27**(12): p. 1835-1848.
66. Konishi, K. and S. Yamaguchi, *Rapid determination of molecular weight distribution of poly(oxyethylene)-type nonionic surfactants by circular thin-layer chromatography*. Analytical Chemistry, 1966. **38**(12): p. 1755-7.
67. Nadeau, H.G., *Separation and analysis of nonylphenoxy polyethylene glycol ether adducts by programmed temperature gas chromatography*. Analytical Chemistry, 1964. **36**(10): p. 1914-1917.
68. Perez, M., et al., *Surfactant-oil-water systems near the affinity inversion. XII. Emulsion drop size versus formulation and composition*. Journal of Dispersion Science and Technology, 2002. **23**(1-3): p. 55-63.
69. Marquez, N., et al., *Partitioning of ethoxylated alkylphenol surfactants in microemulsion-oil-water systems*. Colloids and Surfaces, A: Physicochemical and Engineering Aspects, 1995. **100**: p. 225-31.
70. Salager, J.-L., et al., *Partitioning of Ethoxylated Octylphenol Surfactants in Microemulsion-Oil-Water Systems: Influence of Temperature and Relation between Partitioning Coefficient and Physicochemical Formulation*. Langmuir, 2000. **16**(13): p. 5534-5539.
71. Woll, J.M., T.A. Hatton, and M.L. Yarmush, *Bioaffinity separations using reversed micellar extraction*. Biotechnology Progress, 1989. **5**(2): p. 57-62.
72. Graciaa, A., et al., *The partitioning of complex surfactant mixtures between oil/water/microemulsion phases at high surfactant concentrations*. Journal of Colloid and Interface Science, 1983. **93**(2): p. 474-86.
73. De Maeyer, L., C. Trachimow, and U. Kaatze, *Entropy-Driven Micellar Aggregation*. Journal of Physical Chemistry B, 1998. **102**(43): p. 8480-8491.
74. Bradford, M.M., *A rapid and sensitive method for the quantitation of microgram quantities of protein utilizing the principle of protein-dye binding*. Analytical Biochemistry, 1976. **72**(1-2): p. 248-54.
75. Daniel, R.M., et al., *The effect of temperature on enzyme activity: new insights and their implications*. Extremophiles, 2008. **12**(1): p. 51-59.
76. Adachi, M. and M. Harada, *Solubilization mechanism of cytochrome c in sodium bis(2-ethylhexyl) sulfosuccinate water/oil microemulsion*. Journal of Physical Chemistry, 1993. **97**(14): p. 3631-40.
77. Shin, Y.-O. and J.H. Vera, *Solubilization limit of lysozyme into DODMAC reverse micelles*. Biotechnology and Bioengineering, 2002. **80**(5): p. 537-543.
78. Shin, Y.O., M.E. Weber, and J.H. Vera, *Reverse micellar extraction and precipitation of lysozyme using sodium di(2-ethylhexyl) sulfosuccinate*. Biotechnology Progress, 2003. **19**(3): p. 928-935.
79. Pahlman, S., J. Rosengren, and S. Hjerten, *Hydrophobic interaction chromatography on uncharged Sepharose derivatives. Effects of neutral salts on the adsorption of proteins*. Journal of Chromatography, 1977. **131**: p. 99-108.

80. Mozo-Villarias, A., J. Cedano, and E. Querol, *Hydrophobicity density profiles to predict thermal stability enhancement in proteins*. Protein Journal, 2006. **25**(7-8): p. 529-535.
81. Salager, J.L., et al., *Properties of surfactant/oil/water emulsified systems in the neighborhood of the three-phase transition*. Journal of Colloid and Interface Science, 1980. **77**(1): p. 288-9.
82. Burauer, S., et al., *Bicontinuous microemulsions revisited: a new approach to freeze fracture electron microscopy (FFEM)*. Colloids and Surfaces A: Physicochemical and Engineering Aspects, 2003. **228**(1-3): p. 159-170.
83. Matzke, S.F., et al., *Mechanisms of protein solubilization in reverse micelles*. Biotechnology and Bioengineering, 1992. **40**(1): p. 91-102.
84. Adachi, M. and M. Harada, *Time dependence of the solubilization state of cytochrome c in AOT water-in-oil microemulsion*. Journal of Colloid and Interface Science, 1994. **165**(1): p. 229-35.
85. Lundberg, D., M. Stjern Dahl, and K. Holmberg, *Mixed Micellar Systems of Cleavable Surfactants*. Langmuir, 2005. **21**(19): p. 8658-8663.
86. Bradford, M.M., *A Rapid and Sensitive Method for the Quantification of Microgram Quantities of Protein Utilizing the Principle of Protein Dye Binding*. Analytical Biochemistry, 1976. **72**: p. 248.
87. Mao, Q. and P. Walde, *Substrate Effects on the Enzymatic Activity of  $\alpha$ -Chymotrypsin in Reverse Micelles*. Biochemical and Biophysical Research Communications, 1991. **178**(3): p. 1105-1112.
88. Shin, Y.-O., M.E. Weber, and J.H. Vera, *Comparison of two methods to recover lysozyme from reverse micellar phases*. Separation Science and Technology, 2003. **38**(8): p. 1733-1748.

## VITA

Javier Alejandro Gómez del Río was born in Eldorado, province of Misiones, República Argentina in 1971. He graduated from the “Escuela Privada de Fábrica Celulosa Argentina” high school as chemical technician in 1990. After that, he received the Bachelor of Science in Chemical Engineering in “Universidad Nacional de Misiones” in 1998. After that, he received the Master in Material Science and Technology of the “Instituto de Tecnología Profesor Jorge A. Sábato” (Universidad Nacional de San Martín – Comisión Nacional de Energía Atómica) in 2001. After that, he achieved the Master of Science in Chemical Engineering in the University of Alabama in Huntsville in 2004.

Gómez del Río is currently pursuing his doctorate in Chemical Engineering at The University of Tennessee, Knoxville, TN, United States.